The Photochemistry of Dioxorhenium(V)

Thesis by

H. Holden Thorp

In Partial Fulfillment of the Requirements

for the Degree of

Doctor of Philosophy

California Institute of Technology

Pasadena, California

1989

(Submitted June 1, 1989)

Acknowledgments

The first thanks must go to Harry Gray -- a great man and a great scientist. It is an honor to join the distinguished ranks of students who call Harry their teacher and their friend. Being Harry's student gave me the opportunity to benefit from my own initiative without suffering from my own naive mistakes. I think David Tyler said it best when he thanked Harry for teaching him "how the big boys play the game." (Although in my case, I might thank Harry for teaching me how the big boys play "Stormy Weather.") Thanks, Harry -- you're big.

Next, I would like to mention John Brewer and what a privilege it has been to have him as a colleague and, more important, as a friend. John has been a constant influence on me as a scientist and has taught me a great deal. Sharing an apartment with John and our two Euchre opponents Scotty and Todd (Hi Val!) gave me many of my fond memories of Caltech. Sorry you guys couldn't win more often -- maybe you should learn to keep score the right way.

The rest of the Gray group, what a crew! Pixie (Miriam), it's always comforting to know that you're "wi-i-i-de awake"; thanks for everything -- Go Heels! Ramy, who took me in during my hour of need and has been my friend ever since -- too bad you won't let me decorate your hair more often. Tad, you're a dude (sorry about those hoses). "The Mav" -- what more can I say? Dave Malerba, thanks for helping flatten out my backswing. Josh, Erica, Tom Meade, the "bio girls" (Jenny and Adrienne), Tom Zeitlow, Janet, Mark, Wayne, Brad, Mike Therien, Mike Albin, Bruce, Catherine, Charlie, "Laddie" -- big, one and all. Special thanks also to my good friends Chris Sipes and Ken Graham.

I would like to thank Nick Turro for teaching me about micelles and giving me the chance to work in his laboratory. Thanks to my friends at Columbia, especially Vijay, Alan, Jeff, Sandy, Rachel and William. I'd also like to thank the people at Yale who tolerated and befriended me while I was writing my thesis: Gary, Bob, Warren, Mitch, Neil and Jim.

I have to thank the good folks at the University of North Carolina, without whom I would be cutting on cadavers and memorizing nerve insertions. Tom Meyer has been a continuous source of encouragement and advice; Pat Sullivan and Mitchell Bruce were the first people to show me how to do research and to have fun being a scientist. Also, my high school chemistry teacher, Bill Winfield, first taught me how to understand chemistry and be an interested observer.

I have received undying support from many people, and not only during my graduate career. Nancy and Nick Robinson have been my close friends for many years. Patti, thank you for all of your patience and support -- and your love, some of which I've been lucky enough to give back. My brother, Clay, is my constant friend and my surest champion. I never thought my "little brother" would give me so much to shoot for. My parents, Bo and Herb, have made the largest contribution of all. Their love, support and inspiration have made it all possible for me.

Finally, I would like to thank the National Science Foundation for a graduate fellowship (1987-1989).

to Patti

Abstract

The excited-state properties of *trans*-$ReO_2(py)_4^+$ (ReO_2^+) in acetonitrile solution have been investigated. The excited-state absorption spectrum of ReO_2^+ is dominated by bleaching of the ground state MLCT and d-d systems. The reduction potential of $ReO_2^{2+/+*}$ is estimated from emission and electrochemical data to be -0.7 V (SSCE). The ReO_2^+ excited state efficiently reduces methylviologen and other pyridinium and olefin acceptors. The resulting Re(VI) species oxidizes secondary alcohols and silanes. Acetophenone is the product of *sec*-phenethyl alcohol oxidation.

The emission properties of ReO_2^+ in aqueous solutions of anionic and nonionic surfactants have been investigated. The emission and absorption maxima of ReO_2^+ are dependent on the water content of its environment. Emission lifetimes vary over four orders of magnitude upon shifting from aqueous to nonaqueous environments. The emission lifetime has a large (8.6) isotope effect ($k(H_2O)/k(D_2O)$) that reflects its sensitivity towards the environment. These properties have been used to develop a model for the interactions of ReO_2^+ with sodium dodecyl sulfate (SDS). A hydrophobic ReO_2^+ derivative, $ReO_2(3\text{-Ph-py})_4^+$, has been used to probe micelles of nonionic surfactants, and these results are consistent with those obtained with SDS.

The emission properties of ReO_2^+ in Nafion perfluorosulfonated membranes have been investigated. Absorption and emission spectroscopy indicate that the interior of the membrane is quite polar, similar to ethylene glycol. Two well-resolved emission components show different lifetimes and different isotope effects, indicative of varying degrees of solvent accessibility. These components are taken as evidence for chemically distinct regions in the polymer film, assigned as the interfacial region and the ion cluster region.

The unsubstituted pyridine complex shows monophasic, $\tau = 1.7\ \mu s$, emission decay when bound to calf thymus DNA. Switching to the 3-Ph-py complex yields a biphasic emission decay ($\tau_1 = 2.4\ \mu s$, $\tau_2 = 10\ \mu s$) indicative of an additional, solvent-inaccessible binding mode. Photoinduced electron transfer to methylviologen leads to oxidative cleavage of the DNA as detected by gel electrophoresis. Electrochemical and spectrophotometric techniques used with organic substrates also can be used to monitor the oxidation of DNA. Abstraction of the ribose 4' hydrogen by ReO_2^{2+} is a possible mechanism.

Table of Contents

List of Figures

Chapter 1

Chapter 2

List of Tables

List of Abbreviations

bpy	2,2'-bipyridine
BLM	bleomycin
Brij 35	$CH_3(CH_2)_{11}(OCH_2CH_2)_{23}OH$
cmc	critical micellar concentration
CR-Me_3	meso-2,3,7,11,12-pentamethyl-3,7,11,17-tetraazabicyclo-[11.3.1]heptadeca-1(7),13,15-triene
CTAB	cetyltrimethylammonium bromide
CTDNA	calf thymus DNA
DNA	deoxyribonucleic acid
DIP	4,7-diphenyl-1,10-phenanthroline
DMF	N,N-dimethylformamide
DS^-	dodecyl sulfate anion
$E_{1/2}$	half-wave potential
$E_{0\text{-}0}$	excited state energy
en	1,2-ethylenediamine
HD_{B35}	isotope effect ($k_Q(H_2O)/k_Q(D_2O)$) in aqueous Brij 35 solution
HD_{HS}	isotope effect ($k_Q(H_2O)/k_Q(D_2O)$) in homogeneous solution
$I_{p,a}$	anodic peak current
$I_{p,c}$	cathodic peak current
k_f	bimolecular forward electron transfer rate constant
k_Q	bimolecular Stern-Volmer quenching constant
L-NS_2	2,6-bis(2,2-diphenyl-2-thioethyl)pyridine
MLCT	metal-to-ligand charge transfer
4-Me-py	4-methylpyridine (4-picoline)
MV^{2+}	methylviologen (paraquat)

NHE	normal hydrogen electrode
NMR	nuclear magnetic resonance
OOP	out-of-plane bending mode
OsO_2^{2+}	*trans*-dioxoosmium(VI)
phen	1,10-phenanthroline
3-Ph-py	3-phenylpyridine
pop	$P_2O_5H_2^{2-}$
PAR	Princeton Applied Research
py	pyridine
ReO_2^{+}	*trans*-dioxorhenium(V)
ReO_2^{2+}	*trans*-dioxorhenium(VI)
RuO_2^{2+}	*trans*-dioxoruthenium(VI)
SCE	saturated calomel electrode
SSCE	saturated sodium chloride electrode
SDS	sodium dodecyl sulfate
TBAH	tetra-*n*-butylammonium hexafluorophosphate
TCNE	tetracyanoethylene
TEOA	triethanolamine
THF	tetrahydrofuran
TMS	tetramethylsilane
tmc	1,4,8,11-tetramethyl-1,4,8,11-tetraazacyclotetradecane
Triton X-100	$CH_3C(CH_3)_2CH_2C(CH_3)_2C_6H_4(OCH_2CH_2)_{9.5}OH$
τ	emission lifetime
vs.	versus
Z	solvent polarity parameter

Chapter 1.

Introduction

Metal-oxo reagents are ubiquitous in high-valent transition metal coordination chemistry because of the degree to which both terminal and bridging oxo ligands stabilize high oxidation states.[1,2] Much of the ongoing research in oxidation catalyst development has centered on the synthesis of metal-oxo reagents capable of performing oxygen atom transfer[3] or hydrogen atom transfer[4] organic oxidations. From this rich ground-state chemistry, the development of versatile metal-oxo photooxidants might also be envisioned. To date, however, only a handful of metal-oxo complexes that possess long-lived emissive excited states have been prepared.[5-7] These complexes are based on the d^2 *trans*-$Re^{V}O_2^{+}$ and *trans*-$Os^{VI}O_2^{2+}$ chromophores whose electronic structures can be derived from original calculations by Ballhausen and Gray for the vanadyl ion.[8]

Thermal oxygen atom transfer reactions from high-valent metal-oxo reagents to acceptors such as triphenylphosphine have been observed in many systems (Figure 1.1). Metals of Group 6 such as Cr and Mo cleanly transfer oxo groups and form well-characterized metal containing products (**A**).[9] These reactions often proceed with the formation of μ-oxo dimers as shown in **B**.[10] Berg and Holm have used bulky ligands such as 2,6-bis(2,2-diphenyl-2-thioethyl)pyridine (L-NS_2) to prevent dimerization and to yield mononuclear products (**C**).[11] The only example of an oxygen atom transfer photoreaction involving a complex having a long-lived emissive excited state is shown in **D**.[7] Here, irradiation of *trans*-$OsO_2(tmc)^{2+}$ (tmc = 1,4,8,11-tetramethyl-1,4,8,11-tetrazacyclotetradecane) in the presence of triphenylphosphine leads to the production of triphenylphosphine oxide and an uncharacterized metal complex. This osmium complex is a powerful (> 2 V vs. NHE) one-electron excited state oxidant, and it is presumed that the reaction is induced by one-electron oxidation of triphenylphosphine to form

Figure 1.1. Oxygen atom transfer reactions of metal-oxo reagents.

A $[CrOCl_4]^- + PPh_3 \longrightarrow [Cr_2Cl_9]^{3-} + OPPh_3$

B *cis*-$MoO_2(S_2CNR_2)_2 + PPh_3 \longrightarrow [MoO(S_2CNR_2)_2]_2O + OPPh_3$

C *cis*-MoO_2(L-NS_2) + $PPh_3 \xrightarrow{DMF}$ MoO(L-NS_2)(DMF) + $OPPh_3$

D *trans*-$[OsO_2(tmc)]^{2+} + PPh_3 \xrightarrow{h\nu} OPPh_3$ + ?

PPh_3^+ and the stable complex *trans*-$Os^{V}O_2(tmc)^+$. This is followed by attack of the phosphine radical cation on the oxo group and oxygen atom transfer.

A different type of reactivity exhibited by metal-oxo reagents is hydrogen atom and hydride abstraction from organic substrates (Figure 1.2). Meyer and others have performed a very complete study on the physical properties and reactivity of a versatile oxidant, $Ru^{IV}O(bpy)_2(py)^{2+}$. This complex converts alcohols to ketones via a hydrogen atom transfer mechanism (**E**).[12a] Olefin epoxidation has also been observed (**F**) and a mechanism involving addition of the reactive oxo ligand to the double bond followed by loss of epoxide by the metal complex has been proposed.[12b] Photoreactions of *trans*-$Os^{VI}O_2^{2+}$ and *trans*-$Ru^{VI}O_2^{2+}$ also lead to useful organic conversions (**G** and **H**)[13] (CR-Me_3 = meso-2,3,7,11,12-pentamethyl-3,7,11,17-tetraazabicyclo[11.3.1]-heptadeca-1(7),13,15-triene). The mechanism is unknown and the metal containing products are uncharacterized; however, it is tempting to assume that abstraction of hydrogen atoms by a reactive oxo ligand is the first step, especially in light of the detailed studies of these reactions by others.[4,12]

There is a striking contrast between reactions **A** - **C** and **E** - **H**. In oxo complexes of Cr and Mo, it is the inherently weak M-O bond that leads to the observed reactivity. Thus, these reagents are useful for activating oxygen atom acceptors. The oxidizing capability of complexes of Ru and Os, however, arises from a reactive oxo ligand that activates C-H and C-C bonds in a manner analogous to carbonyl excited states.[14] These trends are seen in biological systems as well where oxomolybdenum enzymes such as xanthine oxidase catalyze oxygen atom transfer.[15] In contrast, cytochrome P_{450} activates C-H bonds in substrates such as toluene where the active form of the enzyme is believed to be an Fe^{IV}=O moiety.[16] In photosynthesis, Nature uses an

Figure 1.2. Activation of C-H and C-C bonds by metal-oxo reagents.

E

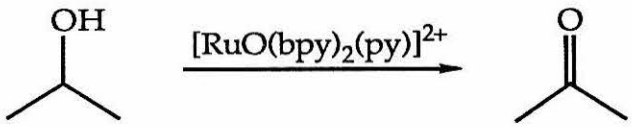
OH
[RuO(bpy)2(py)]2+
O

F

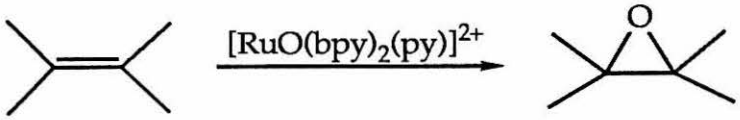
[RuO(bpy)2(py)]2+
O

G

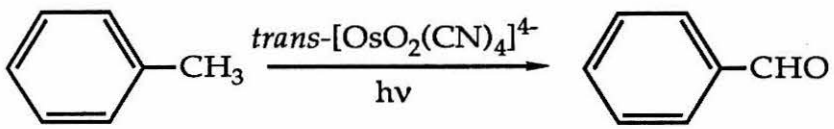
CH3
trans-[OsO2(CN)4]4-
hν
CHO

H

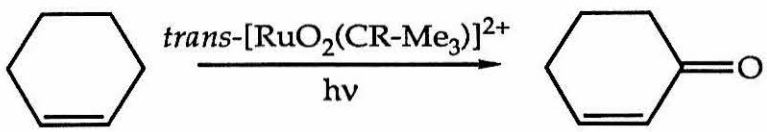
trans-[RuO2(CR-Me3)]2+
hν
O

oxomanganese cluster to store protons and oxidizing equivalents for water oxidation.[17] Surprisingly, this complex can exist in at least six different oxidation states, none of which are reactive towards oxygen atom acceptors or weak C-H bonds in the protein.

Stable d^2 transdioxo complexes have been prepared for Mo(IV),[18,19] Tc(V),[20,21] Re(V),[22-35] Ru(VI),[14,36-43] and Os(VI).[7,44-52] The most detailed investigation of the spectroscopic properties of the *trans*-MO_2 chromophore was performed on *trans*-ReO_2^+ complexes, namely *trans*-$ReO_2(py)_4^+$, *trans*-$ReO_2(en)_2^+$, and *trans*-$ReO_2(CN)_4^{3-}$.[6] The photophysics of these excited states were thoroughly characterized; however, attempts to perform photochemical reactions failed. The subject of this thesis is the development of the solution photochemistry of *trans*-$ReO_2(py)_4^+$, hereinafter referred to as ReO_2^+.

ReO_2^+ - Synthesis and Structure

The aerobic oxidation of K_2ReCl_6 in aqueous pyridine leads to the precipitation of $[ReO_2(py)_4]Cl$.[29] Other salts can be prepared by simple metathesis. The complex is very inert to substitution in the absence of a coordinating anion[53] with a half-time for oxo exchange in $H_2{}^{18}O$ of 8000 minutes.[30] Protonation of the first oxo ligand occurs in concentrated HCl but the second oxo ligand is protonated only in concentrated H_2SO_4.[29] The asymmetric O-Re-O stretch is found at 820 cm^{-1} in the IR spectrum of a $[ReO_2(py)_4]Cl$ Nujol mull,[29] typical of an asymmetric MO_2 stretching mode.[54] This complex was later prepared by the reaction of $ReO_2(PPh_3)_2I$ with pyridine.[31,32] These results had been neglected until the recent discovery that

$ReO_2(PPh_3)_2I$ is a convenient starting material for an extensive series of ReO_2^+ derivatives[53] and other monooxorhenium species.[55]

Many transdioxorhenium complexes have been crystallographically characterized.[22-24,28] A recent structure of a 4-methylpyridine (4-Me-py) complex of ReO_2^+[28] is shown in Figure 1.3. The Re-O and Re-N bond distances and angles are within 0.04 Å for all of the $ReO_2L_4^+$ (L = py, 1/2 en, 4-Me-py) complexes that have been structurally characterized. These angles and distances are given in Table 1.1. An important feature of the py and 4-Me-py structures is the angle of the pyridine rings with respect to the ReN_4 plane. The rings are all within 5 - 23° of being coplanar with the O-Re-O vector.

ReO_2^+ - Electronic Structure and Redox Properties

The electronic spectrum of ReO_2^+ was originally measured in aqueous solution and shows strong bands at 331 nm (ε = 19400 M^{-1} cm^{-1}) and 445 nm (ε = 1200 M^{-1} cm^{-1}).[29] These bands also have been studied in a crystal.[6] Low temperature absorption spectra of single crystals allow the assignment of the low energy band to a $(d_{xy})^2 \rightarrow (d_{xy})^1(d_{xz,yz})^1$ transition leading to a $^{1,3}E_g$ lowest energy excited state. The higher energy band at 331 nm was tentatively assigned to d(Re) $\rightarrow \pi^*$(py) metal-to-ligand charge transfer (MLCT) by Pipes and Meyer on the basis of its shift upon oxo group protonation.[56] Thus, the energy level diagram for ReO_2^+ can be drawn as shown in Figure 1.4.

The ^3E_g excited state of ReO_2^+ (ReO_2^{+*}) shows long-lived emission both in solution and in the solid state.[6] The solid state emission lifetime is quite long (32 μs), as is the solution lifetime in non-hydroxylic solvents ranging from 13 μs in CH_2Cl_2 to 17 μs in pyridine. The lifetime of the ReO_2^{+*}

Figure 1.3. Crystal structure of $[ReO_2(4\text{-Me-py})_4][ReO_4]$ taken from reference 28 (ReO_4^- counterions not shown for clarity).

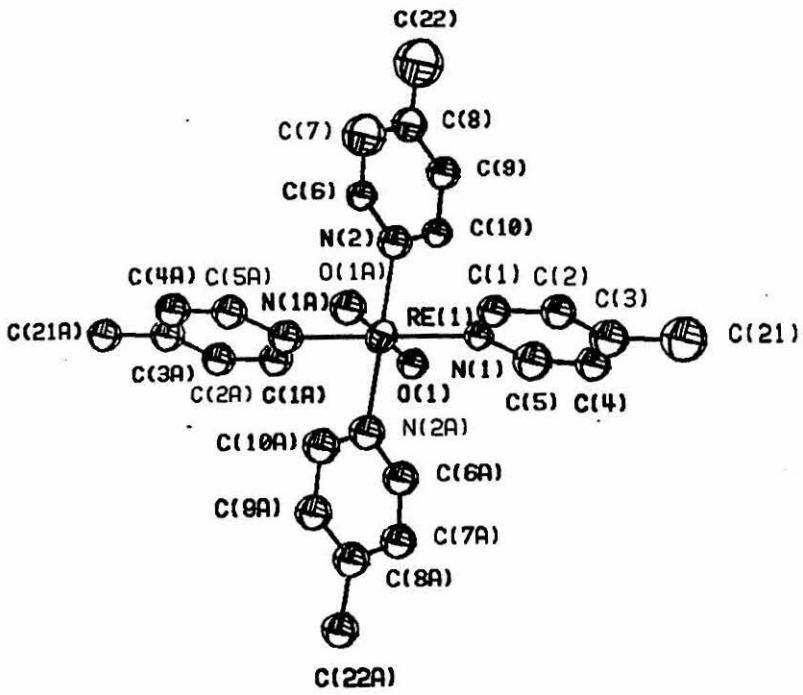
C(22)
C(7)
C(8)
C(9)
C(6)
C(10)
N(2)
O(1A)
C(4A)
C(5A)
N(1A)
C(1)
C(2)
C(3)
C(21A)
RE(1)
C(21)
C(3A)
N(1)
C(2A)
C(1A)
O(1)
C(5)
C(4)
N(2A)
C(10A)
C(6A)
C(9A)
C(7A)
C(8A)
C(22A)

Table 1.1.

Bond Distances and Angles in the Re Coordination Sphere of $ReO_2(4\text{-Me-py})_4^+$ (taken from reference 28).

Bond Distances (Å):	Re(1)-O(1)	1.75 (2)
	Re(1)-N(1)	2.11 (2)
	Re(1)-N(2)	2.14 (2)
Bond Angles (deg):	O(1)-Re(1)-N(1)	89.8 (8)
	O(1)-Re(1)-N(2)	90.1 (8)
	N(1)-Re(1)-N(2)	89.7 (8)

Figure 1.4. Energy level diagram for ReO_2^+ adapted from reference 6.

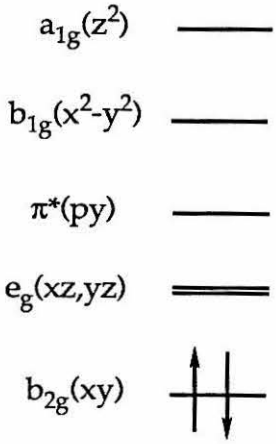
$a_{1g}(z^2)$
$b_{1g}(x^2-y^2)$
$\pi^*(py)$
$e_g(xz,yz)$
$b_{2g}(xy)$

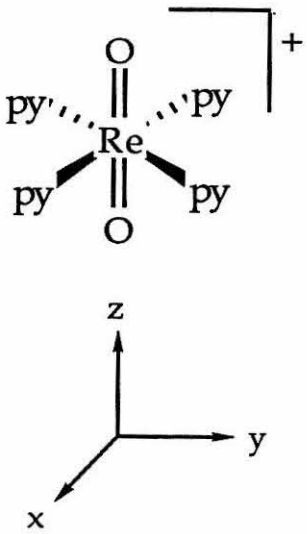
O
py
py
Re
py
py
O
+

z
y
x

emission is quenched by hydroxylic solvents, and Stern-Volmer quenching constants have been measured ($k_Q(H_2O) = 8.2 \times 10^5\ M^{-1}\ s^{-1}$, $k_Q(D_2O) = 9.5 \times 10^4\ M^{-1}\ s^{-1}$). These rate constants show a remarkable (8.6) isotope effect, and the Stern-Volmer plots remain linear over a wide range of quencher concentrations. The solvent dependence of the absorption spectrum of ReO_2^+ was studied much earlier by Beard and Murmann.[57] In both studies, a mechanism involving hydrogen bonding of the solvent to the oxo group was proposed.

In aqueous solution, ReO_2^+ shows rich redox chemistry.[56] In fact, the oxidation states Re(II), III, V and VI all can be reached within the solvent limits. The pH-independent oxidation of ReO_2^+ to $Re^{VI}O_2(py)_4^{2+}$ (ReO_2^{2+}) occurs at +1.25 V (SSCE) and is reversible on the cyclic voltammetry time scale. Attempts to prepare ReO_2^{2+} by bulk electrolysis led to decomposition indicating that the d^1 complex is unstable on the time scale of this experiment.

The properties of ReO_2^+ described here foreshadow the two aspects of photochemistry described in this thesis. First, if the one-electron oxidation can be performed in non-aqueous solution then ReO_2^+ should be a mild excited state reductant. Further, the product of excited state electron transfer, ReO_2^{2+}, might be a useful high-energy intermediate for organic oxidations (Chapter 2). Second, the quenching of ReO_2^{+*} emission by water indicates that this excited state might be a novel probe of microheterogeneous systems including micelles (Chapter 3), polymer films (Chapter 4) and nucleic acids (Chapter 5).

References

1. Griffith, W.P. *Coord. Chem. Rev.* **1970**, *5*, 459.

2. Cotton, F.A.; Wilkinson, G. *Advanced Inorganic Chemistry*, 4th ed.; Wiley, New York, 1980, p. 151-155.

3. Holm, R.H. *Chem. Rev.* **1987**, *87*, 1401.

4. Meyer, T.J. *J. Electrochem. Soc.* **1984**, *131*, 221C.

5. Winkler, J.R.; Gray, H.B. *J. Am. Chem. Soc.* **1983**, *105*, 1373.

6. Winkler, J.R.; Gray, H.B. *Inorg. Chem.* **1985**, *24*, 346.

7. Che, C.-M.; Yam, V.W.-W.; Cho, K.C.; Gray, H.B. *J. Chem. Soc., Chem. Commun.* **1987**, 948.

8. Ballhausen, C.J.; Gray, H.B. *Inorg. Chem.* **1962**, *1*, 111.

9. Miller, K.F.; Wentworth, R.A.D. *Inorg. Chim. Acta* **1979**, *36*, 37.

10. Barral, R.; Bocard, C.; Seree de Roch, I.; Sajus, L. *Tetrahedron Lett.* **1972**, 1693.

11. Holm, R.H.; Berg, J.M. *J. Am. Chem. Soc.* **1985**, *107*, 925.

12. a) Thompson, M.S.; Meyer, T.J. *J. Am. Chem. Soc.* **1982**, *104*, 4106. b) Dobson, J.C.; Seok, W.K.; Meyer, T.J. *Inorg. Chem.* **1986**, *25*, 1314.

13. Yam, V.W.-W.; Che, C.-M.; Tang, W.-T. *J. Chem. Soc., Chem. Commun.* **1988**, 100.

14. Turro, N.J. *Modern Molecular Photochemistry*, Benjamin-Cummings, Menlo Park, CA, 1978.

15. Bray, R.C. *Adv. Enzymol.* **1980**, *51*, 107.

16. Dawson, J.H. *Science* **1988**, *240*, 433.

17. Brudvig, G.W.; Crabtree, R.H. *Proc. Natl. Acad. Sci. USA* **1986**, *83*, 4586.

18. Day, V.W.; Hoard, J.L. *J. Am. Chem. Soc.* **1968**, *90*, 3374.

19. Crayston, J.A.; Almond, M.J.; Downs, A.J.; Poliakoff, M.; Turner, J.J. *Inorg. Chem.* **1984**, 23, 3051.

20. Kastner, M.E.; Lindsay, M.J.; Clarke, M.J. *Inorg. Chem.* **1982**, *21*, 2037.

21. Zuckman, S.A.; Freeman, G.M.; Troutner, D.E.; Volkert, W.A.; Holmes, R.A.; Van DerVeer, D.G.; Barefield, E.K. *Inorg. Chem.* **1981**, *20*, 2386.

22. Calvo, C.; Krischnamachar, N.; Lock, C.J.L. *J. Cryst. Mol. Struct.* **1971**, *1*, 161.

23. Lis, T.; Glowiak, T.; Jerzowska-Trzebiatowska, B. *Bull. Acad. Pol. Sci., Ser. Sci. Chim.* **1975**, *23*, 417.

24. Lock, C.J.L.; Turner, G. *Acta Crystallogr., Sect. B: Struct. Crystallogr. Cryst. Chem.* **1978**, *B34*, 923.

25. Fenn, R.H.; Graham, A.J. *J. Chem. Soc. A* **1971**, 2880.

26. Murmann, R.K.; Schlemper, E.O. *Inorg. Chem.* **1971**, *10*, 2352.

27. Johnson, N.P.; Lock, C.J.L.; Wilkinson, G. *J. Chem. Soc.* **1964**, 1054.

28. Johnson, J.W.; Brody, J.F.; Ansell, G.B.; Zentz, S. *Inorg. Chem.* **1984**, *23*, 2415.

29. Beard, J.H.; Casey, J.; Murmann, R.K. *Inorg. Chem.* **1965**, *4*, 797.

30. Beard, J.H.; Calhoun, C.; Casey, J.; Murmann, R.K. *J. Am. Chem. Soc.* **1968**, *90*, 3384.

31. Freni, M.; Giusto, D.; Romiti, P. *Gazz. Chim. Ital.* **1967**, *97*, 833.

32. Freni, M.; Giusto, D.; Romiti, P.; Minghetti, G. *Gazz. Chim. Ital.* **1969**, *99*, 286.

33. Ciani, G.; D'Alfonso, G.; Romiti, P.; Sironi, A.; Freni, M. *Inorg. Chim. Acta* **1983**, *72*, 29.

34. Murmann, R.K. *Inorg. Synth.* **1976**, *8*, 173.

35. Chakravorti, M.C. *Inorg. Synth.* **1982**, *21*, 116.

36. Takeuchi, K.J.; Samuels, G.J.; Gersten, S.W.; Gilbert, J.A.; Meyer, T.J. *Inorg. Chem.* **1983**, *22*, 1407.

37. Ellis, C.D.; Gilbert, J.A.; Murphy, W.R.; Meyer, T.J. *J. Am. Chem. Soc.* **1983**, *105*, 4842.

38. Gersten, S.W.; Samuels, G.J.; Meyer, T.J. *J. Am. Chem. Soc.* **1982**, *104*, 4029.

39. Che, C.-M.; Wong, K.Y.; Poon, C.K. *Inorg. Chem.* **1985**, *24*, 1797.

40. Mak, T.C.-W.; Che, C.-M.; Wong, K.Y. *J. Chem. Soc., Chem. Commun.* **1985**, 986.

41. Lau, T.C.; Kochi, J.K. *J. Chem. Soc., Chem. Commun.* **1987**, 798.

42. Griffith, W.P.; Pawson, D. *J. Chem. Soc. Dalton Trans.* **1973**, 1315.

43. Green, G.; Griffith, W.P.; Hollinshed, D.M.; Ley, S.V.; Schroder, M. *J. Chem. Soc. Perkin Trans.* **1984**, 1286.

44. Dobson, J.C.; Takeuchi, K.J.; Pipes, D.W.; Geselowitz, D.A.; Meyer, T.J. *Inorg. Chem.* **1986**, *25*, 2357.

45. Pipes, D.W.; Meyer, T.J. *Inorg. Chem.* **1986**, *25*, 4042.

46. Che, C.-M.; Cheng, W.-K. *J. Am. Chem. Soc.* **1986**, *108*, 4644.

47. Kruse, F.H. *Acta Crystallogr.* **1961**, *14*, 1035..

48. Porai-Koshitis, M.A.; Atovmyan, L.O.; Andrianov, V.G. *J. Struct. Chem.* **1961**, *2*, 686.

49. Malin, J.M.; Schlemper, E.O.; Murmann, R.K. *Inorg. Chem.* **1977**, *16*, 615.

50. Anson, F.C.; Collins, T.J.; Gipson, S.L.; Keech, J.T.; Krafft, T.E.; Peake, G.T. *J. Am. Chem. Soc.* **1986**, *108*, 6593.

51. Anson, F.C.; Christie, J.A.; Collins, T.J.; Coots, R.J.; Furutani, T.T.; Gipson, S.L.; Keech, J.T.; Krafft, T.E.; Santarsiero, B.D.; Spies, G.H. *J. Am. Chem. Soc.* **1984**, *106*, 4460.

52. Malin, J.M.; Schlemper, E.O.; Murmann, R.K. *Inorg. Chem.* **1977**, *16*, 615.

53. Brewer, J.C.; Gray, H.B. *Inorg. Chem* . Submitted for publication.

54. Lock, C.J.L.; Wilkinson, G. *Chem. Ind.* (London), **1962**, 40.

55. Mayer, J.M.; Tulip, T.H.; Calabrese, J.C.; Valencia, E. *J. Am. Chem. Soc.* **1987**, *109*, 157.

56. Pipes, D.W.; Meyer, T.J. *Inorg. Chem.* **1986**, *25*, 3256.

57. Beard, J.H.; Murmann, R.K. *J. Inorg. Nucl. Chem.* **1968**, *30*, 2467.

Chapter 2.

Excited-State Properties of Dioxorhenium(V). Generation and Reactivity of Dioxorhenium(VI).

Introduction

The generation of oxidizing transition metal complexes by photophysical and photochemical processes is an area of intense study.[1-5] An immediate goal of this research is to develop compounds whose ground states are unreactive in solution but become versatile oxidants after either photoexcitation or photoinduced electron transfer to a sacrificial acceptor. Much effort has centered on the development of photocatalysts based on ruthenium polypyridyl complexes.[1] These molecules are not well-suited for bond-breaking or bond-making chemistry because they do not possess open coordination sites or potentially reactive ligands. The d^8-d^8 dimer, $Pt_2(pop)_4^{4-}$, has a strongly oxidizing excited state whose reactivity arises from two open platinum coordination sites.[6] Alternatively, the relatively inert oxo ligands of $OsO_2(tmc)^{2+}$ become reactive upon photoexcitation.[7]

The complex *trans*-$ReO_2(py)_4^+$ (ReO_2^+) possesses a long-lived (τ = 10-15 μs) excited state in non-aqueous solution.[8] This excited state arises from a d-d transition ($(d_{xy})^2 \rightarrow (d_{xy})^1(d_{xz,yz})^1$) that leads to the population of an orbital that is formally Re-O antibonding. In addition, it has been reported that this complex can be oxidized reversibly by one electron at +1.25 V (SSCE) in aqueous solution.[9] We report here that this oxidation also can be performed reversibly in non-aqueous solution and that the product of this oxidation, ReO_2^{2+}, can be generated by bimolecular excited state electron transfer quenching. Further, this d^1 intermediate oxidizes organic molecules such as secondary alcohols, halocarbons and silanes.

Experimental

Materials. Solvents used for synthesis were reagent grade. Solvents used for physical measurements were freshly distilled from appropriate

drying agents under vacuum or inert atmosphere. $KReO_4$ (Aesar), tribenzylsilane (Aldrich), and *sec*-phenethyl alcohol (Aldrich, Gold Label) were used as received. Tetra-(*n*-butyl)-ammonium hexafluorophosphate (TBAH) was prepared by the addition of a dilute HPF_6 solution to a saturated aqueous solution of tetra-(*n*-butyl)-ammonium bromide. White crystals were obtained after repeated recrystallization from hot ethanol. Quenchers (mono- and bi-pyridinium ions, TCNE) were prepared, metathesized and purified by the usual techniques.[10] Proton NMR spectra were obtained using a JEOL FX-90Q spectrometer.

$[ReO_2(py)_4]PF_6$. The chloride salt was prepared by the method of Beard et al.[11] The PF_6^- salt was obtained by addition of a saturated aqueous NH_4PF_6 solution to an aqueous solution of the chloride. This yellow solid was recrystallized from 5:1 acetone/pyridine by the addition of petroleum ether.

Electrochemistry. Cyclic voltammetry measurements were made using a Princeton Applied Research (PAR) 173 potentiostat and a PAR 175 universal programmer. Platinum button working electrodes were prepared by polishing with 5 μm alumina, washing with water, and sonicating in 1:1 MeOH/water. Solutions were degassed with argon and kept under an argon blanket during the experiment. A Pt wire/glass joint was used to hold the SSCE reference electrode and to prevent water from leaking into the cell. A Pt wire was used as the auxiliary electrode. Solutions were 0.1 M in TBAH and ~1 mM in compound. Bulk electrolysis experiments were conducted at a Pt gauze working electrode using the PAR 173 potentiostat equipped with a digital coulometer. The bulk electrolysis cell was a two compartment cell fitted with an argon inlet and a Pt wire/glass joint for holding the SSCE reference electrode. Argon flow and stirring were continued throughout the experiment. Electrolysis solutions were exhaustively extracted with pentane

for analysis of the organic products by UV spectroscopy. Standard solutions of appropriate concentrations were used for quantitating the conversion efficiency.

Photochemical experiments. Nanosecond laser flash photolysis and resonance Raman experiments were performed at Columbia University in the laboratories of Prof. N.J. Turro as described previously.[12] Time-resolved absorption measurements were made using 308 nm excitation from a Lambda Physik EMG-201 MSC Excimer laser. A xenon lamp (150 W, Oriel Corp.) powered by a PRA Model M301 power supply and M305 pulser was used as the monitoring source. The lamp was pulsed to produce very bright, 1 ms wide, spectrally broad and highly reproducible lamp profiles. The monitoring light after passage through the sample was collimated and focused onto the entrance slit of a monochromator and data were collected by standard photomultiplier tube/transient digitizer techniques. Decay curves were collected at individual wavelengths and fit to single exponentials by standard algorithms. These decay curves were used to construct transient absorption spectra.

The resonance Raman experiments were conducted by using a homemade laser Raman spectrometer. The samples were excited by a Nd:YAG laser (DCR-2, 532 nm). The laser power was high enough to saturate the excited-state population and also to scatter off from the excited state formed during a single laser pulse. The sample solution was pumped through a nozzle to form a smooth thin jet, which was intercepted by the laser. The back-scattered light was collected at a small angle to the pump beam and focused onto the entrance slit of the Spex Triplemate spectrograph. The third stage of the spectrograph contained a 2400 groove/mm grating to provide high resolution for the Raman experiments. This grating covers a

range of ~900-1800 cm^{-1} in the Raman spectrum with ~2 cm^{-1} resolution. The dispersed light was detected by a PARC Model 1420 gated (10 ns), intensified diode array detector (1024 elements) that was interfaced to a PARC Model 1460 controller. The entire experiment was run by a homemade, menu-driven program with special graphics, written in the Heminway Basic operating system. The Raman spectrum of CH_3CN was routinely subtracted from the data. The spectra were calibrated using toluene.

Optical absorption spectra were obtained using a Shimadzu UV-260 recording spectrophotometer. Steady-state photolysis was performed using a high pressure Hg/Xe arc lamp equipped with water and air cooling and Corning cutoff filters. Emission spectra were recorded on an instrument that has been described previously.[13] Emission lifetime measurements were made using a pulsed Nd:YAG system that has been described previously.[14] A 532 nm excitation pulse was used in all of these measurements. Emission lifetime quenching experiments were performed under vacuum using a two-compartment cell that has been described previously.[15]

Results and Discussion

Excited State Properties. The absorption spectrum of ReO_2^+ in acetonitrile solution (Figure 2.1) exhibits a very intense band at 360 nm that is attributable to d(Re) $\rightarrow \pi^*$(py) MLCT.[9] Further experiments in our laboratory have confirmed this assignment.[16] The weak band at 416 nm has been assigned as $(d_{xy})^2 \rightarrow (d_{xy})^1(d_{xz,yz})^1$, and this transition leads to population of the long-lived triplet excited state, ^3E_g.

The emission properties of ReO_2^+ in nonaqueous solution (pyridine, THF, CH_2Cl_2) were also reported by Winkler and Gray.[8] We have investigated these properties in acetonitrile solution, and observe similar emission at λ_{max} = 640 nm with an emission lifetime of 10 μs. Time-resolved

Figure 2.1. Ground state absorption spectrum of $[ReO_2(py)_4]PF_6$ in CH_3CN.

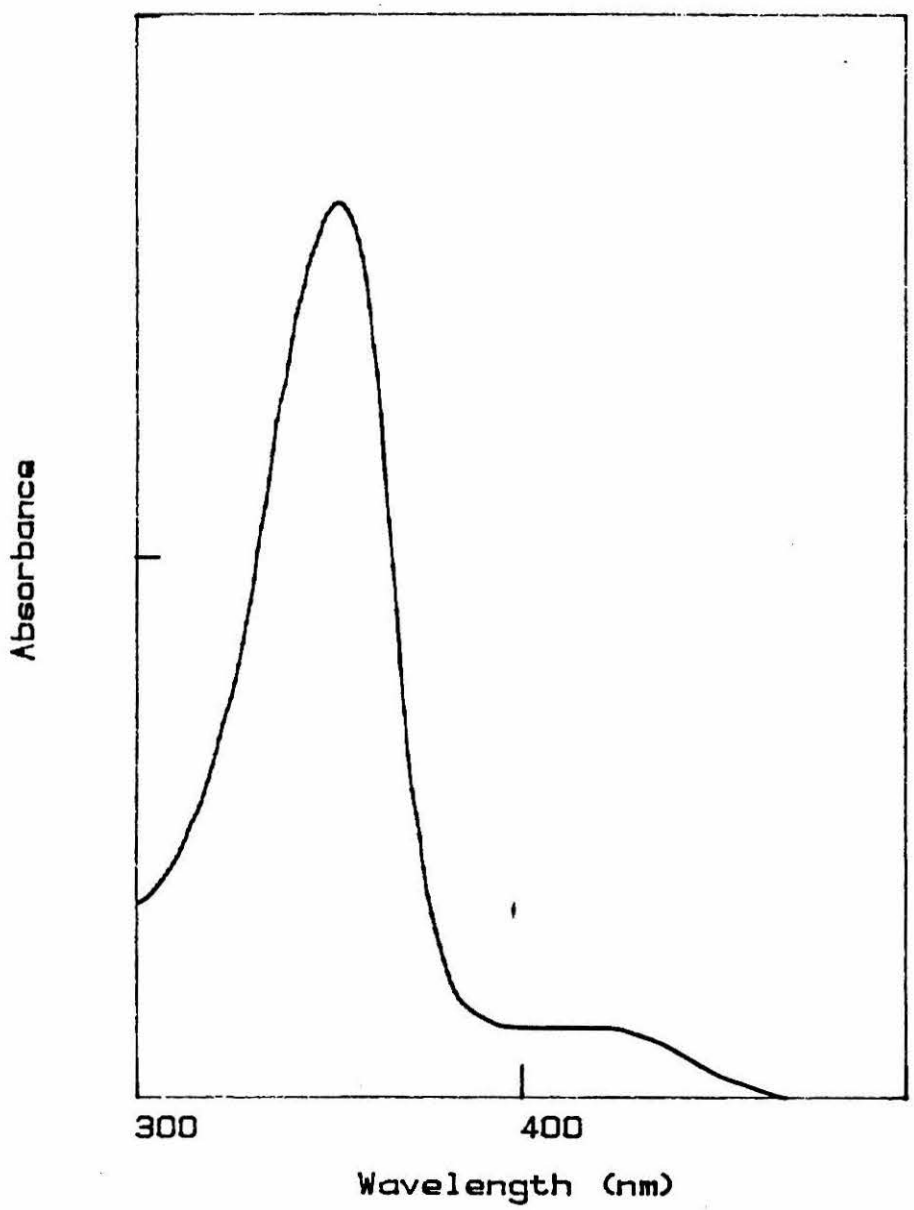
Absorbance
300
400
Wavelength (nm)

absorption spectra taken 80 ns after laser flash photolysis of these solutions are dominated by bleaching of the ground-state MLCT and d-d transitions at 340 nm and 420 nm (Figure 2.2). This bleaching recovers by first-order kinetics with a lifetime equal to the emission lifetime. A broad, weak excited state absorption at ~500 nm decays with the same lifetime as the emission and the ground state bleach.

The weak excited state absorption can be assigned by considering the energy level diagram shown in Figure 2.3. As shown, the excited triplet configuration is $(d_{xy})^1(d_{xz,yz})^1$. From the energy of the ground state MLCT band, the π^*(py) orbital is estimated to lie ~28400 cm^{-1} above the d_{xy} orbital, thereby making the energy for an excited state $(d_{xy})^1(d_{xz,yz})^1 \rightarrow (d_{xz,yz})^1(\pi^*(py))^1$ transition much higher than that of the observed ~500 nm absorption. It is likely that if this transition occurs, it is unobserved because of the strong ground state bleach occurring in the same region. Likewise, the $(d_{xy})^1(d_{xz,yz})^1 \rightarrow (d_{xy})^1(\pi^*(py))^1$ transition should occur at ~2270 nm (~4400 cm^{-1}), an energy a great deal lower than that observed. From energy considerations, it is thus reasonable to assign the observed excited state absorption band to a $(d_{xy})^1(d_{xz,yz})^1 \rightarrow (d_{xz,yz})^2$ transition.

The resonance Raman spectrum of ReO_2^+ obtained in acetonitrile solution is shown in Figure 2.4. This spectrum shows a very strong band at 916 cm^{-1} that can be assigned to the symmetric M-O stretch. This frequency is the same as that observed in vibrational progressions of low temperature emission spectra of ReO_2^+ crystals.[8] Recently, this same progression has been observed from ReO_2^+ intercalated in smectite clays.[17]

Redox Properties and Excited State Electron Transfer. In aqueous solution, ReO_2^+ can be oxidized reversibly to ReO_2^{2+} at +1.25 V(SSCE).[9] The cyclic voltammogram of ReO_2^+ in 0.1 M TBAH/CH_3CN solution (Figure 2.5a)

Figure 2.2. Excited state absorption spectrum of ReO_2^{+*} taken 80 ns after 308 nm excitation in CH_3CN.

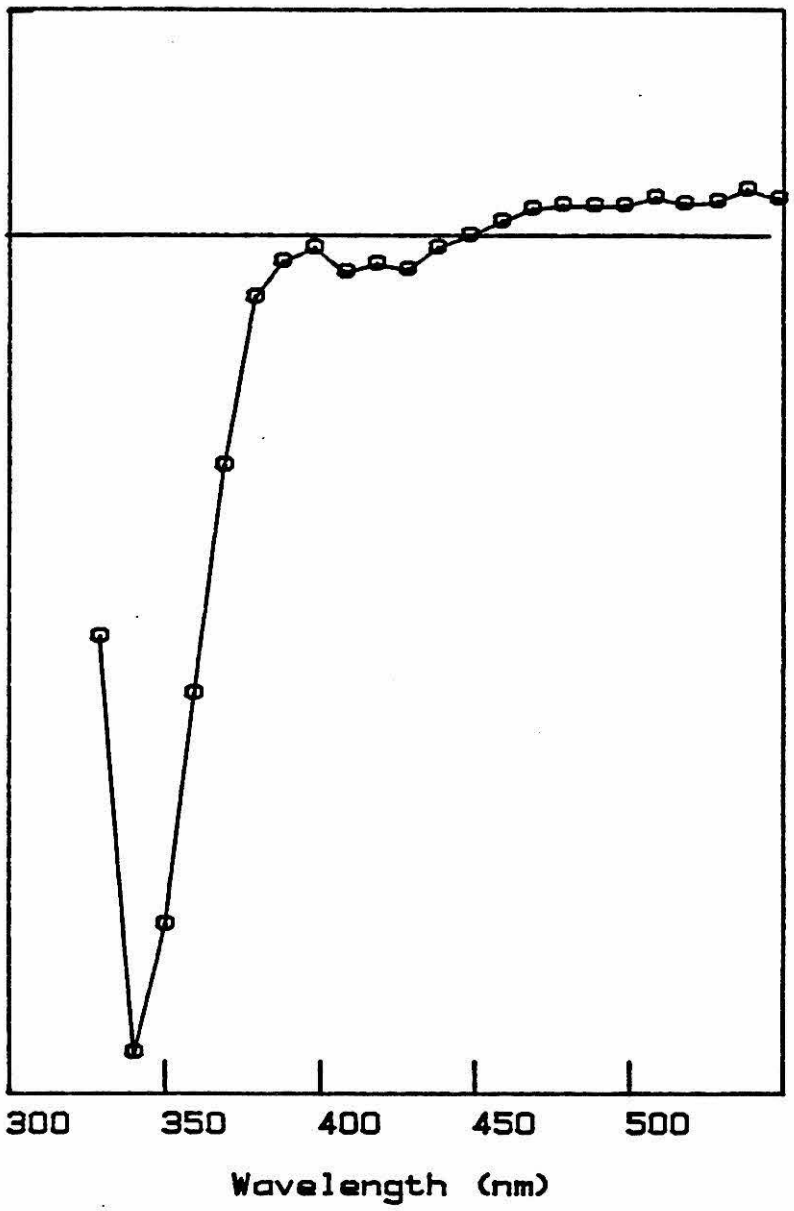
300
350
400
450
500
Wavelength (nm)

Figure 2.3. Energy level diagram showing the relative energies of potential excited state absorptions.

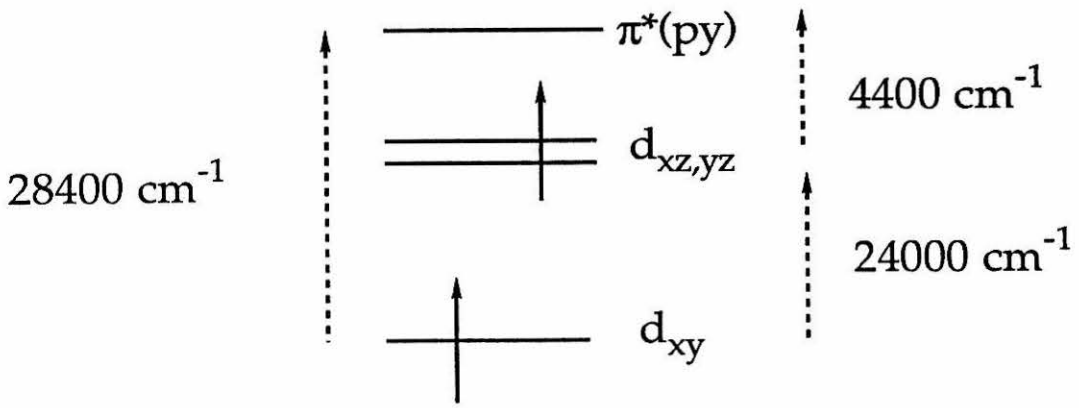
π*(py)
4400 cm-1
dxz,yz
28400 cm-1
24000 cm-1
dxy

Figure 2.4. Resonance Raman spectrum of ReO_2^+ obtained with 532 nm excitation in CH_3CN.

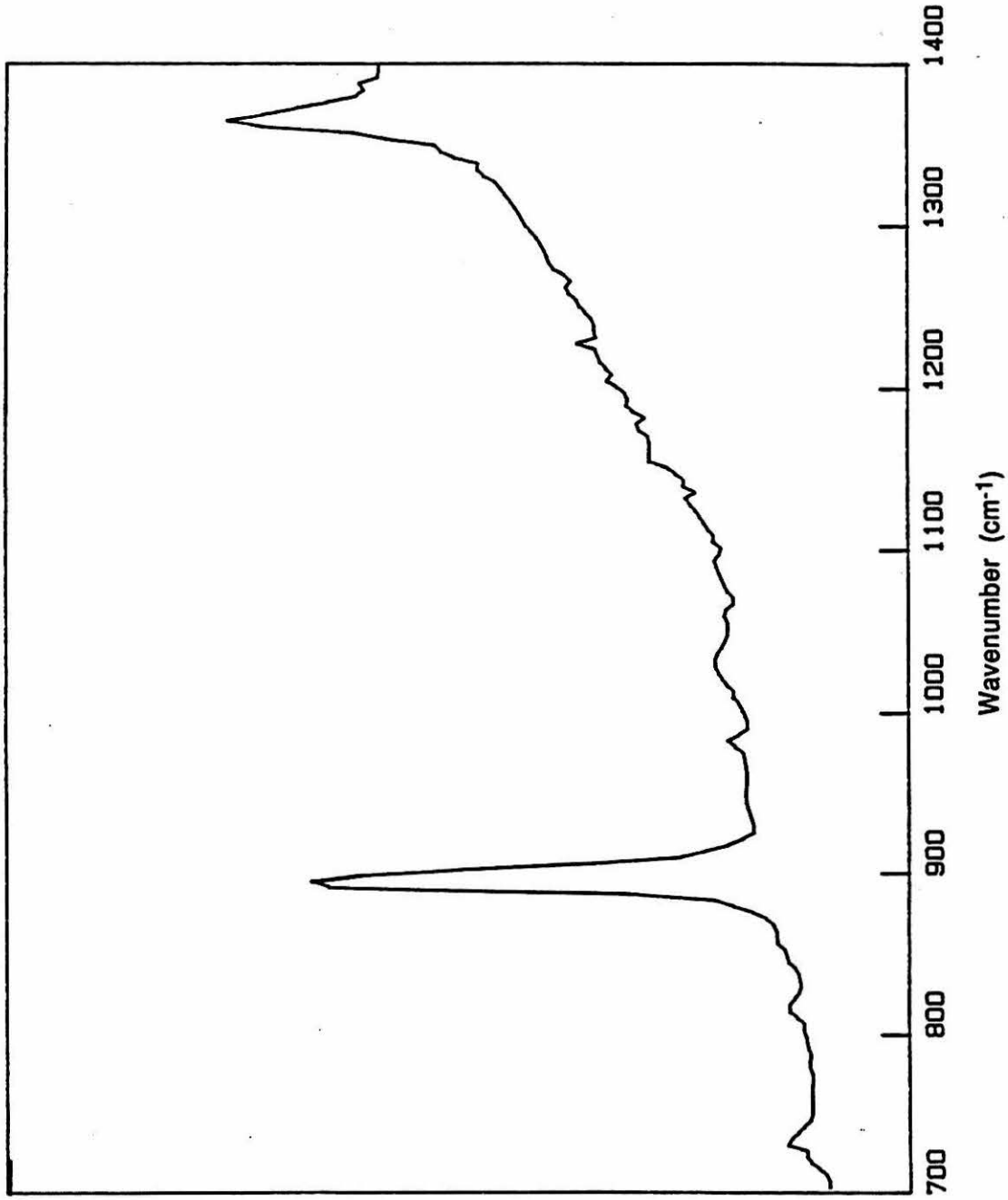
700
800
900
1000
1100
1200
1300
1400
Wavenumber (cm-1)

Figure 2.5. Cyclic voltammograms of ReO_2^+ in 0.1 M TBAH in (a) CH_3CN and (b) CH_2Cl_2. Scan rate: 200 mV/s.

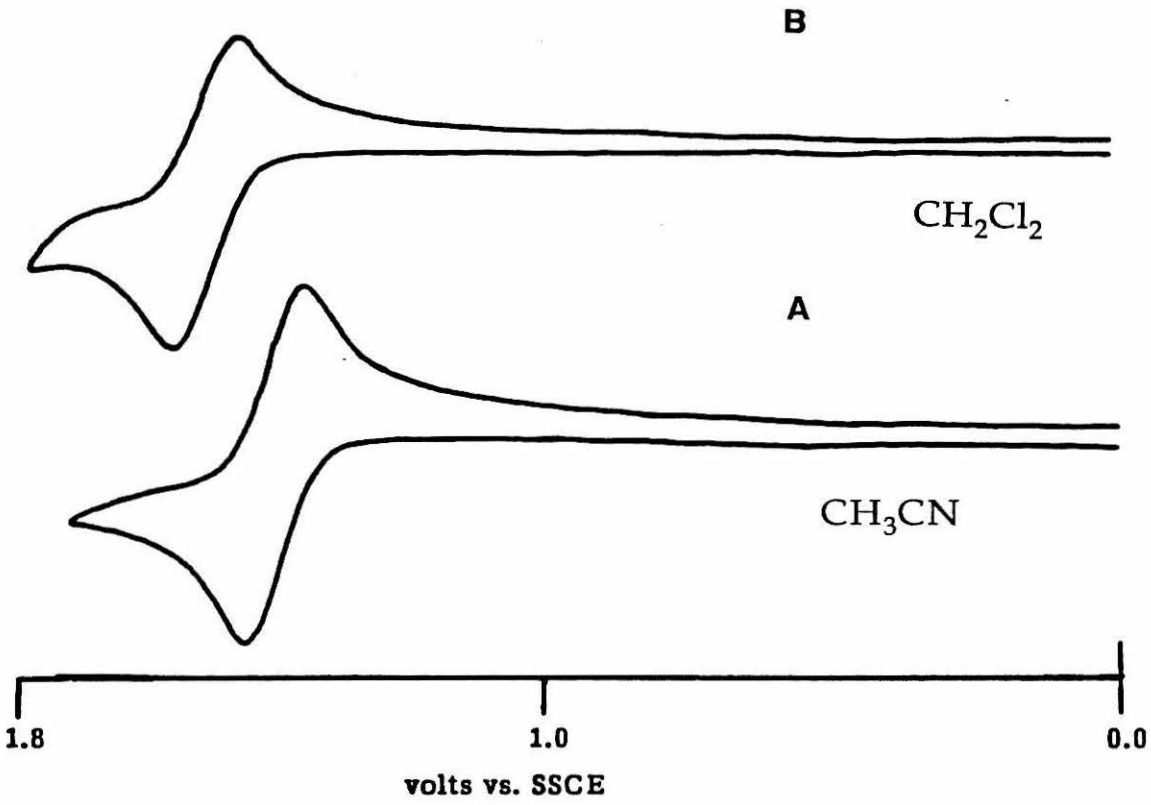
B
CH_2Cl_2
A
CH_3CN
1.8
1.0
0.0
volts vs. SSCE

consists of a single wave at +1.37 V corresponding to this same reversible (ΔE = 60-70 mV, $I_{p,c}/I_{p,a}$ ~1) one-electron oxidation. In dichloromethane solution, however, this wave becomes only quasi-reversible (Figure 2.5b, ΔE ~100 mV, $I_{p,c}/I_{p,a} < 1$), a point that will be discussed later.

Using the emission maximum of ReO_2^+ in acetonitrile as an estimate of $E_{0\text{-}0}(ReO_2^{+*})$, along with the electrochemical data discussed above, the excited state potential can be estimated as shown in equation (1).[3]

$$E(ReO_2^{2+/+*}) = E(ReO_2^{2+/+}) - E_{0\text{-}0}(ReO_2^{+*}) \sim -0.7 \text{ V} \quad (1)$$

Given this potential, reduction of methylviologen (N,N'-dimethyl-4,4'-bipyridinium, MV^{2+}) should be favored by ~0.25 V ($E(MV^{2+/+})$ = -0.45 V).[10] Figure 2.6 shows the Stern-Volmer plot for quenching of ReO_2^{+*} emission by MV^{2+}. From the slope of this plot, a bimolecular quenching rate constant of $k_f = 3.6 \times 10^8\ M^{-1}\ s^{-1}$ can be calculated.

To establish that an electron transfer reaction is responsible for the quenching of the ReO_2^+ emission, time-resolved absorption experiments were performed. Shown in Figure 2.7 is the absorption spectrum of an acetonitrile solution of ReO_2^+ and MV^{2+} obtained 2 μs after laser flash photolysis. The spectrum contains two strong bands at 390 nm and 600 nm that are attributable to the MV^+ radical.[18a] The bleaching at 330 nm is due to ReO_2^{2+} but is not as pronounced as that for ReO_2^{+*}.

The dynamics of the transient species produced in the electron transfer reaction also were investigated. The rate of MV^+ production determined by the appearance of the transient absorption signals at 390 nm and 605 nm was first order and agreed with the rate calculated from the rate constant for Stern-Volmer emission quenching. The decay trace at 330 nm shows a decrease in bleaching from an initial level due to ReO_2^{+*} to a lower level due to ReO_2^{2+}. This decay is first order and proceeds at the same rate as the

Figure 2.6. Stern-Volmer plot for the quenching of the ReO_2^{+*} emission lifetime by MV^{2+}.

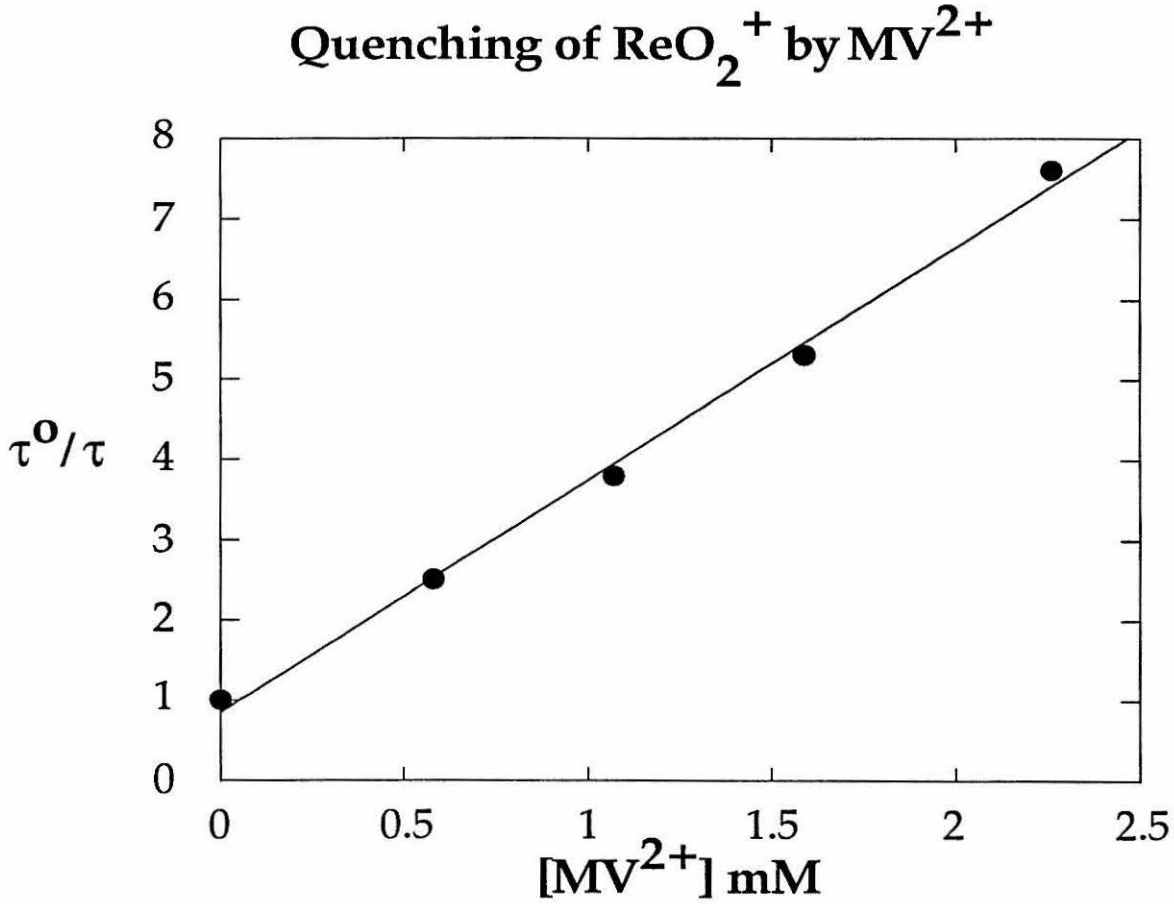
Quenching of ReO_2^+ by MV^{2+}
τ^o/τ
0
1
2
3
4
5
6
7
8
0
0.5
1
1.5
2
2.5
$[MV^{2+}]$ mM

Figure 2.7. Absorption spectrum of a CH_3CN solution of ReO_2^+ and MV^{2+} taken 2 μs after 308 nm excitation.

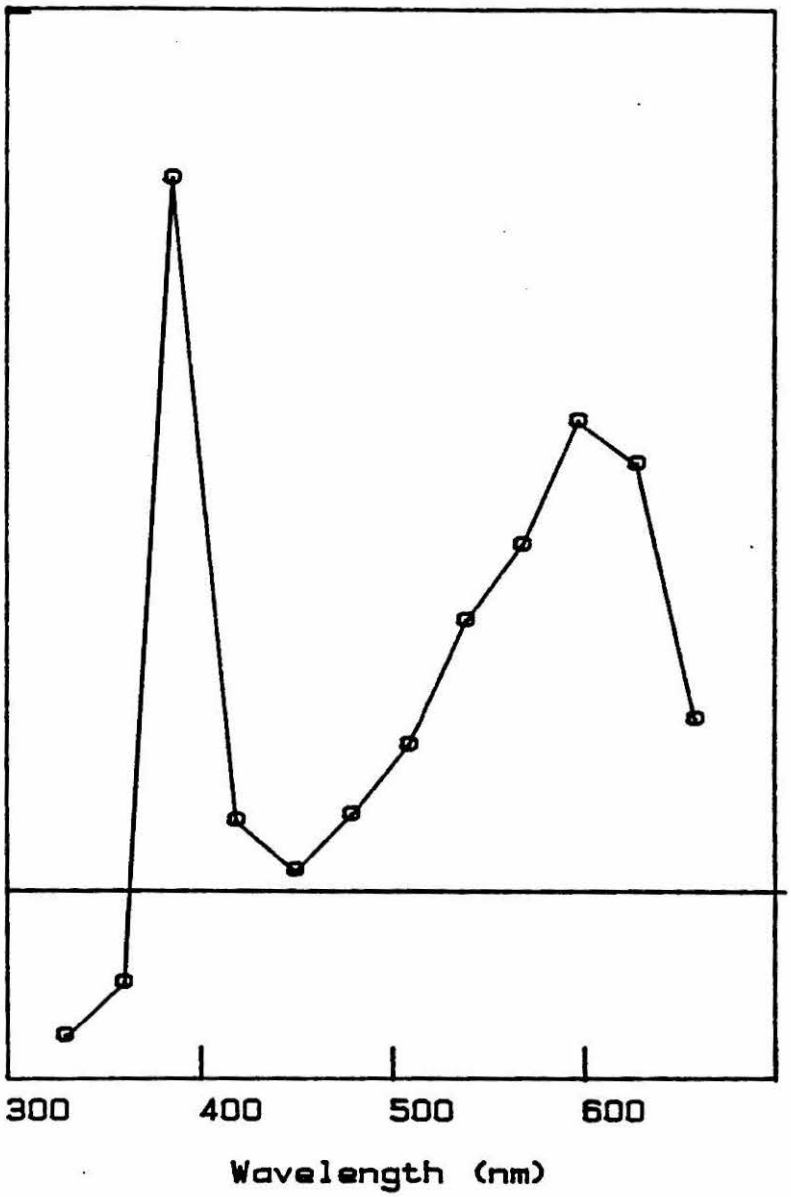
300
400
500
600
Wavelength (nm)

increase in absorption due to MV^+. The disappearance of the MV^+ signal at 605 nm was second-order, and least squares fitting of a $1/[MV^+]$ plot (Figure 2.8) using the procedure of Marshall[10,18b] gave a bimolecular rate constant for charge recombination of $k_b = 2.1 \times 10^{10}\ M^{-1}\ s^{-1}$. This corresponds to the diffusion-controlled limit in acetonitrile calculated by the method of Meyer et al.[19] The extremely efficient recombination is due to the large (~1.82 V) driving force for back electron transfer in this system. In addition, k_b also was determined from the MV^+ signal at 390 nm and the ReO_2^{2+} ground state bleach at 330 nm. Each of these rate constants were within experimental error of the k_b determined at 605 nm, indicating that excited-state electron transfer in this solvent is completely reversible.

The excited state of ReO_2^+ also efficiently reduces other electron acceptors (Table 2.1). The rate constants show that the excited state reduction potential of -0.7 V estimated from emission and electrochemical measurements is quite reasonable.[3,19] Further, k_b was estimated for 4-cyano-N-benzylpyridinium, 4-cyano-N-methylpyridinium, and 4-carbomethoxy-N-methylpyridinium. The rate constants in all of these cases were diffusion-controlled with driving forces greater than 2.0 V. Again, reversibility was verified by comparing the rate constant determined from the pyridinium radical absorption with the rate constant determined from the ReO_2^+ ground state bleach.

Reactivity of ReO_2^{2+}. As shown in Figure 2.5, the oxidation of ReO_2^+ in acetonitrile is reversible on the cyclic voltammetry time scale. This reversibility is supported by the transient absorption experiments. In CH_2Cl_2, however, the cyclic voltammogram exhibits only a quasi-reversible oxidation wave. Analysis of the scan-rate dependence of this wave[20] indicates that an EC mechanism is operating with a chemical reaction rate of $0.04 \pm 0.01\ s^{-1}$.

Figure 2.8. Plot of $1/\Delta A$ at 605 nm vs. time for the back-electron transfer reaction between ReO_2^{2+} and MV^+.

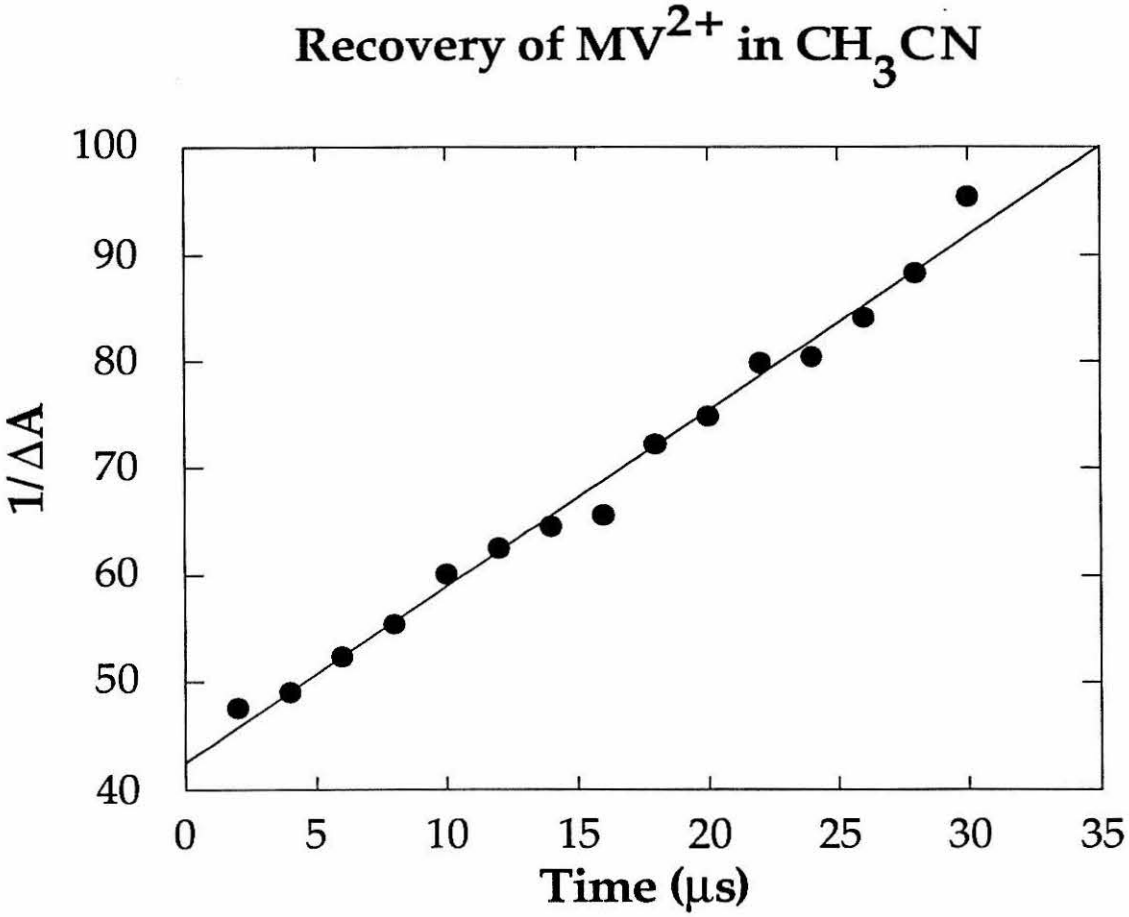
Recovery of MV^{2+} in CH_3CN
100
90
80
70
60
50
40
1/ΔA
0
5
10
15
20
25
30
35
Time (μs)

Table 2.1.

Bimolecular Electron Transfer Rate Constants from Stern-Volmer Quenching of the Emission Lifetime of ReO_2^{+*}.

Q	$E_{1/2}(Q^{+/0})$[a]	k_f (M^{-1} s^{-1})
tetracyanoethylene	+0.24	9.0×10^9
N,N'-propylene-1,10-phenanthrolinium	-0.27	4.5×10^8
N,N'-dimethyl-4,4'-bipyridinium	-0.45	3.6×10^8
4-cyano-N-benzylpyridinium	-0.59	2.6×10^8
4-cyano-N-methylpyridinium	-0.67	1.1×10^8
4-carbomethoxy-N-methylpyridinium	-0.78	1.1×10^7
4-amido-N-ethylpyridinium	-0.93	4.1×10^6

[a]References 5 and 10.

Steady-state photolysis of CH_2Cl_2 solutions of ReO_2^+ and MV^{2+} at $\lambda > 450$ nm leads to net production of MV^+ (Figure 2.9), thereby indicating that ReO_2^{2+} is reacting with CH_2Cl_2 in competition with back electron transfer, allowing MV^+ to accumulate. Photolysis of ReO_2^+ and MV^{2+} in THF also led to production of MV^+; however, no absorption changes were observed after 24 h of irradiation of ReO_2^+ and MV^{2+} in CH_3CN.

The oxidized species, ReO_2^{2+}, also reacts with other organic substrates. Shown in Figure 2.10a is the oxidation wave of ReO_2^+ with increasing amounts of tribenzylsilane ($(PhCH_2)_3SiH$) added to the CH_3CN solution. The silane reacts with ReO_2^{2+}, producing an oxidation wave that becomes increasingly irreversible with addition of $(PhCH_2)_3SiH$. Figure 2.10b shows the same experiment performed with a secondary alcohol, *sec*-phenethyl alcohol ($PhCH(OH)CH_3$), as the substrate.

Bulk electrolysis of degassed CH_3CN solutions of ReO_2^+ containing $PhCH(OH)CH_3$ was performed at $E > 1.5$ V (SSCE). The electrolysis was run for 3 turnovers based on the one-electron oxidation of ReO_2^+. Analysis of the organic products by UV spectroscopy showed that $PhCH(OH)CH_3$ is converted to acetophenone. By monitoring the intense ketone π-π^* absorption,[21] a current efficiency of 90 ± 5 % for conversion of the alcohol to the ketone (a two-electron process) was determined.

Oxidation Mechanism. A key question is whether a ReO_2^+-alcohol complex is formed prior to oxidation of the metal complex. Hydrogen bonding was proposed originally to explain the quenching of ReO_2^+ emission by molecules containing hydroxylic protons.[8] Figure 2.11a shows the proton NMR spectrum of 1-propanol in acetonitrile that contains sharp quartet and triplet resonances between 3 and 4 ppm that are due to the α-CH_2 and OH protons, respectively. Upon the addition of « 1 equivalent of ReO_2^+ these

Figure 2.9. Absorption spectra taken at 15 min. intervals during steady-state photolysis of ReO_2^+ and MV^{2+} in CH_2Cl_2.

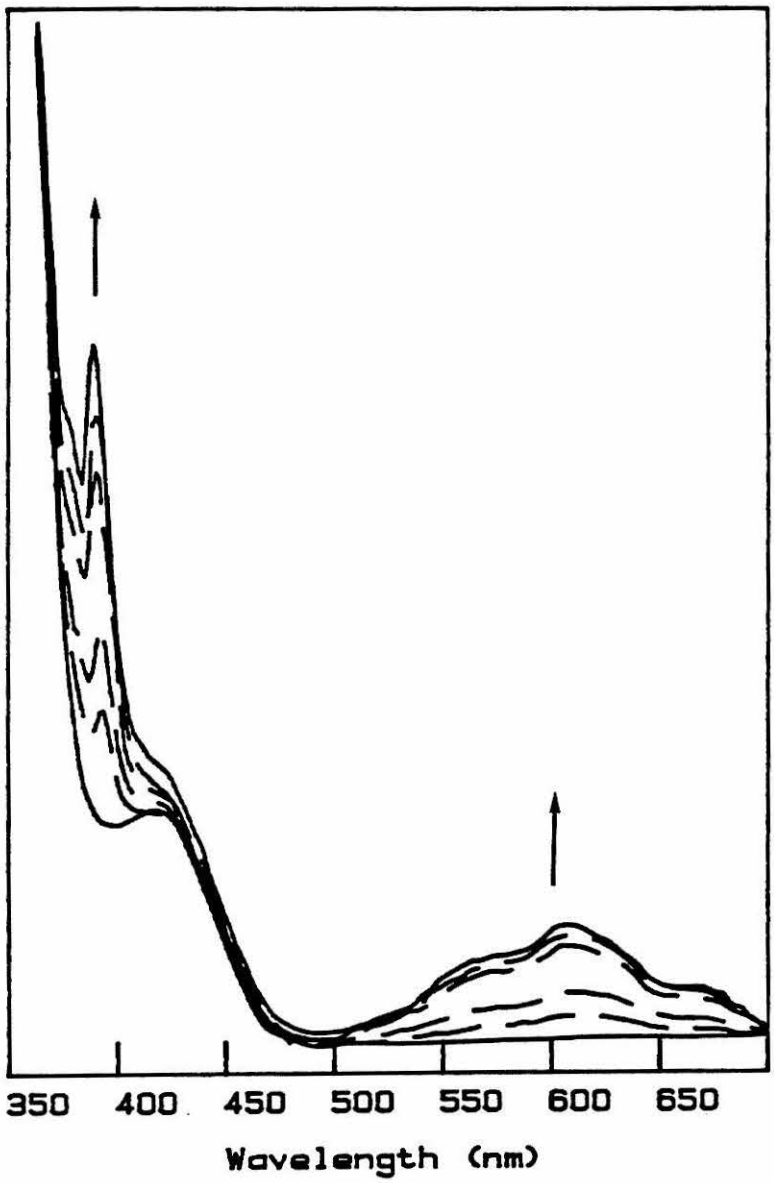
350
400
450
500
550
600
650
Wavelength (nm)

Figure 2.10. Cyclic voltammograms of ReO_2^+ in CH_3CN with increasing amounts of added (a) $(PhCH_2)_3SiH$ and (b) $PhCH(OH)CH_3$.

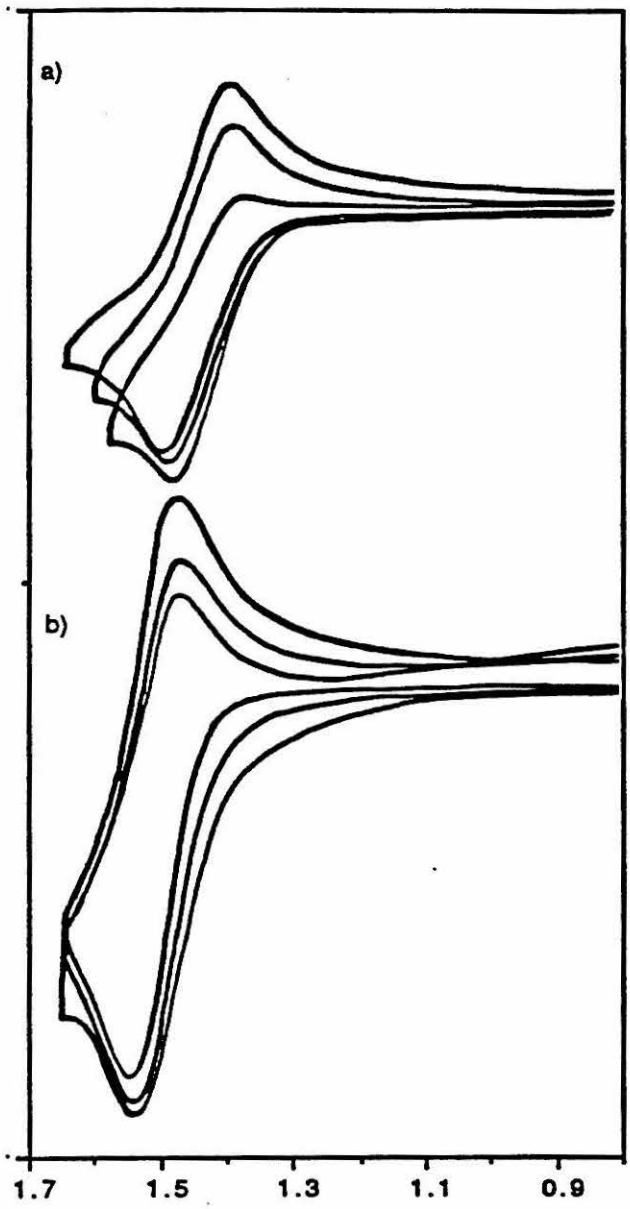
a)
b)
1.7
1.5
1.3
1.1
0.9
V(SSCE)

Figure 2.11. Proton NMR spectra of (a) 1-propanol in CD_3CN and (b) 1-propanol in CD_3CN with « 1 equivalent of ReO_2^+ added to the solution.

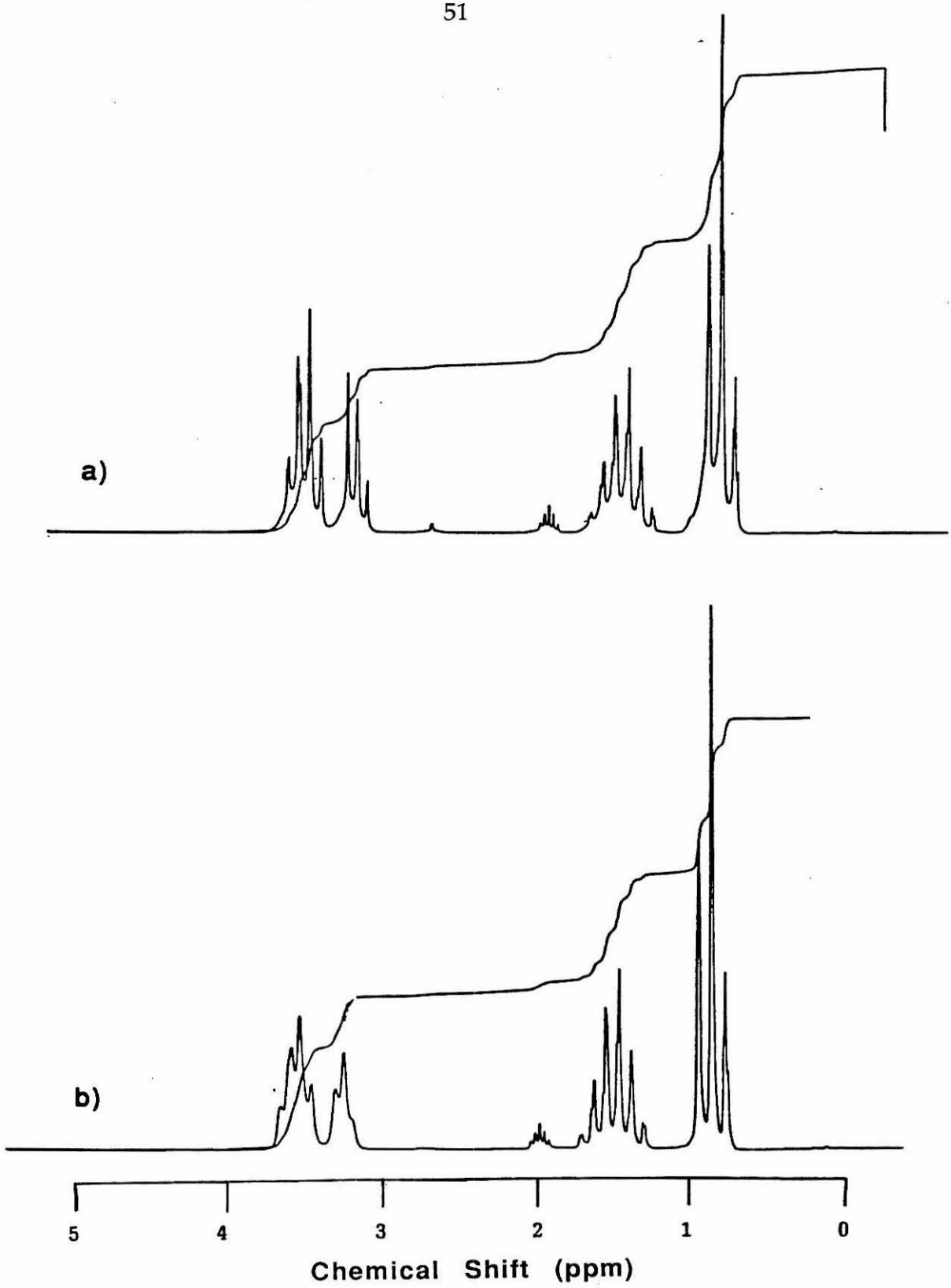
a)
b)
5
4
3
2
1
0
Chemical Shift (ppm)

resonances become dramatically broadened, strongly indicating that some type of complex has been formed. Similar observations have been made by Fox et al., in polyoxotungstate systems.[22]

We also have observed similar effects with the $PhCH(OH)CH_3$ substrate. Figure 2.12a shows the proton NMR spectrum of *sec*-phenethyl alcohol in CH_3CN. The hydroxyl proton resonance appears as a doublet centered at 3.4 ppm. The α-methyne proton resonance centered at 4.8 ppm is a quartet of doublets due to coupling to the three protons of the terminal methyl group and to the hydroxyl proton. Upon addition of ~10^{-3} equivalents of ReO_2^+ (Figure 2.12b), the hydroxyl proton resonance is observed to broaden and become decoupled from the α-methyne proton resonance, which now appears as a clean quartet due to coupling only to the terminal methyl protons. This observation is taken as strong evidence for complex formation between the hydroxyl proton and ReO_2^+.

The metal-containing species present after catalytic activity has ceased is currently uncharacterized. The resulting solution is colorless, suggesting that ReO_4^- might be the deactivation product. This is ruled out, however, by cyclic voltammograms that show a single irreversible reduction wave at -0.8 V, much less than the reduction potential for ReO_4^-.[23] Synthesis aimed at lowering the oxidation potential for ReO_2^+ should lead to a catalyst that is active at lower potentials.[16] Tuning of the potential so that activity is retained while the absolute potential is minimized may lead to smoother substrate oxidation.

It is likely that ReO_2^{2+} abstracts a hydrogen atom from substrate in the initial step of oxidation. One resonance form of ReO_2^{2+} is a $Re(d^2)$ bonded to an oxo radical (Figure 2.13), a structure that resembles a carbonyl n,π^* excited state. Recall that n,π^* states efficiently abstract hydrogen atoms from many

Figure 2.12. Proton NMR spectra (TMS reference) of (a) *sec*-phenethyl alcohol in CD_3CN and (b) *sec*-phenethyl alcohol in CD_3CN with ~10^{-3} equivalents of ReO_2^+ added to the solution.

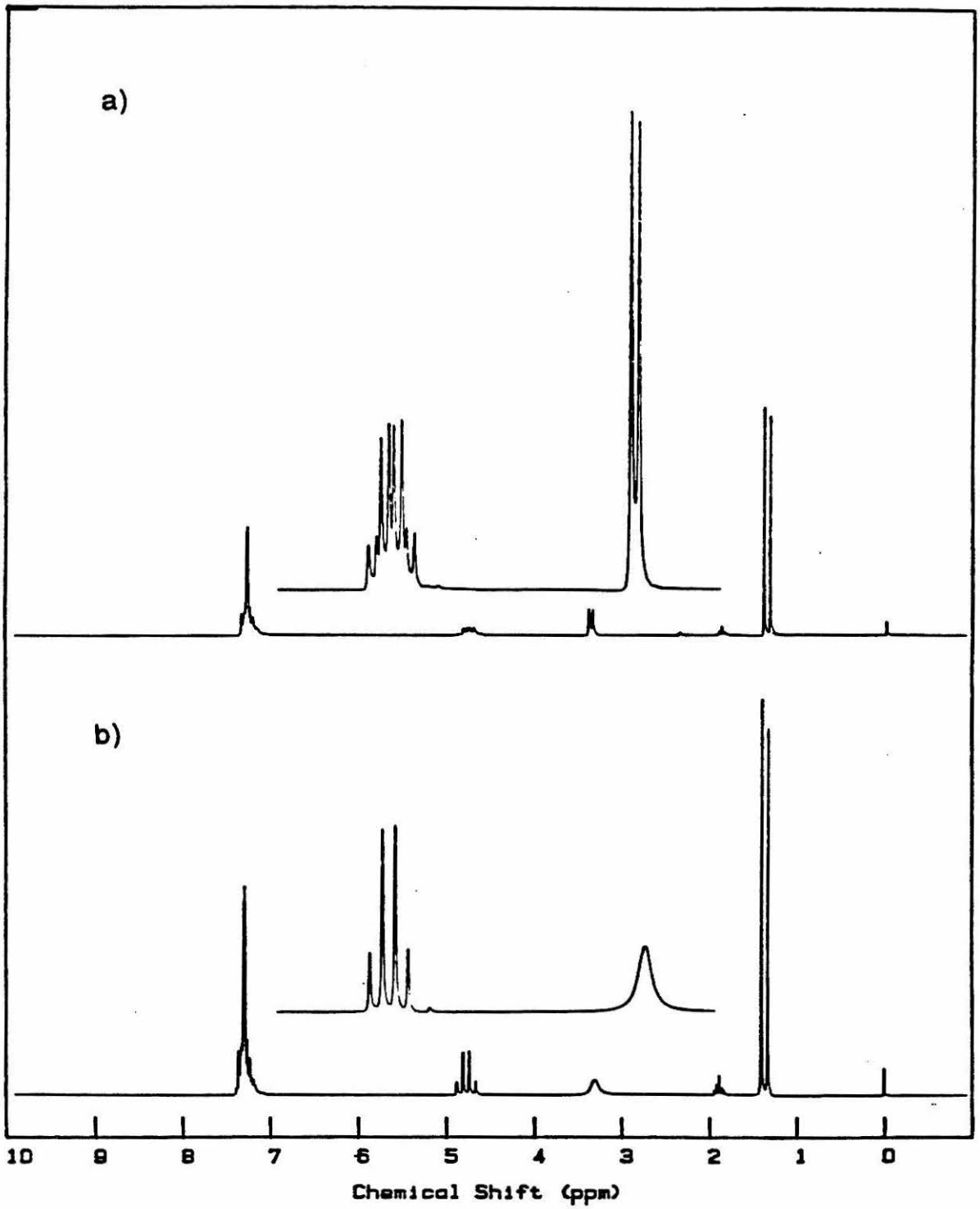
a)
b)
10
9
8
7
6
5
4
3
2
1
0
Chemical Shift (ppm)

Figure 2.13. Scheme showing a potential mechanism for the H-atom abstraction reactivity of ReO_2^{2+}.

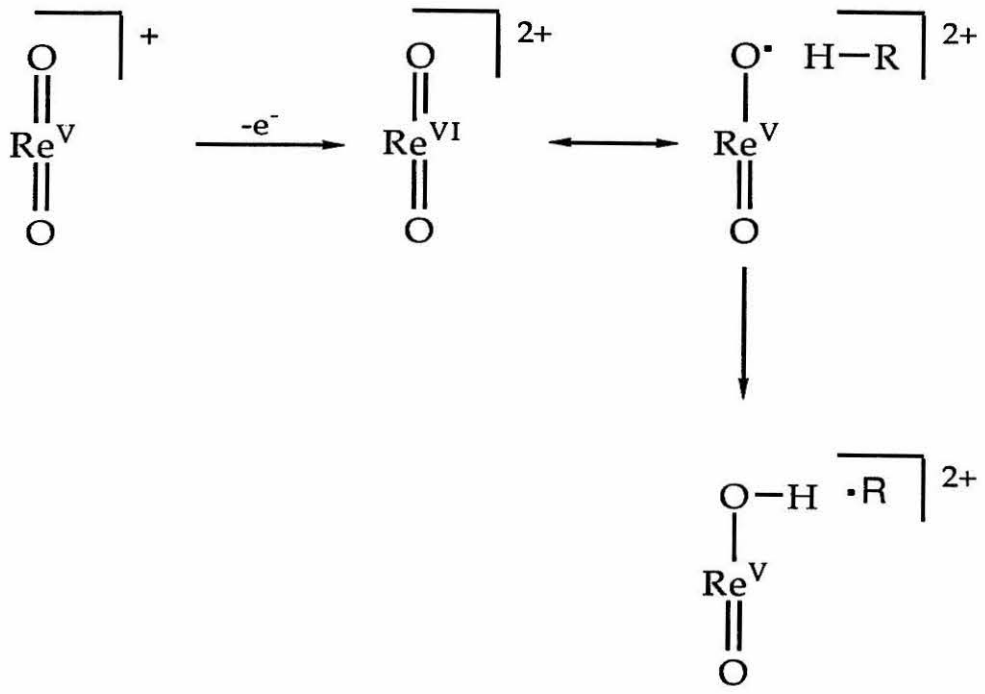
+
O
Re V
O
-e-
2+
O
Re VI
O
O·
H—R
2+
Re V
O
O—H
·R
2+
Re V
O

types of substrates,[21] and Ru(IV) monooxo and Ru(VI) and Os(VI) dioxo complexes undergo the same types of conversions stoichiometrically by H-atom abstraction.[7,24,25] The fact that greater than stoichiometric amounts of organic product have been observed under electrolysis conditions indicates that it would be fruitful to search for novel photocatalytic H-atom abstraction reactions that could be initiated by electron transfer from ReO_2^{+*} complexes.

Conclusions

These findings illustrate a number of potentially important trends in metal-oxo complexes. The photophysics of ReO_2^+ and OsO_2^{2+} are quite similar;[7] however, their redox properties and resulting excited state chemistry are quite distinct. The osmium complex is a powerful (> 2 V vs. NHE) excited state oxidant owing to the relative stability of Os(V). In striking contrast, Re(IV) is unobservable in our system and it is Re(VI) that is actually accessible. The ReO_2^+ complex is therefore a weak excited state reductant as shown in Figure 2.14. It is noteworthy that the observed redox couple for each system is VI/V regardless of the number of d-electrons involved.

The importance of these observations is evident in the reactivity of ReO_2^+. In the iron family complexes,[7,24,25] reactivity similar to carbonyl excited states[21] is observed with Ru(IV), Ru(VI) and Os(VI) as stated in Chapter 1 of this thesis. In terms of the mechanism of Figure 2.13, this implies that the oxo radical intermediates of Ru(III), Ru(V) and Os(V) are thermally (or photochemically) accessible. This is clearly not the case for the analogous Re(IV) species. Oxidation of ReO_2^+ to Re(VI) creates a thermally accessible oxo radical state on Re(V), a very stable oxidation state. This permits H-atom abstraction reactions such as alcohol oxidation to occur.

This work has far-reaching consequences for the design of photoredox catalysts. Clearly, excited state electron transfer is a powerful method for

Figure 2.14. Modified Latimer diagram for ReO_2^+.

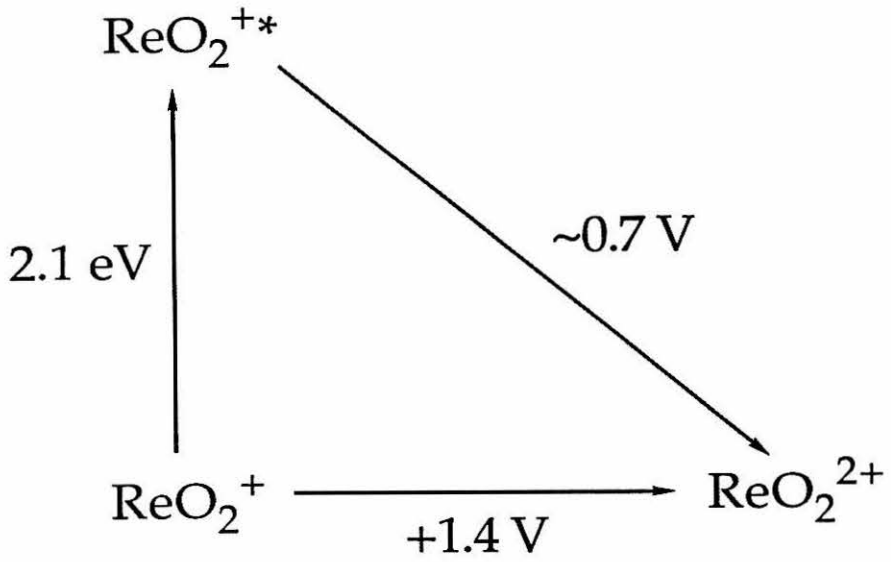
ReO_2^{+*}
2.1 eV
~0.7 V
ReO_2^{+}
+1.4 V
ReO_2^{2+}

activating stable catalysts. This energy can be harvested more effectively, however, when the catalyst has a reactive site such as an oxo ligand that has been activated by the redox event. In particular, the extremely stable oxo ligands of ReO_2^+ acquire oxo radical reactivity upon complex oxidation. In contrast, storage of a comparable amount of energy in $Ru(bpy)_3^{2+}$ does not lead to bond-breaking or bond-making chemistry[1] because there is no potentially reactive site in the metal complex. It is thereby fruitful to search for excited states capable of performing redox reactions that lead to an activated metal complex with a potentially reactive functionality.

References

1. a) Kalyanasundaram, K. *Coord. Chem. Rev.* **1982**, *46*, 159. b) Meyer, T.J. *Pure and Appl. Chem.* **1986**, *58*, 1193. c) Krause, R.A. *Struct. and Bonding* **1987**, *67*, 1.

2. Lees, A.J. *Chem. Rev.* **1987**, *87*, 711.

3. Balzani, V.; Bolletta, F.; Scandola, F.; Ballardini, R. *Pure and Appl. Chem.* **1979**, *51*, 229.

4. Maverick, A.M.; Gray, H.B. *Pure Appl. Chem.* **1980**, *52*, 2339.

5. Kavarnos, G.J.; Turro, N.J. *Chem. Rev.* **1986**, *86*, 401.

6. a) Vlcek, A.A.; Gray, H.B. *J. Am. Chem. Soc.* **1987**, *109*, 286. b) Vlcek, A.A., Jr.; Gray, H.B. *Inorg. Chem.* **1987**, *26*, 1997. c) Harvey, E.L.; Stiegman, A.E.; Vlcek, A.A., Jr.; Gray, H.B. *J. Am. Chem. Soc.* **1987**, *109*, 5233.

7. a) Che, C.-M.; Yam, V.W.-W.; Cho, K.C.; Gray, H.B. *J. Chem. Soc., Chem. Commun.* **1987**, 948. b) Yam, V.W.-W.; Che, C.-M.; Tang, W.-T. *J. Chem. Soc., Chem. Commun.* **1988**, 100.

8. Winkler, J.R.; Gray, H.B. *Inorg. Chem.* **1985**, *24*, 346.

9. Pipes, D.W.; Meyer, T.J. *Inorg. Chem.* **1986**, *25*, 3256.

10. Marshall, J.L., Ph.D. Thesis, California Institute of Technology, Pasadena, CA, **1986**.

11. Beard, J.H.; Casey, J.; Murmann, K.R. *Inorg. Chem.* **1965**, *4*, 797.

12. Kumar, C.V.; Barton, J.K.; Gould, I.R.; Turro, N.J.; Van Houten, J. *Inorg. Chem.* **1988**, *27*, 648.

13. Rice, S.F.; Gray, H.B. *J. Am. Chem. Soc.* **1983**, *105*, 4571.

14. Nocera, D.G.; Winkler, J.R.; Yocum, K.M.; Bordignon, E.; Gray, H.B. *J. Am. Chem. Soc.* **1984**, *106*, 5145.

15. Marshall, J.L.; Hopkins, M.D.; Gray, H.B. *ACS Symp. Ser.* **1987**, *357*, 254.

16. Brewer, J.C.; Gray, H.B. *Inorg. Chem.* submitted for publication.

17. Newsham, M.D.; Giannelis, E.P.; Pinnavaia, T.J.; Nocera, D.G. *J. Am. Chem. Soc.* **1988**, *110*, 3885.

18. a) Kosower, E.M.; Cotter, J.L. *J. Am. Chem. Soc.* **1964**, *86*, 5524. b) Marshall, J.L.; Stobart, S.R.; Gray, H.B. *J. Am. Chem. Soc.* **1984**, *106*, 3027.

19. Bock, C.R.; Connor, J.A.; Gutierrez, A.R.; Meyer, T.J.; Whitten, D.G.; Sullivan, B.P.; Nagle, J.K. *J. Am. Chem. Soc.* **1979**, *101*, 4815.

20. a) Schwarz, W.M.; Shain, I. *J. Phys. Chem.* **1966**, *70*, 845. b) Nicholson, R.S. *Anal. Chem.* **1965**, *37*, 1351. c) Nicholson, R.S.; Shain, I. *Anal. Chem.* **1964**, *36*, 706.

21. Turro, N.J., "Modern Molecular Photochemistry," Benjamin Cummings, Menlo Park, CA, **1978**.

22. Fox, M.A.; Cardona, R.; Gaillard, E. *J. Am. Chem. Soc.* **1987**, *109*, 6347.

23. Astheimer, L.; Schwochau, K. *J. Inorg. Nucl. Chem.* **1976**, *38*, 1131.

24. a) Thompson, M.S.; DeGiovani, W.F.; Moyer, B.A.; Meyer, T.J. *J. Org. Chem.* **1984**, *49*, 4972. b) Dobson, J.C.; Seok, W.K.; Meyer, T.J. *Inorg. Chem.* **1986**, *25*, 1514.

25. Marmion, M.E.; Takeuchi, K.J. *J. Am. Chem. Soc.* **1988**, *110*, 1472.

26. The bulk of this chapter has been published: Thorp, H.H.; Van Houten, J.; Gray, H.B. *Inorg. Chem.* **1989**, *28*, 889.

Chapter 3.

Emission Properties of d^2 Transdioxo Complexes in Aqueous Solutions of Anionic and Nonionic Surfactants: A Sensitive Probe of Hydrophobic Binding Regions.

The photochemistry of small guest molecules included in microheterogeneous environments is an area of continuing interest in biomimetic chemistry.[1] Transition metal complexes are attractive candidates for inclusion in these environments because of the diversity of their photophysics and redox properties.[2] The two-fold purpose of this research is to probe the structure and dynamics of the environment using novel properties of the guest molecule and to develop new photochemistry of the guest molecule through the use of a novel environment.[3] The transdioxo Re(V) complex, $ReO_2(py)_4^+$, abbreviated hereafter as ReO_2^+, is a potentially sensitive probe of interfacial regions of microheterogeneous environments because its emission lifetime varies over four orders of magnitude upon shifting from aqueous to increasingly nonaqueous regions. The Re(V) complex can be oxidized photochemically to $Re(VI)O_2(py)_4^{2+}$, and this Re(VI) complex is reactive towards a number of organic substrates.[4]

In order to develop fully the microheterogeneous photochemistry of ReO_2^+, we have studied its emission properties in aqueous solutions of anionic and neutral surfactants. A model for cationic metal complexes in anionic surfactant solutions has been developed through numerous detailed investigations involving $Ru(bpy)_3^{2+}$ (bpy = 2,2'-bipyridine).[5] Because the emission lifetime of $Ru(bpy)_3^{2+}$ is not strongly dependent on the aqueous character of its environment, bimolecular quenching experiments were employed to develop this model.[6-8] We will show that a similar model can be developed for ReO_2^+ by varying surfactant concentration, H_2O/D_2O ratio, incident laser power, and ionic strength.

Previous work with $Ru(bpy)_3^{2+}$ and sodium dodecyl sulfate (SDS) has shown that a number of different interactions between cationic metal complexes and anionic surfactants can occur. At very low surfactant

concentration, insoluble dodecyl sulfate (DS^-) salts can precipitate (Figure 3.1, **1**).[9] Above the critical micellar concentration (cmc(SDS) = 8.1 mM), these salts are solubilized by the anionic micelles (**2**).[6,7,9] At intermediate concentrations below the cmc (3 - 6 mM), clusters have been shown to form that resemble very diffuse inverse micelles with one or more $Ru(bpy)_3^{2+}$ cations in the center (**3**).[8] Based on our data, we propose that ReO_2^+ obeys the model shown in Figure 3.1. This model is consistent with similar $Ru(bpy)_3^{2+}$ schemes, and we have been able to show for the first time that extramicellar clusters (**3**) persist at surfactant concentrations well above the cmc.

Dioxorhenium(V) and SDS

NMR spectra. The NMR spectra of ReO_2^+ in micellar D_2O solutions of SDS are typical for complexes bound to aqueous micelles.[9c-f] The spectra in Figure 3.2 show two important characteristic changes. First, the signal arising from the surfactant protons on the carbon that is α to the sulfonate group is shifted from δ = 3.90 ppm (Figure 3.2b) to δ = 3.85 ppm (Figure 3.2c). This indicates that ReO_2^+ is residing near the α-carbon, most probably near the sulfonate/water interface. The second change in the spectrum is a shift of the pyridine α-proton resonance from δ = 8.71 ppm (Figure 3.2a) to δ = 8.87 ppm (Figure 3.2c). This shift increases monotonically as ReO_2^+ is added to the solution (Figure 3.3). This shift is observed for free pyridine as well as for the metal complex, indicating that this effect is not unique to ReO_2^+. Thus, this NMR shift serves as a potentially useful environmental marker that is not coupled to the exquisitely sensitive electronic properties to be discussed below.

Steady-state electronic spectra. The absorption spectrum of ReO_2^+ in aqueous solution exhibits band maxima at 445 (ε 1200) and 331 nm (ε = 19400

Figure 3.1. Model for SDS/ReO_2^+ interactions.

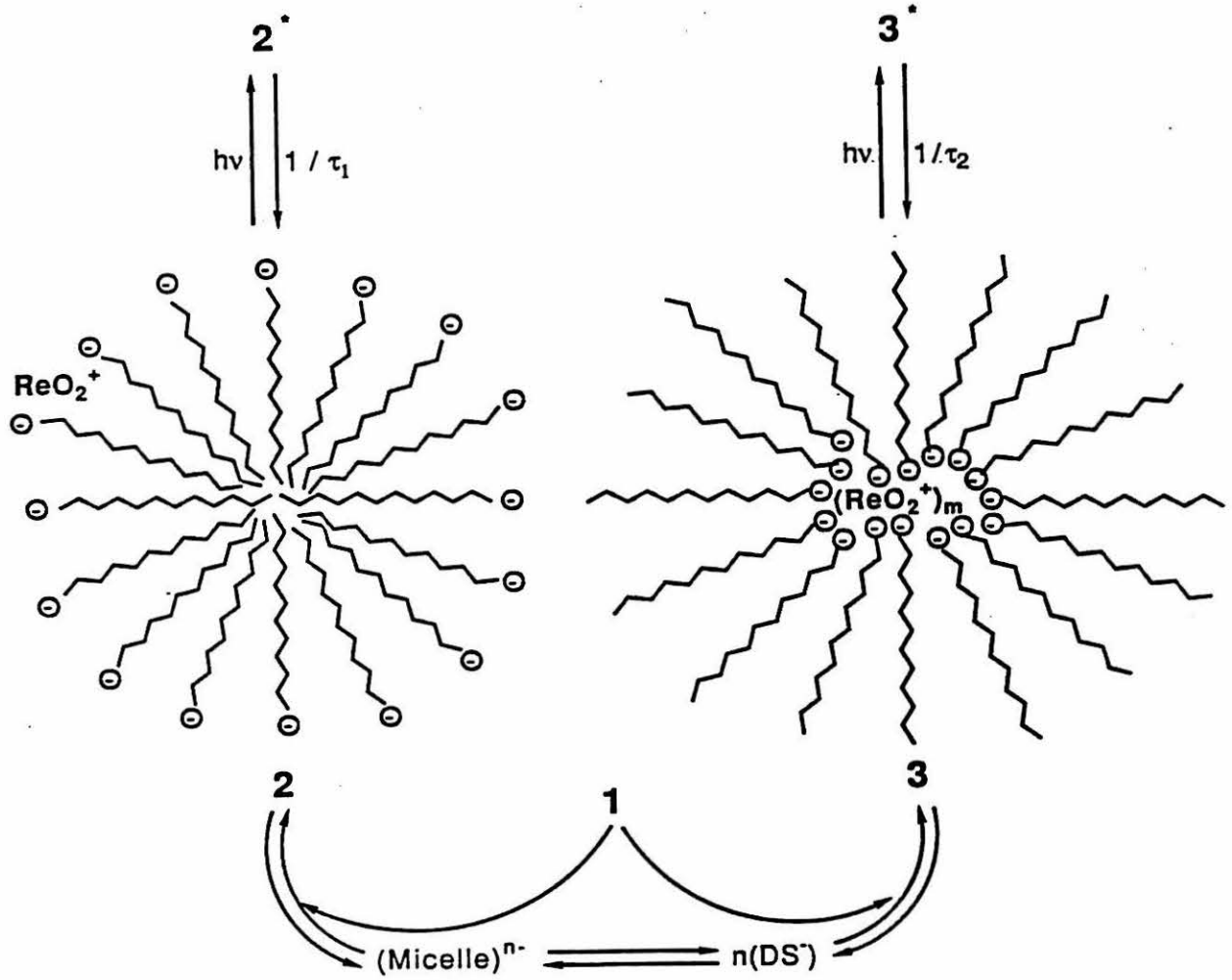

$$ReO_2^+ + DS^- \longrightarrow (ReO_2)(DS)\downarrow$$

1

$DS^- = {}^-OSO_3(CH_2)_{11}CH_3$

Figure 3.2. NMR spectra of (a) ReO_2^+ in D_2O, (b) SDS in D_2O, (c) ReO_2^+ and SDS in D_2O, where the mole fraction of ReO_2^+ relative to SDS is 0.10.

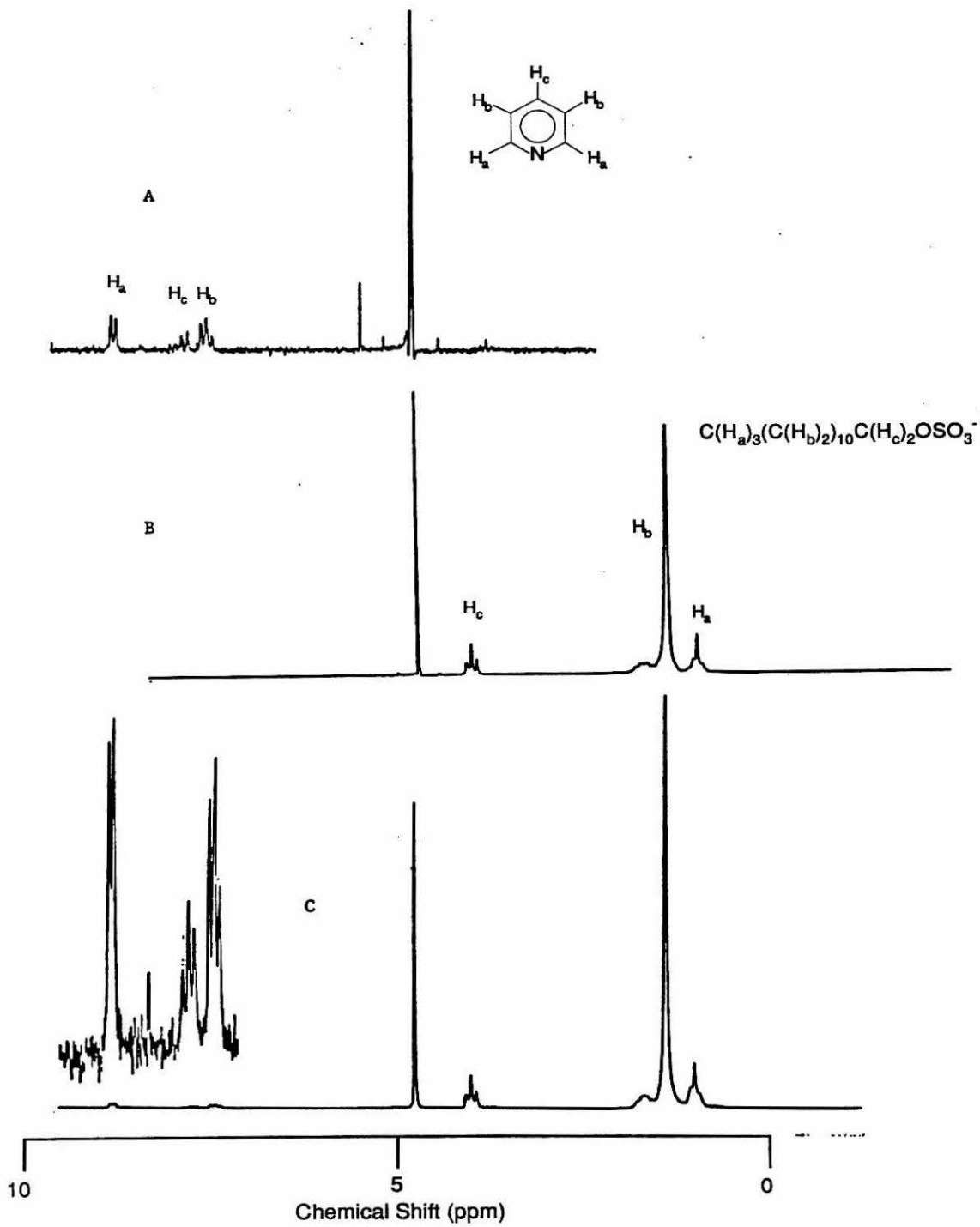
A
B
C
H_a
H_c H_b
H_c
H_b
H_b
H_a
N
H_a
$C(H_a)_3(C(H_b)_2)_{10}C(H_c)_2OSO_3^-$
H_b
H_c
H_a
10
5
0
Chemical Shift (ppm)

Figure 3.3. Plot of the chemical shift of the H_a for ReO_2^+ (see Figure 3.2) versus the mole fraction of ReO_2^+ relative to SDS.

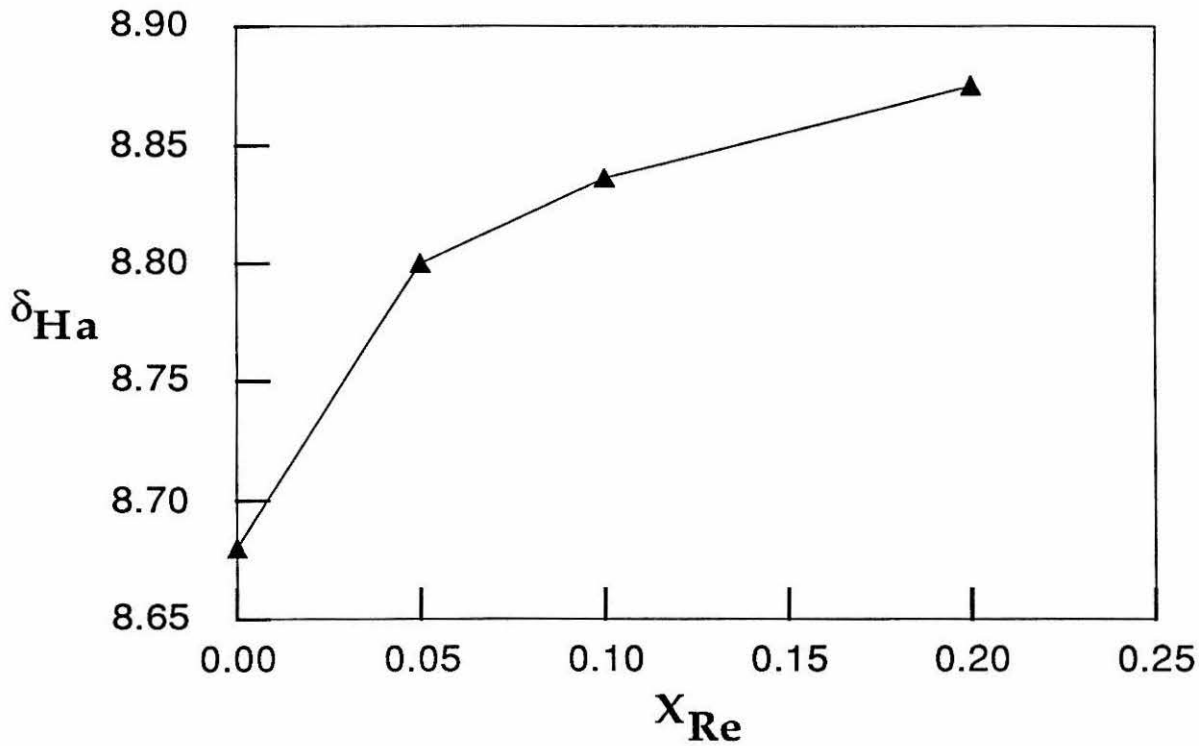
8.90
8.85
8.80
8.75
8.70
8.65
δ_{Ha}
0.00
0.05
0.10
0.15
0.20
0.25
X_{Re}

M^{-1} cm^{-1})[10] (Figure 3.4a). The low-energy band has been assigned[11] to $(d_{xy})^2 \rightarrow (d_{xy})^1(d_{xz,yz})^1$. The intense band at 331 nm is attributable to d(Re) $\rightarrow$ π^*(py) MLCT on the basis of its shift upon protonation of the oxo group.[10] Several experiments in our laboratory support this assignment.[12] The MLCT λ_{max} shifts to lower energy in less-polar solvents (Figure 3.4c).

The energy of the MLCT transition is linearly dependent on the solvent polarity parameter, Z (Figure 3.5).[13] These data correlate equally well with the Gutmann acceptor number,[14] a phenomenon that has been observed frequently for MLCT transitions in other complexes.[15] Figure 3.4b shows that this band also shifts to lower energy upon addition of 20 mM SDS to an aqueous solution of ReO_2^+. This energy can be used to calculate an average polarity of the SDS environment that is between MeOH and EtOH, a result consistent with other measures of the SDS micellar polarity near the interfacial region.[16]

The emission properties of ReO_2^+ were first investigated by Winkler and Gray.[11] The emission spectrum of this complex in nonaqueous solution (Figure 3.6a) is essentially featureless with $\lambda_{max}^{em}(CH_3CN)$ at 640 nm. The lifetime of this emission varies slightly with solvent, ranging from 10-17 μs depending on the nonaqueous medium (Table 3.1). The emission is quenched by protic solvents with a large isotope effect (in pyridine), $k(H_2O)/k(D_2O) = 8.6$; $k_Q(H_2O) = 8.2 \times 10^5$, $k_Q(D_2O) = 9.4 \times 10^5$ M^{-1} s^{-1}.[11b] In neat H_2O or D_2O this emission is quenched completely ($\tau < 10$ ns). Addition of SDS to aqueous solutions of ReO_2^+ leads to emission with λ_{max} at 675 nm (Figure 3.6b); precisely the same behavior is observed in experiments on nonaqueous (pyridine) solutions of ReO_2^+ to which small amounts of H_2O have been added.[11b]

Figure 3.4. Absorption spectra of ~1 mM solutions of $[ReO_2(py)_4]PF_6$ in (a) water (dotted line), (b) 20 mM SDS (solid line) and (c) N,N-dimethylformamide (dashed line).

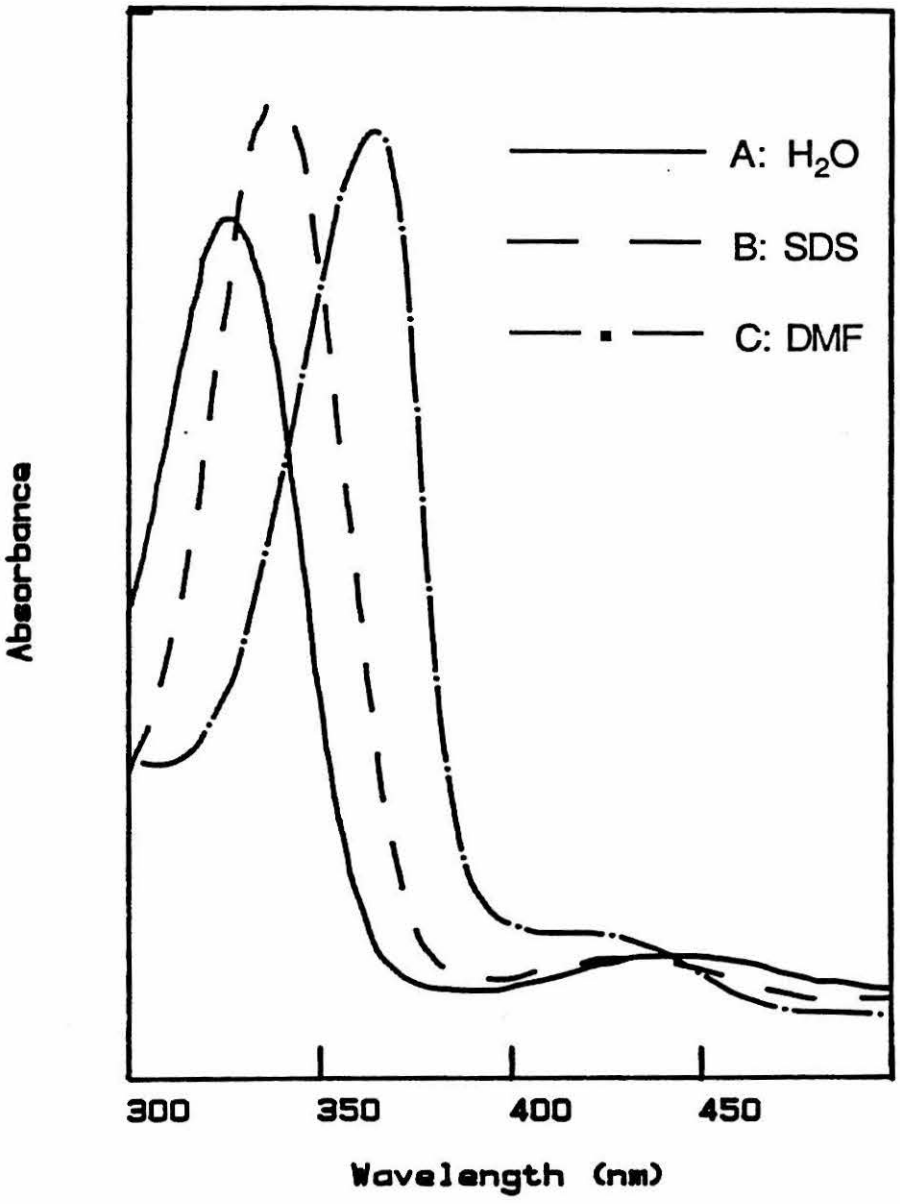
A: H_2O
B: SDS
C: DMF
Absorbance
300
350
400
450
Wavelength (nm)

Figure 3.5. Plot of ReO_2^+ MLCT energy (absorption maximum) vs. the solvent polarity parameter, Z.

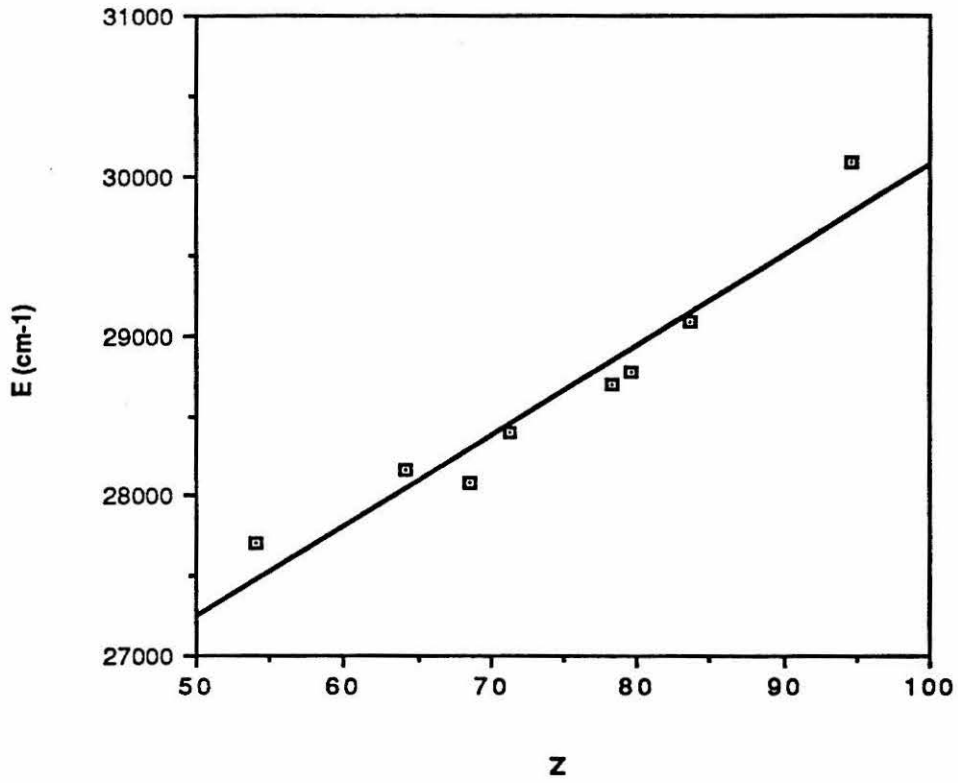
31000
30000
29000
28000
27000
E (cm-1)
50
60
70
80
90
100
Z

Figure 3.6. Uncorrected room-temperature emission spectra of $[ReO_2(py)_4]PF_6$ in (a) acetonitrile solution, (b) 40 mM SDS/H_2O.

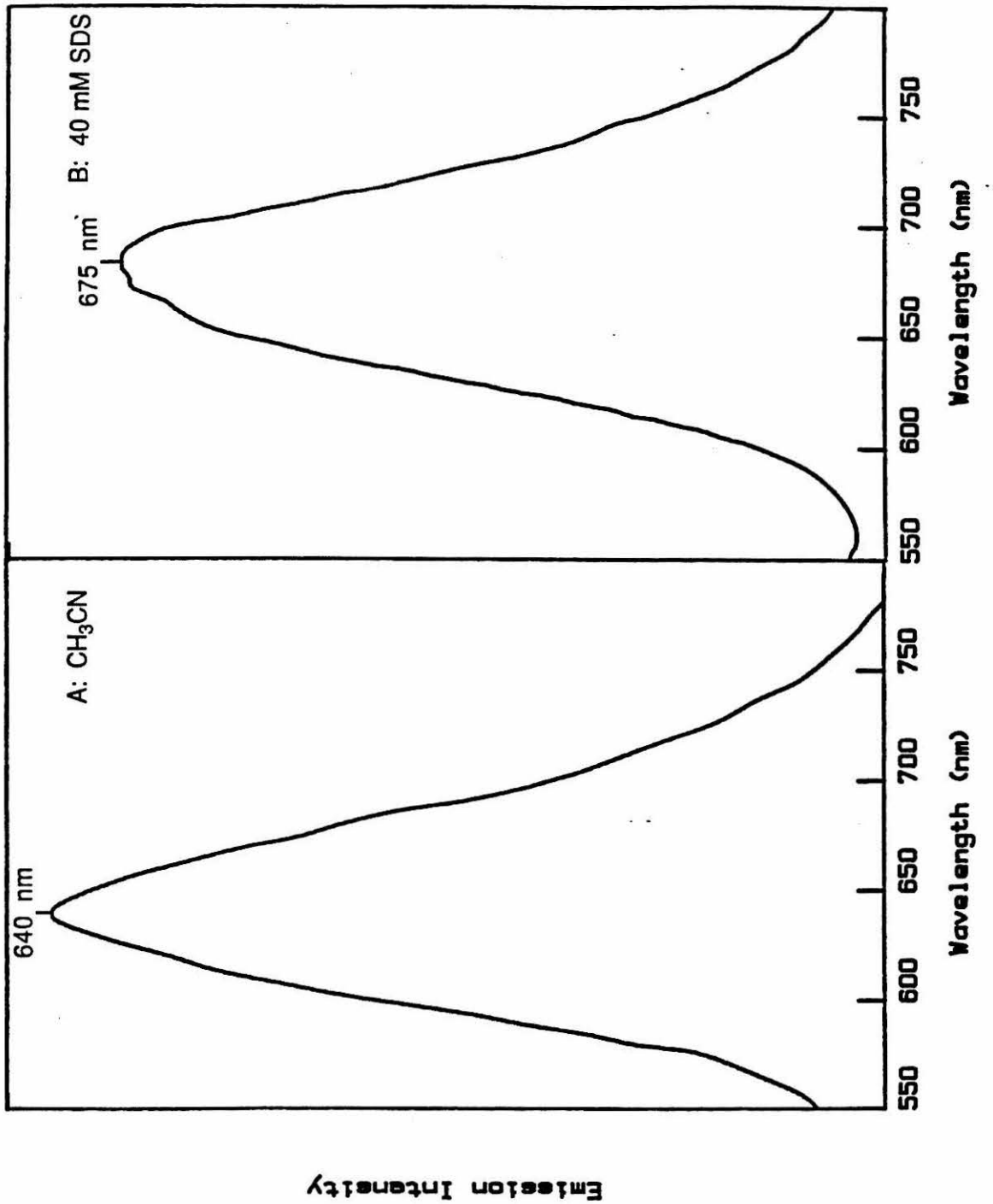
A: CH_3CN
640 nm
B: 40 mM SDS
675 nm
550
600
650
700
750
Wavelength (nm)
Emission Intenseity

Table 3.1.

Emission Lifetime Data for $[ReO_2(py)_4]PF_6$.

surfactant	solvent	τ
-----	H_2O	< 10 ns
-----	CH_3CN	10 μs
-----	CH_2Cl_2	12.5 μs
SDS	H_2O	67 ns/900 ns
SDS	D_2O	570 ns/900 ns
SDS	4:1 H_2O/D_2O	120 ns/900 ns
SDS	4:1 H_2O/D_2O/0.2 M NaCl	70 ns/900 ns
Brij 35	H_2O	< 10 ns
CTAB	H_2O	< 10 ns

Emission lifetime measurements. The decay curves of aqueous micellar SDS solutions of ReO_2^+ are biphasic with $\tau_1 = 67$ and $\tau_2 = 900$ ns. The value of τ_1 is increased in D_2O (570 ns) with $k(H_2O)/k(D_2O) = 8.6$, the same ratio that was obtained in homogeneous nonaqueous solution.[11b] Data obtained in H_2O/D_2O mixtures show a linear dependence of τ_1 on $[H_2O]$ following equation (1) (Figure 3.7).

$$\tau_1(D_2O)/\tau_1(H_2O,D_2O) = 1 + k_Q(H_2O) * \tau_1(D_2O) * [H_2O] \qquad (1)$$

From this equation we estimate values of $k_Q(H_2O) = 2.4 \times 10^5$ and $k_Q(D_2O) = 2.8 \times 10^4$ $M^{-1}s^{-1}$. These rate constants are of the same order as those measured in homogeneous solution, thereby suggesting that the same deactivation mechanism is operating under these conditions. The similarity of these results with those obtained in homogeneous solution indicates that τ_1 arises from ReO_2^+ residing in an environment of reduced water concentration. In contrast the component τ_2 is independent of the H_2O/D_2O ratio, suggesting that it is not exposed to the bulk aqueous medium.

The magnitude of τ_1 is strongly dependent on the surfactant concentration (Figure 3.8). There is a marked increase of τ_1 in the vicinity of the cmc, indicative of association with a normal SDS micelle as shown in **2**.[3] The longer component, τ_2, shows a different dependence on surfactant concentration (Figure 3.9). The lifetime increases as a function of the surfactant concentration and maximizes at the cmc. At low surfactant concentrations, clusters containing more than one ReO_2^+ can participate in triplet-triplet annihilation, resulting in shorter lifetimes.[8] As the surfactant concentration is increased, more clusters are formed, and the multiply occupied clusters are reduced in concentration. Since the ReO_2^+ concentration

Figure 3.7. Stern-Volmer plot for equation (1).

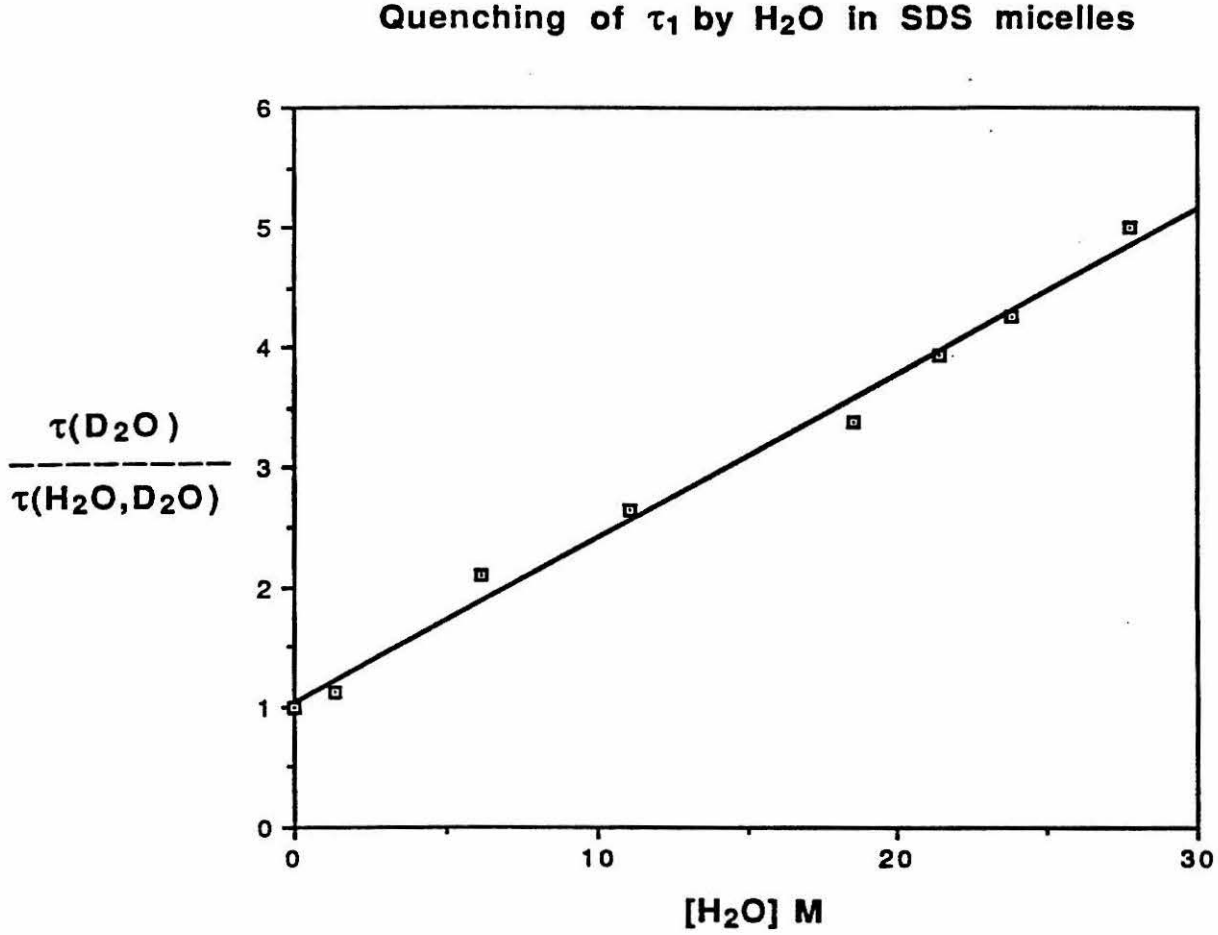
Quenching of τ_1 by H_2O in SDS micelles
$\frac{\tau(D_2O)}{\tau(H_2O,D_2O)}$
0
1
2
3
4
5
6
0
10
20
30
$[H_2O]$ M

Figure 3.8. Dependence of τ_1 on SDS concentration.

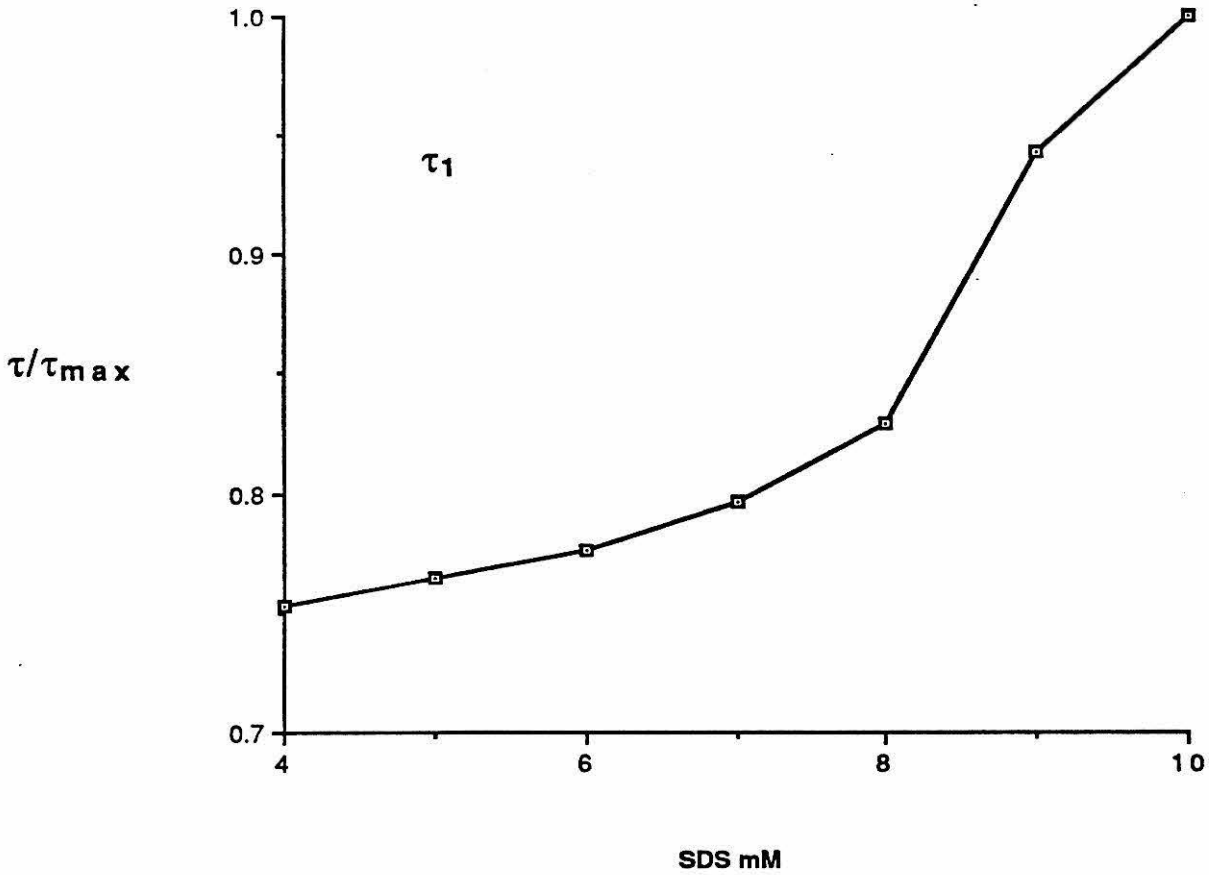
1.0
0.9
0.8
0.7
τ1
τ/τmax
4
6
8
10
SDS mM

Figure 3.9. Dependence of τ_2 on SDS concentration.

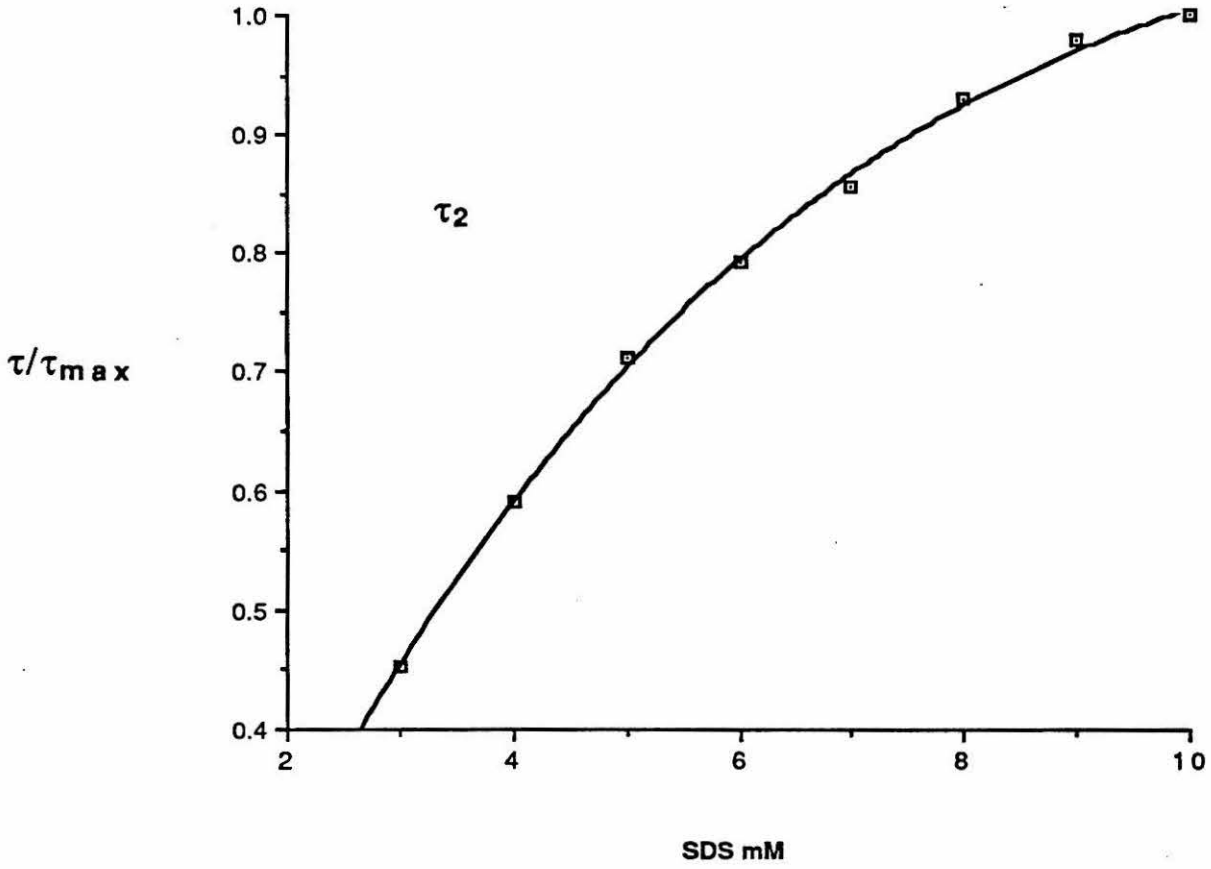
1.0
0.9
0.8
0.7
0.6
0.5
0.4
τ/τmax
τ2
2
4
6
8
10
SDS mM

is constant, the probability for two probes to be within the same cluster decreases with increase in the SDS concentration, and therefore a lengthening of the lifetime can be observed.

The inverse dependence of τ_2 on the incident laser power further supports this model (Figure 3.10). At SDS concentrations below the cmc (3.6 mM), τ_2 is inversely dependent on the laser power and levels off to a maximum at low excitation intensities. This is consistent with the self-annihilation mechanism associated with clusters containing more than one ReO_2^+ ion. At SDS concentrations well above the cmc (40 mM), τ_2 is only slightly dependent on the laser power, indicating that most of the clusters are singly occupied at these SDS concentrations.

The value of τ_1 can be reduced significantly by the addition of NaCl (Table 3.1). Greater ionic strength increases the average micellar size and raises water concentration at the interface.[17] Increased exposure to water results in a reduced value of τ_1. In contrast, τ_2 is not dependent on [NaCl]. The decay profiles of ReO_2^+ in cationic cetyltrimethylammonium bromide (CTAB) and non-ionic Brij 35 ($CH_3(CH_2)_{11}(OCH_2CH_2)_{23}OH$) micellar solutions are single exponentials and short, as in water. This further supports the proposal that the long-lived emission observed in SDS arises from a unique environment associated with SDS. The negatively charged surfactant can cluster with the positively charged (ReO_2^+) probe ions, and a probe embedded in such cluster is least exposed to the bulk aqueous environment. On the other hand, the short lived emission arises from probe ions bound to micelles at the negatively charged interfacial region.

Time-resolved emission spectra. In acetonitrile solution, the steady-state emission spectrum of ReO_2^+ (Figure 3.6a) is typical of complexes of this type. Time-resolved emission measurements in CH_3CN show that this

Figure 3.10. Dependence of τ_2 on laser power intensity in (a) 3.6 mM SDS, (b) 40 mM SDS.

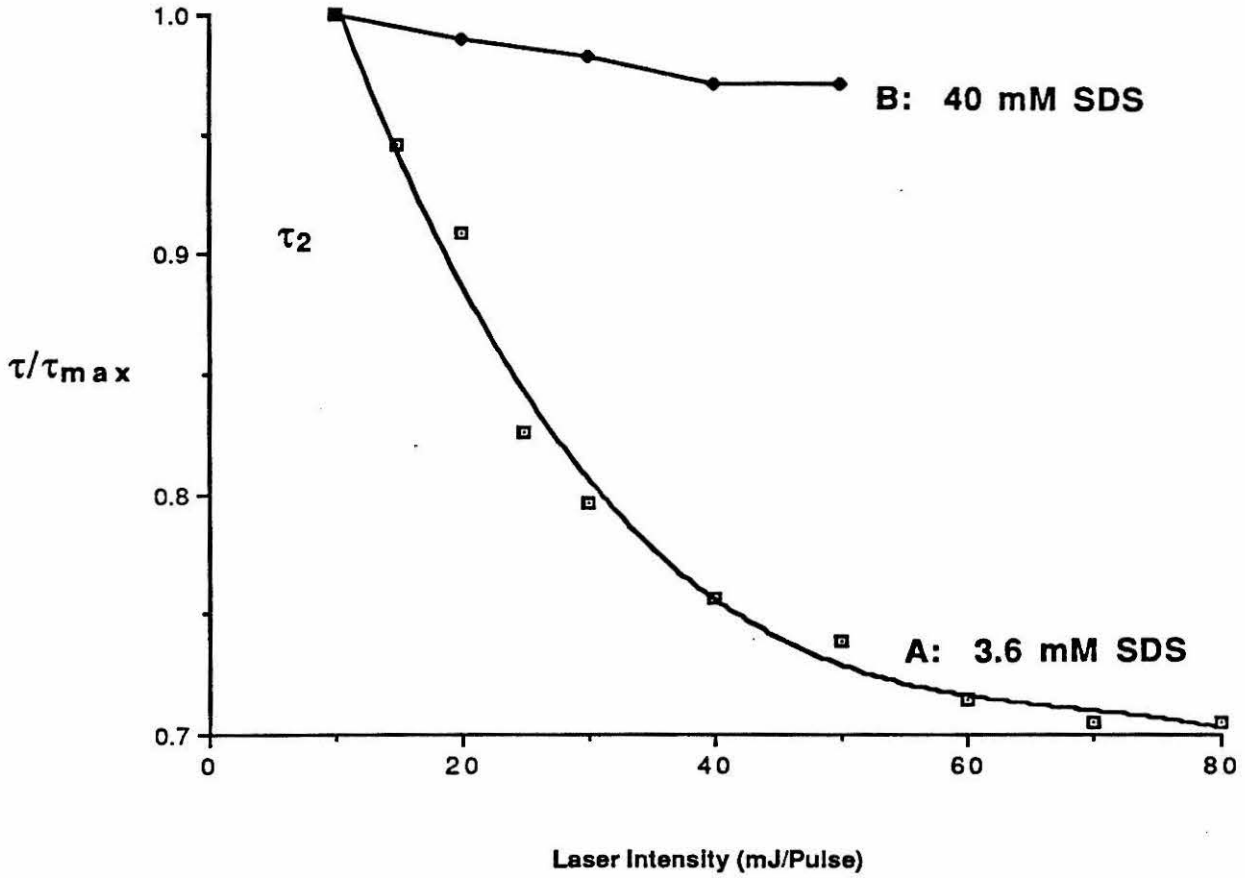
1.0
0.9
0.8
0.7
τ/τmax
τ2
B: 40 mM SDS
A: 3.6 mM SDS
0
20
40
60
80
Laser Intensity (mJ/Pulse)

emission spectrum remains unchanged (λ_{max} 640 nm) over a period of 10 μs. The corresponding decay curves are strictly monoexponential and independent of the monitoring as well as the excitation wavelength (300 - 550 nm). Thus, only one emissive state is observed in homogeneous, nonaqueous solution.

The steady-state emission spectrum of ReO_2^+ obtained in SDS is red-shifted relative to CH_3CN (Figure 3.6b). Qualitatively, the spectrum broadens slightly, and the emission maximum is moved to lower energy. Time-resolved emission spectra taken in SDS at 50 ns intervals over a period of 200 ns show a blue shift in the emission maximum with time (Figure 3.11). This is consistent with two emissive states, a short-lived species with emission at longer wavelengths and a longer-lived state with emission at shorter wavelengths.[18] The fact that the longer-lived component emits at higher energy suggests that this species is less relaxed by the surrounding environment. The ordered structure of the cluster would restrict reorganization and therefore could not relax the excited state very effectively. Thus, this species would be expected to emit at higher energies. In steady-state emission experiments involving other aqueous microheterogeneous environments, including nucleic acids (Chapter 5) and polyelectrolyte films (Chapter 4),[18b] we have observed that more polar environments (as indicated by MLCT absorption maxima) lead to emission at longer wavelengths.

Dioxorhenium(V) and Nonionic Surfactants

Preparation of ReO_2(3-Ph-py)$_4^+$. One of the advantages of the ReO_2^+ system is the ability to alter the axial nitrogen ligands.[12] This allows the hydrophobic properties to be tuned over a wide range. The CN^- complex ($K_3ReO_2(CN)_4$) does not bind to ionic or neutral micelles. The pyridine

Figure 3.11. Time-resolved emission spectra of $[ReO_2(py)_4]PF_6$ in 40 mM SDS, 4:1 H_2O/D_2O. Inset: plot of emission maximum versus time.

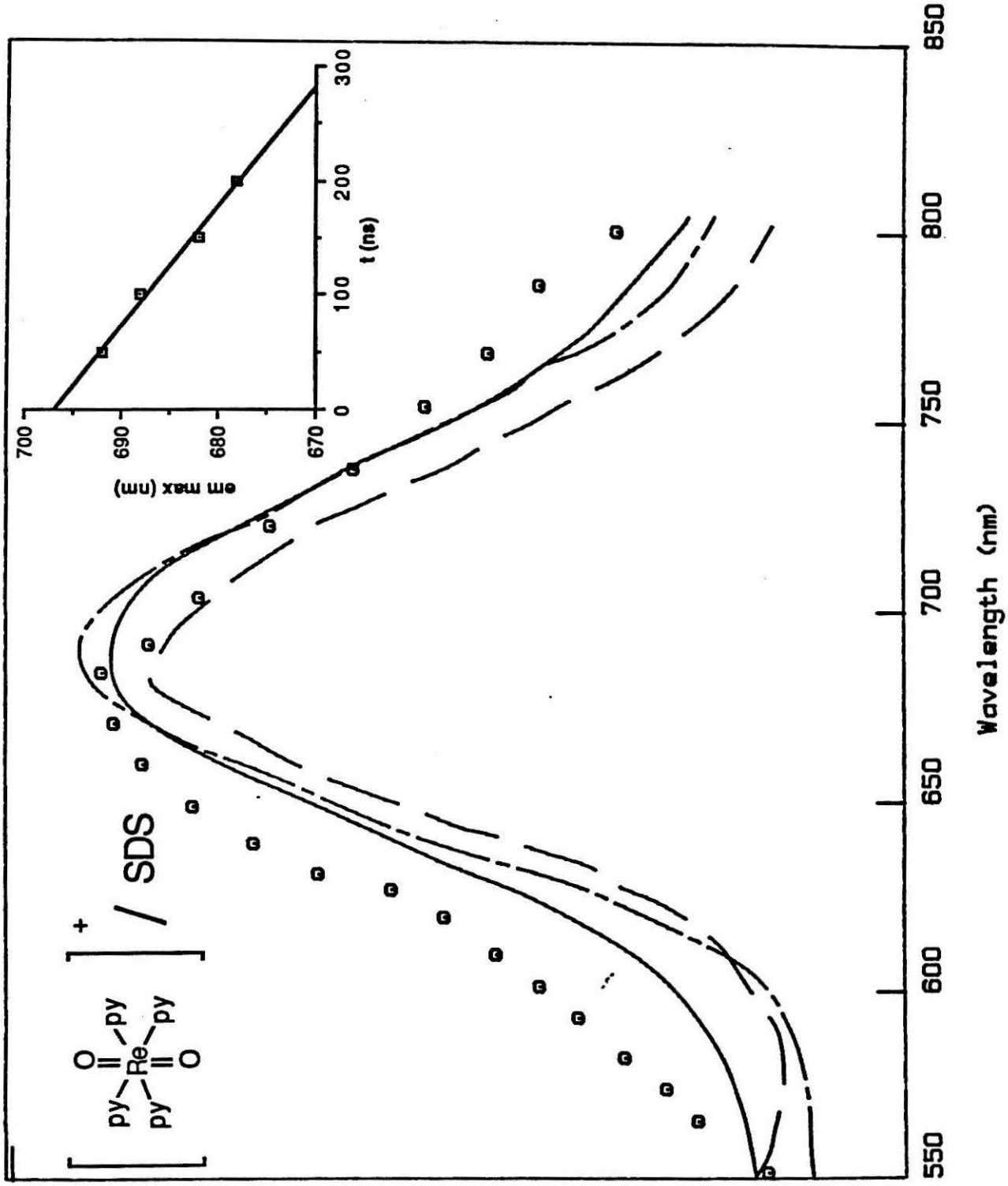
Emission Intensity
Wavelength (nm)
550
600
650
700
750
800
850
SDS
+
O
py
Re
py
O
py
em max (nm)
670
680
690
700
t (ns)
0
100
200
300

complex associates with anionic micelles but not neutral or cationic aggregates. A new derivative, $ReO_2(3\text{-Ph-py})_4^+$, has been prepared, and this complex is sufficiently hydrophobic to bind to neutral as well as anionic micelles. This presents an interesting balance of hydrophobic and hydrophilic properties. The ReO_2^+ unit is very hydrophilic, containing two oxo ligands that are of formal charge -2 and therefore extremely good hydrogen bond acceptors. At the same time, it is possible to add four very hydrophobic ligands, such as 3-phenylpyridine, to this hydrophilic ReO_2^+ moiety.

The 4-picoline and 4-*tert*-butylpyridine derivatives of ReO_2^+ were prepared by Winkler and Gray, and their non-aqueous homogeneous solution emission properties have been reported.[11] The 3-phenylpyridine complex is prepared by substituting 3-phenylpyridine for pyridine in the usual preparation of ReO_2^+. Once purified, this derivative is quite similar to the unsubstituted complex. As in the methyl and *tert*-butyl derivatives, addition of the substituent does not alter greatly the electronic properties of ReO_2^+. The asymmetric MO_2 stretch is present at 810 cm^{-1} (Figure 3.12a), as are the PF_6^- stretch (840 cm^{-1}) and the out of plane bending modes for monosubstituted phenyl rings (750 cm^{-1} and 695 cm^{-1}). The aromatic region of the NMR spectrum (Figure 3.12b) shows four resonances. The peaks at δ = 8.0, 9.1 and 9.4 ppm arise from three of the four pyridyl resonances. The final pyridyl resonance is covered partly by the large multiplet at δ = 7.52 arising from the five phenyl protons. The cyclic voltammogram (Figure 3.13) shows the same reversible $ReO_2^{+/2+}$ couple seen in the unsubstituted complex. The $E_{1/2}$ for this couple is 40 mV less positive than the same couple for the unsubstituted pyridine complex, indicating that the phenyl rings are donating a *very small* amount of electron density to the metal center. The absorption spectrum (Figure 3.14) shows the $^{3,1}E_g$ bands at 425 nm and 490 nm,

Figure 3.12. (A) Metal-oxo stretching region of the IR spectrum (Nujol mull) of $[ReO_2(3\text{-Ph-py})_4]PF_6$. (B) Aromatic region of the NMR spectrum of $[ReO_2(3\text{-Ph-py})_4]PF_6$.

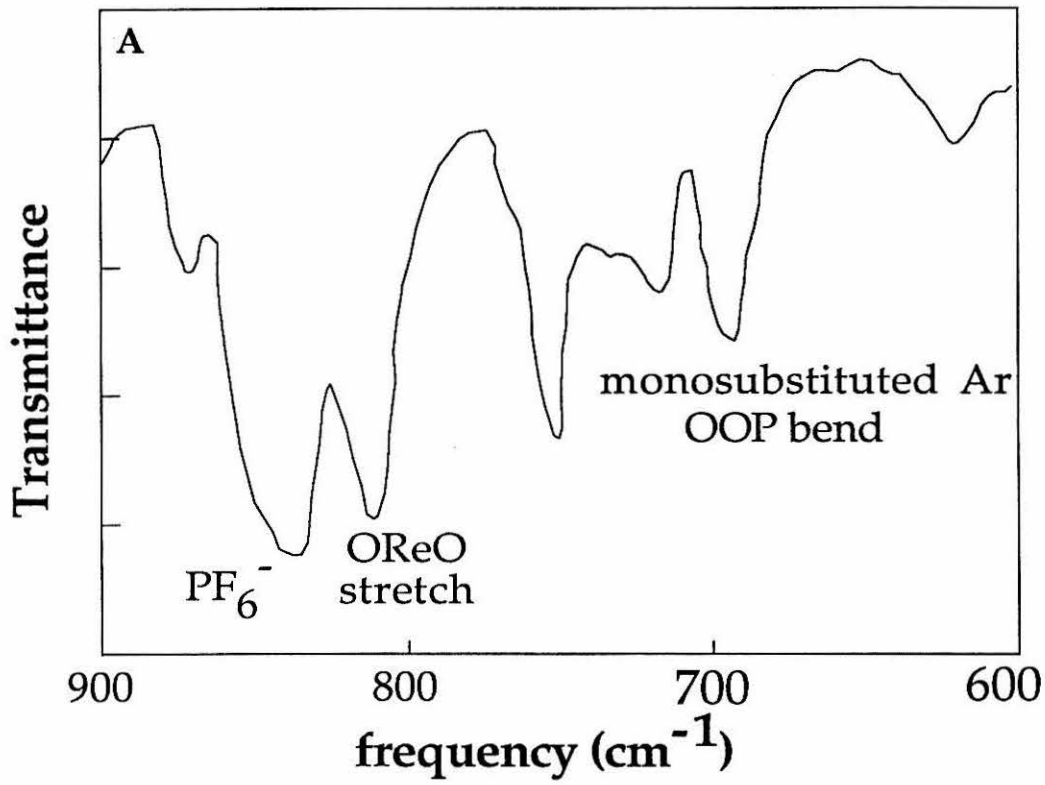
A
Transmittance
monosubstituted Ar
OOP bend
ORe=O
stretch
PF_6^-
900
800
700
600
frequency (cm^{-1})

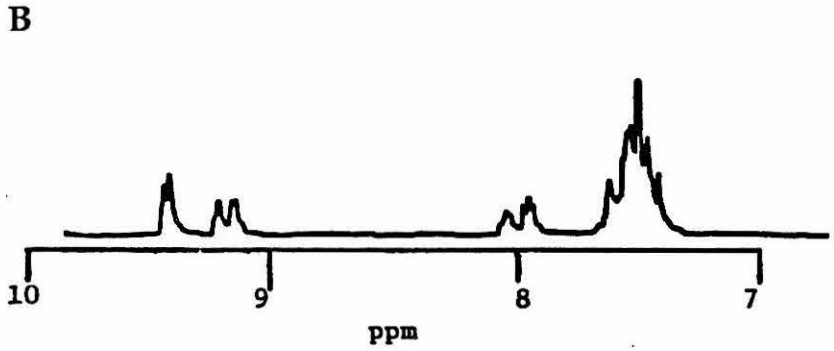
B
10
9
8
7
ppm

Figure 3.13. Cyclic voltammogram of $[ReO_2(3\text{-Ph-py})_4]PF_6$ in acetonitrile, 0.1 M TBAH. Scan rate: 200 mV/s.

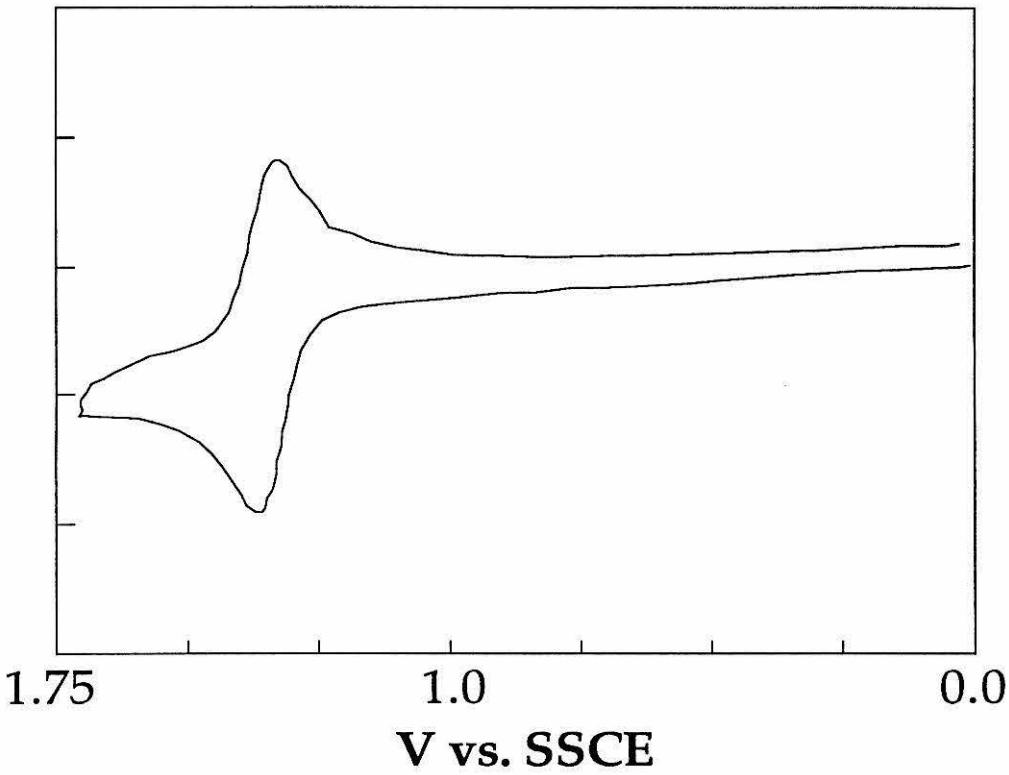
1.75
1.0
0.0
V vs. SSCE

Figure 3.14. Ligand field region of the absorption spectrum of $[ReO_2(3\text{-Ph-py})_4]PF_6$.

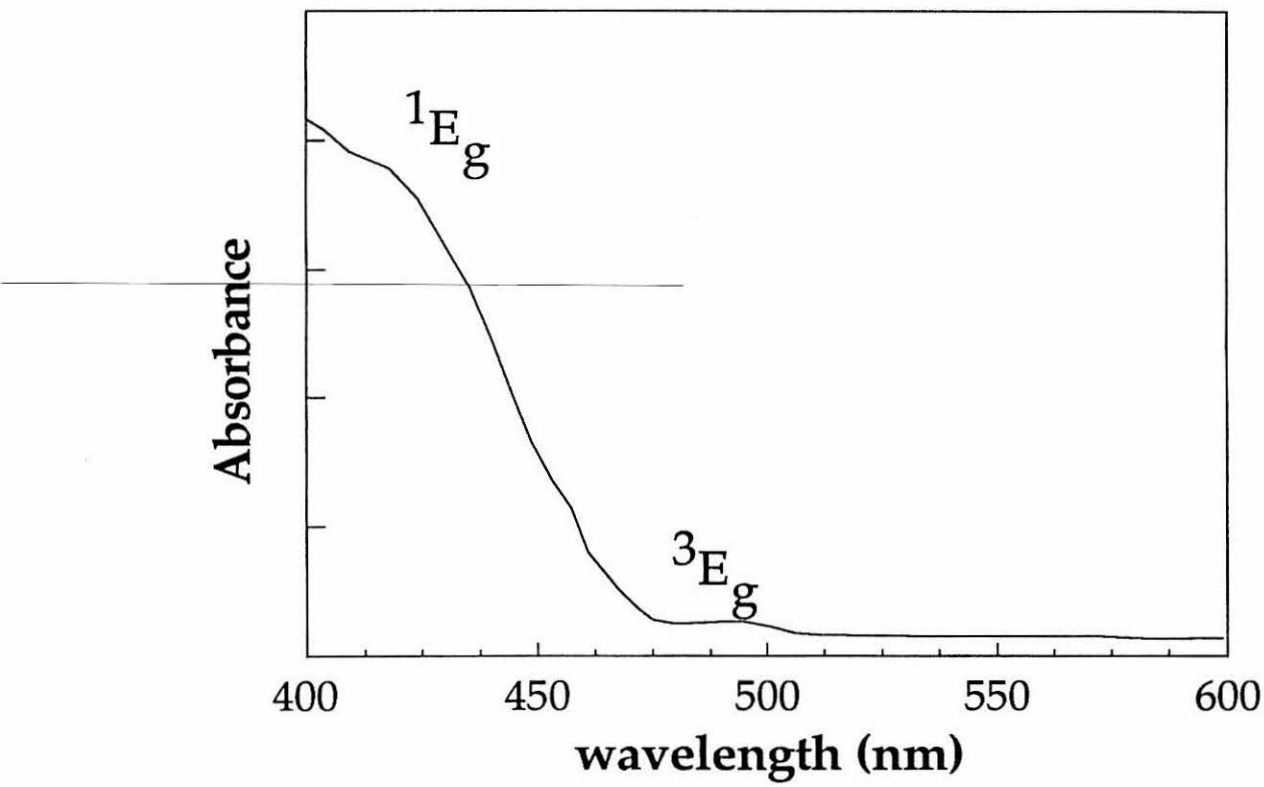
^1E_g
^3E_g
Absorbance
400
450
500
550
600
wavelength (nm)

essentially identical to the unsubstituted analog. Finally, the same structureless emission in room temperature fluid solution is observed (Figure 3.15a). The similarity of the electronic properties of these complexes is summarized in Table 3.2. Thus, the hydrophobic character of the complex has been increased while the desired electronic properties and photophysics have been retained.

Steady-state emission spectra. The steady-state emission spectrum of this complex in CH_3CN shown in Figure 3.15a is unstructured at room temperature. When placed in aqueous solutions of Brij 35, $ReO_2(3\text{-Ph-py})_4^+$ shows vibronically structured emission (Figure 3.15b). This progression ($\Delta\nu$ ~900 cm^{-1}) corresponds to the symmetric ReO_2 stretch and is similar to that seen in low-temperature emission spectra[11] of $ReO_2(py)_4^+$ and in room-temperature emission spectra of $ReO_2(py)_4^+$ intercalated in some types of complex layered oxides.[20] The appearance of this progression indicates that the ReO_2^+ chromophore is in a viscous environment.

Emission lifetime measurements. The lifetime data for $ReO_2(3\text{-Ph-py})_4^+$ are given in Table 3.3. In Brij 35, owing to the absence of electrostatic interactions (which can lead to the formation of **3**), it is reasonable to expect that the major interaction that may occur is hydrophobic binding of $ReO_2(3\text{-Ph-py})_4^+$ to the micellar core. Accordingly, in Brij 35, the decay curve is monophasic (τ 500 ns) and shows only a small isotope effect ($k(H_2O)/k(D_2O) = 1.1$). The increased lifetime and the small isotope effect are consistent with local ordering of the chromophore (Figure 3.15), with limited exposure to the aqueous environment. Thus, $k(H_2O)/k(D_2O)$ is an effective measure of the solvent accessibility of the probe molecule.[21] In aqueous solutions of Triton X-100 ($CH_3C(CH_3)_2CH_2C(CH_3)_2C_6H_4(OCH_2CH_2)_{9.5}OH$),[6] a

Figure 3.15. Uncorrected room-temperature emission spectra of $[ReO_2(3\text{-Ph-py})_4]PF_6$ in (a) acetonitrile and (b) Brij $35/H_2O$.

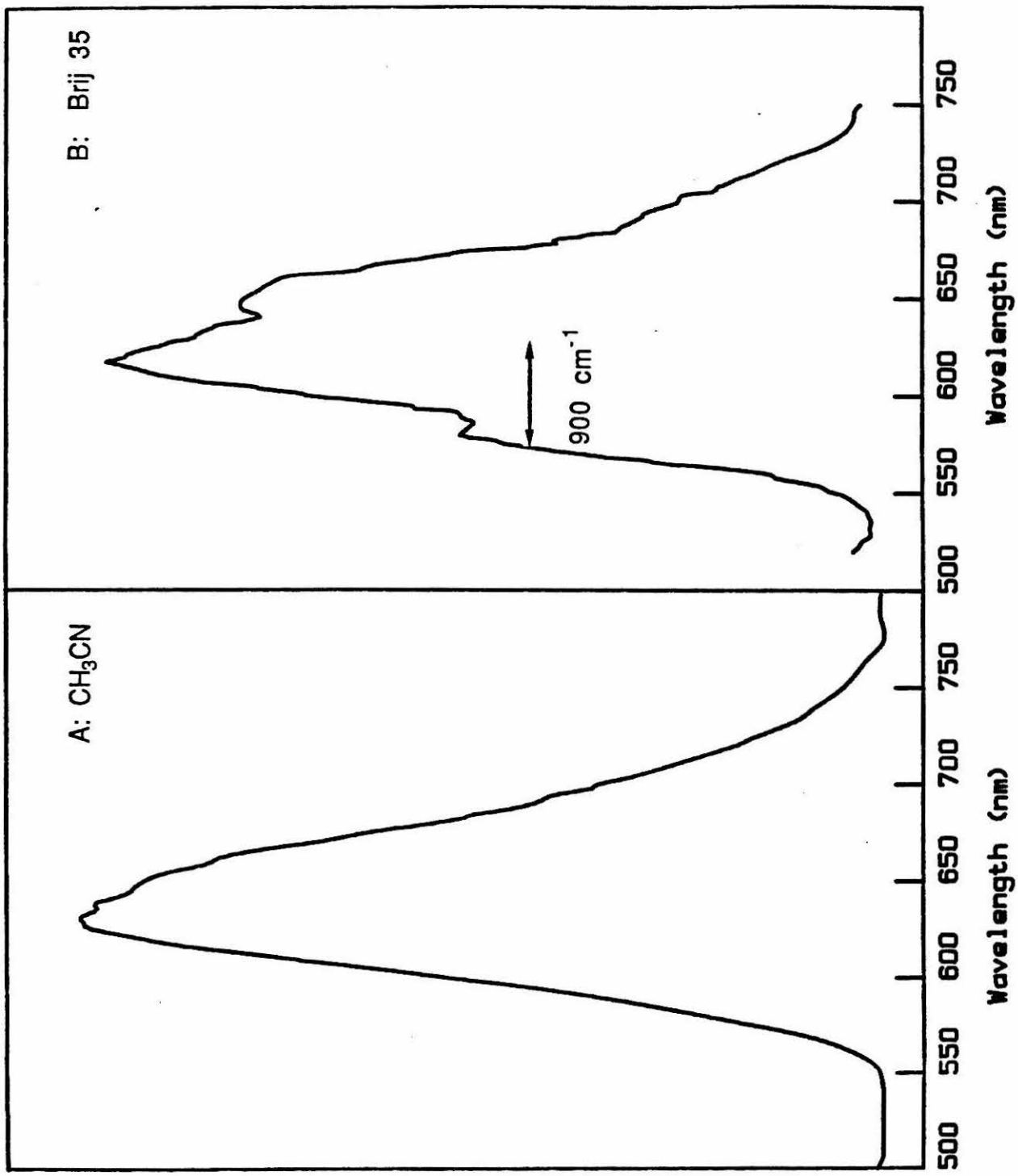
A: CH_3CN
B: Brij 35
900 cm^{-1}
500
550
600
650
700
750
Wavelength (nm)
Emission Intenseity

Table 3.2.

Electronic Properties of Dioxorhenium Complexes.

	$[ReO_2(py)_4]PF_6$	$[ReO_2(3\text{-Ph-py})_4]PF_6$
ν(Re-O)[a]	815 cm^{-1}[b]	810 cm^{-1}
$E_{1/2}(ReO_2^{2+/+})$[c]	+1.37 V	+1.34 V
λ_{max}^{abs}(d-d)[d]	435 nm	425 nm
λ_{max}^{em} [e]	640 nm	625 nm

[a]Nujol mull.

[b]from ref. 11b.

[c]Acetonitrile solution, 0.1 M tetra-n-butylammonium hexafluorophosphate.

[d]Acetonitrile solution.

[e]Acetonitrile solution, 400 nm excitation.

Table 3.3.

Emission Lifetime Data for Other Transdioxo Complexes.

complex	medium	τ
$[ReO_2(3\text{-Ph-py})_4]PF_6$	H_2O	< 10 ns
	CH_3CN	10 μs
	Brij 35/H_2O	500 ns
	Brij 35/D_2O	570 ns
	Triton X-100/D_2O	1.36 μs
	SDS/D_2O	1.3 μs
	CTAB	< 10 ns
$[OsO_2(tmc)](ClO_4)_2$	H_2O	1.45 μs
	CH_3CN	1.0 μs
	SDS/H_2O	1.3 μs

nonionic surfactant with a larger hydrophobic chain than Brij 35, a similar isotope-independent, long-lived emission was observed (τ = 1.36 μs).

In micellar SDS solution, the decay curve of $ReO_2(3\text{-Ph-py})_4^+$ is monophasic and shows no isotope effect. The emission properties (lack of an isotope effect, and a long-lived (1.3 μs), single-component decay) indicate that $ReO_2(3\text{-Ph-py})_4^+$ is bound in cluster aggregates (**3**) rather than at the interfacial region of the anionic micelles (**2**). Further, $ReO_2(3\text{-Ph-py})_4^+$ shows no interaction with positively charged CTAB micelles, thereby suggesting that the complex is not sufficiently hydrophobic to allow it to bind to positively charged micelles.

Dioxoosmium(VI)

The electronically related complex $OsO_2(tmc)^{2+}$ (tmc = 1,4,8,11-tetramethyl-1,4,8,11-tetraazacyclotetradecane),[22] shows a different type of environmentally dependent emission lifetime (λ_{max}^{em} 630 nm). The lifetime increases marginally with solvent polarity from 1.0 μs in CH_3CN to 1.45 μs in H_2O. The lifetime in micellar SDS solution is 1.30 μs, and it shows no deuterium isotope effect. This behavior may result from encapsulation of the oxo groups by the bulky tmc macrocycle, making the complex less sensitive to hydrogen bond donors in the outer coordination sphere. From infrared spectroscopy,[22] it may be concluded that the metal-oxo bonds of OsO_2^{2+} are much stronger than those in ReO_2^+ and that the oxo ligands might be poorer hydrogen bond acceptors.

The OsO_2^{2+} system clearly is not as attractive as the ReO_2^+ system for characterization of microenvironments, but there is also a distinct disadvantage for aqueous photochemistry in general. Shown in Figure 3.16 is the absorption spectrum of OsO_2^{2+}, taken at 2 min intervals during photolysis

Figure 3.16. Absorption spectra of $[OsO_2(tmc)](ClO_4)_2$ taken at 2 min intervals during photolysis at $\lambda > 360$ nm.

Photolysis of $OsO_2(tmc)^{2+}$ in H_2O, λ>360 nm

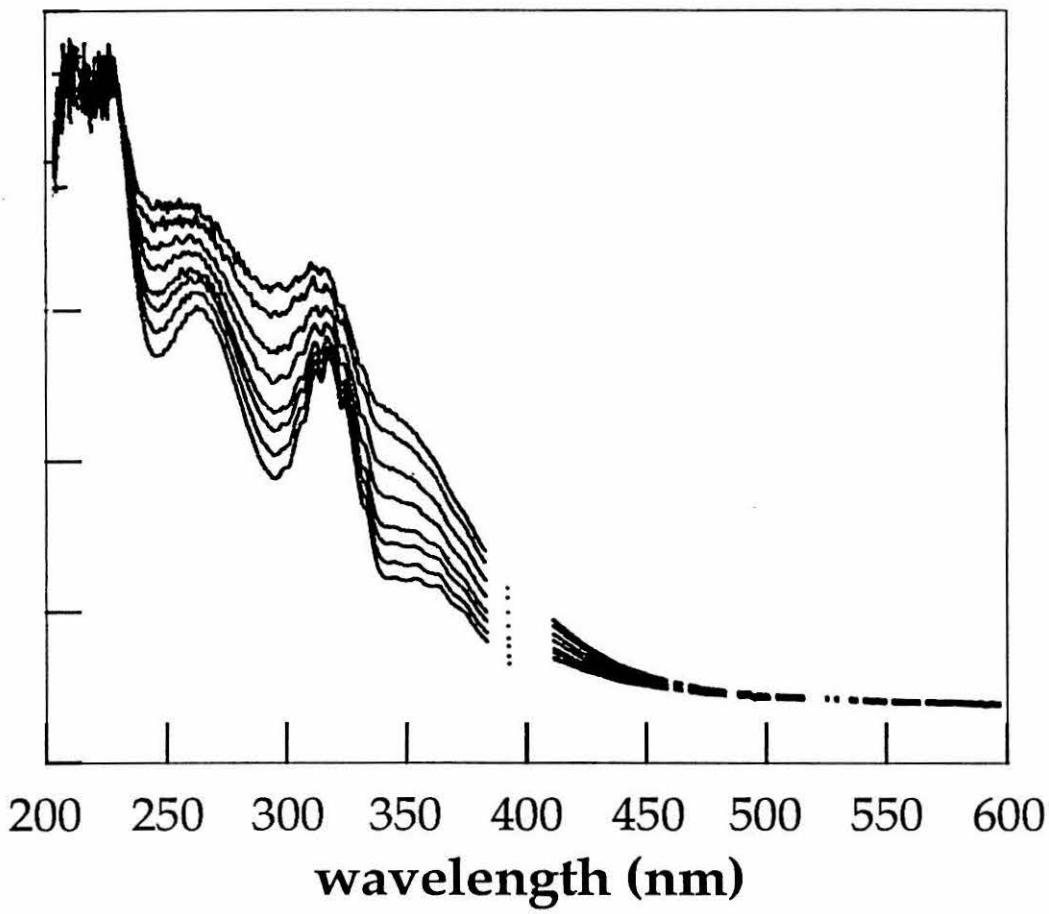

at $\lambda > 360$ nm. The complex clearly is decomposing to yield a spectroscopically nondescript product. Thermodynamic arguments might predict the formation of a μ-oxo dimer as the photolysis product.[23]

Conclusions

We have shown that the d^2 transdioxo complex $ReO_2(py)_4^+$ is a very sensitive probe for hydrophobic binding regions in aqueous surfactant solutions. A number of properties of this chromophore can be used to delineate its microenvironment. These properties include (1) a polarity-dependent UV absorption band and emission maximum, (2) a strong vibrational progression that can be observed when the complex is in an ordered cluster, (3) an emissive excited state that is strongly coupled to the water molecules of its surroundings and (4) a large H_2O/D_2O isotope effect on the excited state properties. We have used these properties together with the fact that the excited state of ReO_2^+ is capable of triplet-triplet annihilation to show that the pre-micellar cluster model proposed for $Ru(bpy)_3^{2+}$ can be generalized to dioxo cations (Figure 3.1). In our case, we have shown that this model is valid by varying the surfactant concentration, incident laser power intensity, H_2O/D_2O ratio, and ionic strength.

We also have synthesized a hydrophobic ReO_2^+ derivative, $ReO_2(3\text{-Ph-py})_4^+$, whose electronic properties are virtually identical with those of the unsubstituted complex. With this hydrophobic derivative, we have been able to probe other environments (e.g., nonionic micelles) by means of the SDS/ReO_2^+ model. An electronically related osmium complex is not nearly as useful for studying aqueous systems, or for aqueous photochemistry in general.

Experimental Section

Materials. Solvents used for synthesis were reagent grade. Photochemical measurements were made in spectrograde solvents that were freshly distilled from appropriate drying agents under inert atmosphere. Triton X-100 was used as received. Sodium dodecyl sulfate (Aldrich) and Brij 35 (Aldrich) were recrystallized from acetone/water. Water was purified by a nanopure water system. Na_2OsCl_6 and $KReO_4$ (Aesar) were used as received. The 1,4,8,11-tetramethyl-1,4,8,11-tetraazacyclotetradecane ligand (Aldrich) was recrystallized from acetone and dried at room temperature under high vacuum. Deuterium oxide (Aldrich, 99.8 atom%) was placed under vacuum immediately after opening and was distilled just before use.

Dioxo complexes. The chloride salt of $ReO_2(py)_4^+$ was prepared by the method of Beard et al.[24a] The PF_6^- salt was precipitated by addition of saturated aqueous NH_4PF_6 to a water solution of the chloride and recrystallized from 5:1 acetone/pyridine. K_2ReCl_6 was prepared by a known method.[24b]

$[ReO_2(3\text{-Ph-py})_4]PF_6$: A 0.5 g sample of K_2ReCl_6 was added to 5 g of 3-phenylpyridine and 1 mL of nanopure H_2O and boiled under reflux for 6 h. The solution was cooled to room temperature and dissolved in acetone. An excess of NH_4PF_6 (Aldrich) was added, and addition of petroleum ether precipitated a crude yellow solid. A dichloromethane solution of this solid was loaded onto a silica gel column. Elution with dichloromethane separated a yellow band and a green band that were discarded. Elution with acetonitrile separated the desired orange band, which was collected and evaporated to dryness. Slow crystallization from 1:1 acetone/petroleum ether produced an orange microcrystalline solid that was dried for 6 h in a vacuum oven at 60° C. Crystals were soluble in dichloromethane, acetonitrile, acetone, toluene,

and diethyl ether and insoluble in petroleum ether and water. Elemental analysis: C, 51.87%; H, 3.70 %; N, 5.55%. Calculated for $[ReO_2(3\text{-Ph-py})_4]PF_6$: C, 53.7%; H, 3.69%; N, 5.69%.

$[OsO_2(tmc)](ClO_4)_2$: A 0.5 g sample of tmc (Aldrich) was added to 150 mL of absolute ethanol containing 12 g of tin plates cut from tin foil (Aldrich). After bringing to reflux, a solution of 0.5 g of Na_2OsCl_6 in 200 mL of absolute ethanol was slowly added over ~2 h. The entire mixture was refluxed overnight and then cooled to room temperature. The solvent was removed on a rotary evaporator and the residue was dissolved in a minimum amount of water. After filtering a small amount of insoluble material, the solution was heated at ~80° C for 15 min. After cooling to room temperature, 1.5 mL of hydrogen peroxide (Baker, 30% in water) was added slowly. When effervescence had ceased, a saturated solution of $NaClO_4$ was added. The solution was cooled overnight, and 62 mg of light brown crystals were recovered. Elemental analysis: C, 24.5%; H, 4.56%; N, 8.25%. Calculated for $[OsO_2(tmc)](ClO_4)_2$: C, 24.8%; H, 4.76%; N, 8.27%.

Physical measurements. Electrochemistry was performed as described elsewhere.[4] Time-resolved emission measurements were performed using an OMA system that has been described previously.[25] The spectra were averaged for 15 - 25 shots and smoothed by two-point smoothing. Electronic absorption spectra were obtained using a Shimadzu UV-260 recording spectrophotometer. Steady-state emission spectra[26] and emission decay curves[27] were obtained as described previously. Four parameter biexponential fits were performed using a program written by M. Albin. This program is based on the techniques of Marquadt as described by Bevington.[28] In all cases described here, the ratio of integrated intensities τ_1/τ_2 was ~2:1.

Sample preparation. Solutions for emission lifetime measurements were prepared in a two-compartment cell fitted with a 10 mL Pyrex bulb and a 1 cm pathlength cuvette.[29] Solvent was transferred on a high vacuum line and degassed by five freeze-pump-thaw cycles. For surfactant solutions, the metal complex was added to the bulb and the surfactant was placed in the cuvette. Nanopure water was added directly and D_2O was vacuum transferred into the bulb. Thus, the metal complex was dissolved before mixing with the surfactant. In "Stern-Volmer" experiments, the "quencher" (H_2O, D_2O, NaCl, SDS) was added to the cuvette while the the solution was kept in the bulb under vacuum. Liquids were degassed by three freeze-pump-thaw cycles before mixing with the solution. Repeating the emission lifetime measurements using less rigorous degassing methods did not quantitatively effect the decay curve. Extreme care was taken to insure that the surfactant, metal complex, and NaCl were completely dissolved.

References and Notes

1. Fendler, J.H. *Membrane Mimetic Chemistry* Wiley-Interscience, N.Y., **1982.**

2. Kalyanasundaram, K. *Photochemistry in Microheterogeneous Systems* Academic Press, N.Y., **1987.**

3. Turro, N.J.; Graetzel, M.; Braun, M. *Angew. Chem. Int. Ed. Engl.* **1980**, *19*, 675.

4. Thorp, H.H.; Van Houten, J.; Gray, H.B. *Inorg. Chem.* **1989**, *28*, 889.

5. Kalyanasundaram, K. *Coord. Chem. Rev.* **1982**, *46*, 159.

6. a) Dressick, W.J.; Raney, K.W.; Demas, J.N.; DeGraff, B.A. *Inorg. Chem.* **1984**, *23*, 875. b) Hauenstein, B.L.; Dressick, W.J.; Buell, S.L.; Demas, J.N.; DeGraff, B.A. *J. Am. Chem. Soc.* **1983**, *105*, 4251. c) Dressick, W.J.; Hauenstein, B.L.; Gilbert, T.B.; Demas, J.N.; DeGraff, B.A. *J. Phys. Chem.* **1984**, *88*, 3337. d) Mandal, K.; Hauenstein, B.L.; Demas, J.N.; DeGraff, B.A. *J. Phys. Chem.* **1983**, *87*, 328.

7. a) Schmehl, R.H.; Whitten, D.G. *J. Am. Chem. Soc.* **1980**, *102*, 1938. b) Foreman, T.K.; Sobol, W.M.; Whitten, D.G. *J. Am. Chem. Soc.* **1981**, *103*, 5333.

8. Baxendale, J.H.; Rodgers, M.A.J. *J. Phys. Chem.* **1982**, *86*, 4906.

9. a) Turro, N.J.; Yekta, A. *J. Am. Chem. Soc.* **1978**, *100*, 3931. b) Meisel, D.; Matheson, M.S.; Rabani, J. *J. Am. Chem. Soc.* **1978**, *100*, 117. c) Menger, F.M. *Acc. Chem. Res.* **1979**, *12*, 1. d) Menger, F.M.; Jerkunika, J.M.; Johnston, J.C. *J. Am. Chem. Soc.* **1978**, *100*, 4676. e) Erikson, J.C.; Gillberg, G. *Acta Chem. Scand.* **1966**, *20*, 2019. f) Hansen, J.R.; Mast, R.C. *Adv. Chem. Ser.* **1982**, *208*, 440.

10. Pipes, D.W.; Meyer, T.J. *Inorg. Chem.* **1986**, *25*, 3256.

11. a) Winkler, J.R.; Gray, H.B. *J. Am. Chem. Soc.* **1983**, *105*, 1371. b) Winkler, J.R.; Gray, H.B. *Inorg. Chem.* **1985**, *24*, 346.

12. Brewer, J.C.; Gray, H.B. *Inorg. Chem.* Manuscript in preparation.

13. Gordon, A.J.; Ford, R.A. *The Chemist's Companion: A Handbook of Practical Data, Techniques and References,* Wiley-Interscience, N.Y., **1972.**

14. Gutmann, V. *Electrochim. Acta* **1976,** *21,* 661.

15. a) Curtis, J.C.; Sullivan, B.P.; Meyer, T.J. *Inorg. Chem.* **1983,** *22,* 224. b) Pyle, A.M.; Barton, J.K. *Inorg. Chem.* **1987,** *26,* 3820. c) Fung, E.Y.; Chua, A.C.M.; Curtis, J.C. *Inorg. Chem.* **1988,** *27,* 1294.

16. a) Kalyanasundaram, K.; Thomas, J.K. *J. Phys. Chem.* **1977,** *81,* 2176. b) Menger, F.M.; Jerkunika, J.M.; Johnston, J.C. *J. Am. Chem. Soc.* **1978,** *100,* 4676.

17. Turro, N.J.; Zimmt, M.B.; Lei, X.G.; Gould, I.R.; Nitsche, K.S.; Cha, Y. *J. Phys. Chem.* **1987,** *91,* 4544.

18. a) Turro, N.J., *Modern Molecular Photochemistry,* Benjamin-Cummings, Menlo Park, CA, **1978.** b) Thorp, H.H.; Gray, H.B., unpublished results.

19. In addition, the longer-lived component would be expected to emit at higher energy than the short-lived component from energy-gap law considerations. (Caspar, J.V.; Meyer, T.J. *J. Phys. Chem.* **1983,** *87,* 952.) Synthesis of ReO_2^+ compounds having a range of different emission maxima confirms that the energy-gap law applies to the ReO_2^+ chromophore.[12]

20. Newsham, M.D.; Giannelis, E.P.; Pinnavaia, T.J.; Nocera, D.G. *J. Am. Chem. Soc.* **1988,** *110,* 3885.

21. Using the ratio of the isotope effect in Brij 35 (HD_{B35}) to the isotope effect in homogeneous solution (HD_{HS}) as a scaling factor, a corrected lifetime that potentially eliminates rigidity can be calculated as in (2).

$$\tau_c = \tau(\text{Brij 35}) * (HD_{B35})/(HD_{HS}) \qquad (2)$$

This calculation gives 66 ns, within experimental error of τ_1(SDS) where the isotope effect is the same as in homogeneous solution. This is encouraging

since SDS and Brij 35 have the same hydrophobic groups. Further experimentation using a wide range of surfactants and ReO_2^+ derivatives might allow us to quantify the contribution of rigidity to the emission enhancement.

22. a) Che, C.-M.; Cheng, W.-K. *J. Am. Chem. Soc.* **1986,** *108,* 4644. b) Che, C.-M.; Yam, V.W.-W.; Cho, K.C.; Gray, H.B. *J. Chem. Soc., Chem. Commun.* **1987,** 948. c) Yam, V.W.-W., Ph.D. Thesis, University of Hong Kong, **1988.**

23. Holm, R.H. *Chem. Rev.* **1987,** *87,* 1401.

24. a) Beard, J.H.; Casey, J.; Murmann, K.R. *Inorg. Chem.* **1965,** *4,* 797. b) Watt, G.W.; Thompson, R.J. *Inorg. Synth.* **1963,** *4,* 797.

25. Kumar, C.V.; Barton, J.K.; Gould, I.R.; Turro, N.J.; Van Houten, J. *Inorg. Chem.* **1988,** *27,* 648.

26 Rice, S.F.; Gray, H.B. *J. Am. Chem. Soc.* **1983,** *105,* 4571.

27. Nocera, D.G.; Winkler, J.R.; Yocum, K.M.; Bordignon, E.; Gray, H.B. *J. Am. Chem. Soc.* **1980,** *102,* 6761.

28. Bevington, P.R. *Data Reduction and Error Analysis for the Physical Sciences,* McGraw-Hill, N.Y., **1969.**

29. Marshall, J.L.; Hopkins, M.D.; Gray, H.B. *ACS Symp. Ser.* **1987,** *357,* 254.

Chapter 4.

Photophysics of Dioxorhenium(V) in Polymer Membranes: Direct Evidence for Chemically Distinct Regions in Nafion.

Introduction

The structure of Nafion (Figure 4.1) perfluorosulfonated membranes and thin films has been investigated by numerous electrochemical,[1-6] spectroelectrochemical[7, 8] and photophysical[9] methods and is an area of continuing interest in redox chemistry. The most widely accepted model for Nafion structure originally was developed by Yeager and Steck[5], who proposed that small ions could occupy three distinct regions of the polymer. These regions include a hydrophobic region, a hydrophilic ion cluster region, and an interfacial region between the two. It is believed that the hydrophobic region is composed of aggregated polymer chain material and that the ion cluster region contains most of the SO_3^- sites, adsorbed water and counterions. The interfacial region is believed to contain some pendant side chain material, a small number of SO_3^- sites, some adsorbed water and some counterions. Recent work by Rubinstein[4] using ferrocene as a hydrophobic electrochemical probe has shown that $Ru(bpy)_3^{2+}$ occupies both the interfacial and ion cluster regions and that *these regions become more hydrophobic upon incorporation of the complex.* Additionally, Vining and Meyer[6] have demonstrated that all three regions can be occupied by Ru(II) aqua-polypyridyl complexes depending on the pH of the bulk solution. A working model for Nafion structure based on the current literature is shown in Figure 4.2. The emission lifetime of $Ru(bpy)_3^{2+}$ is not altered by incorporation into the membrane; however, a 12 nm blue-shift of the MLCT emission is observed.

The photophysics of $ReO_2(py)_4^+$ (ReO_2^+) are altered greatly by incorporation into Nafion polymer membranes. The emissive excited state of ReO_2^+, efficiently quenched in aqueous solution, is long-lived in the presence of sodium dodecyl sulfate at concentrations both above and below the cmc (Chapter 3).[10] Anionic polymers containing potentially hydrophobic regions

Figure 4.1. Chemical structure of Nafion.

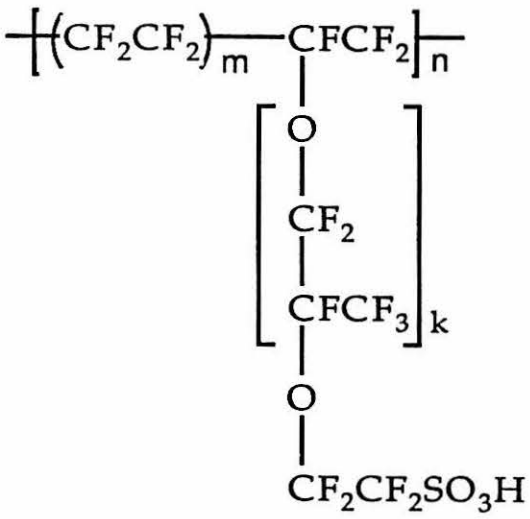

Nafion

$$\left\{ \begin{array}{l} m = 5\text{-}13.5 \\ n = \text{ca. } 1000 \\ k = 1, 2, 3, \ldots \end{array} \right\}$$

Figure 4.2. Working model for Nafion structure based on reference 5 showing (a) hydrophobic fluorocarbon region, (b) interfacial region and (c) ion cluster region.

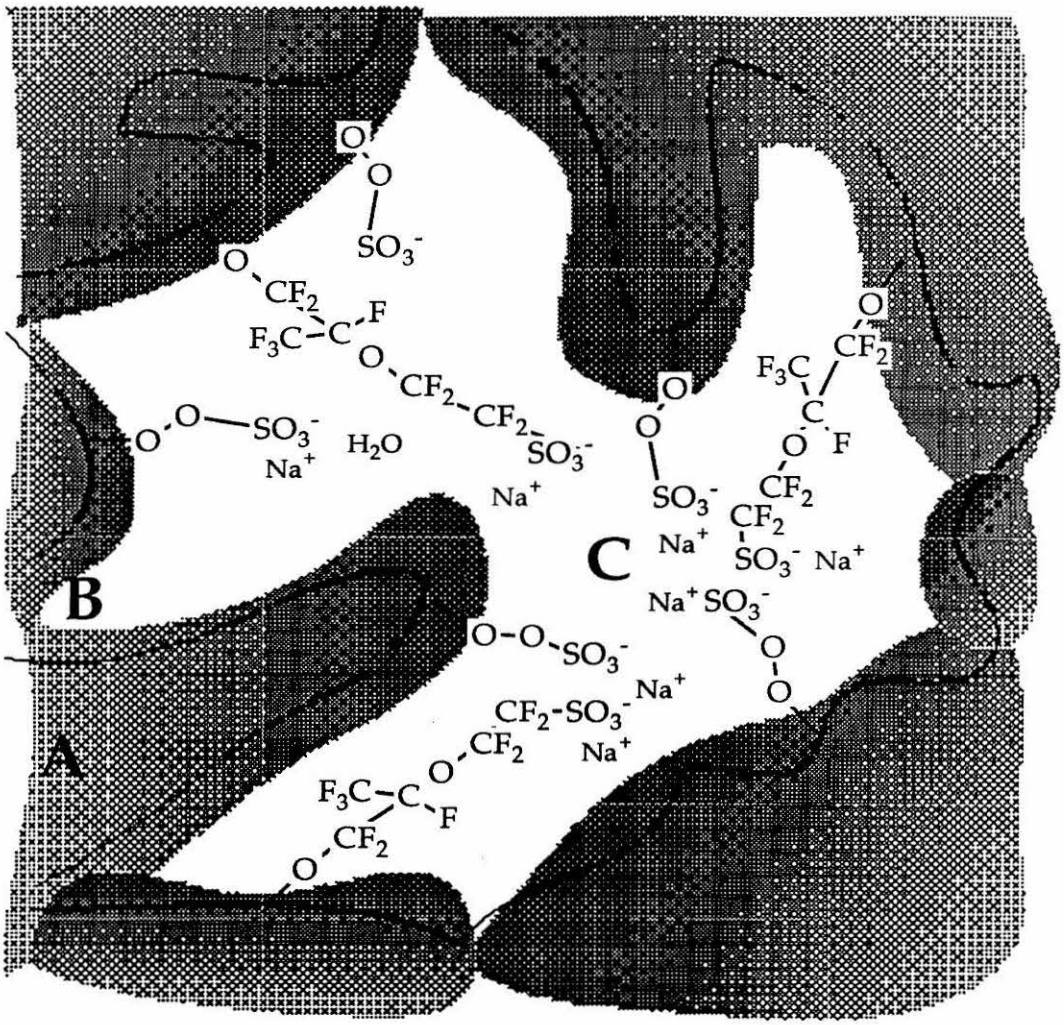
A
B
C
SO_3^-
CF_2
F_3C
H_2O
Na^+
$CF_2-SO_3^-$

also induce long-lived emission from aqueous solutions of ReO_2^+. The photophysics of ReO_2^+ in these systems will be interpreted in terms of the general model[10] of Chapter 3 and previous work involving $Ru(bpy)_3^{2+}$.

Results and Discussion

Nafion membranes quantitatively incorporate ReO_2^+ upon soaking in aqueous solutions of the complex. The absorption spectrum of an ReO_2^+-exchanged membrane is shown in Figure 4.3. The average polarity calculated from this spectrum is Z~85.3, similar to ethylene glycol.[10] This environment seems to be even more polar than aqueous micellar solutions of SDS.

In nonaqueous solution, the emission spectrum of ReO_2^+ is broad and featureless, with λ_{max} = 650 nm (Figure 3.6).[11a] The emission spectra of ReO_2^+ in Nafion membranes prepared in H_2O and D_2O are also broad, with an emission maximum (695 nm, Figure 4.4) that is red shifted 45 nm relative to nonaqueous solution. This red shift is 20 nm greater than that seen in SDS, consistent with the relative polarities of these environments as indicated by the absorption spectra. In addition, there is a large emission enhancement in D_2O that is reflected in the emission lifetime.

The emission decay curves of ReO_2^+-exchanged membranes show two well-resolved components. In H_2O, these components exhibit lifetimes of τ_1 = 250 ns and τ_2 = 1.3 μs, and the integrated intensities of these components are essentially equal (Figure 4.5). These values are independent of laser power and loading levels between 20 and 200 μmoles/cm^2. In membranes prepared in D_2O, τ_1 = 750 ns and τ_2 = 2.9 μs. This gives isotope effects of 3 and 2.4 for τ_1 and τ_2, respectively. The isotope effect potentially reflects the solvent accessibility of certain environments.[10] These results clearly indicate that ReO_2^+ occupies two distinct regions of the polymer membrane.

Figure 4.3. Absorption spectra of ReO_2^+ in (a) H_2O, (b) Nafion membrane/H_2O, (c) DMF.

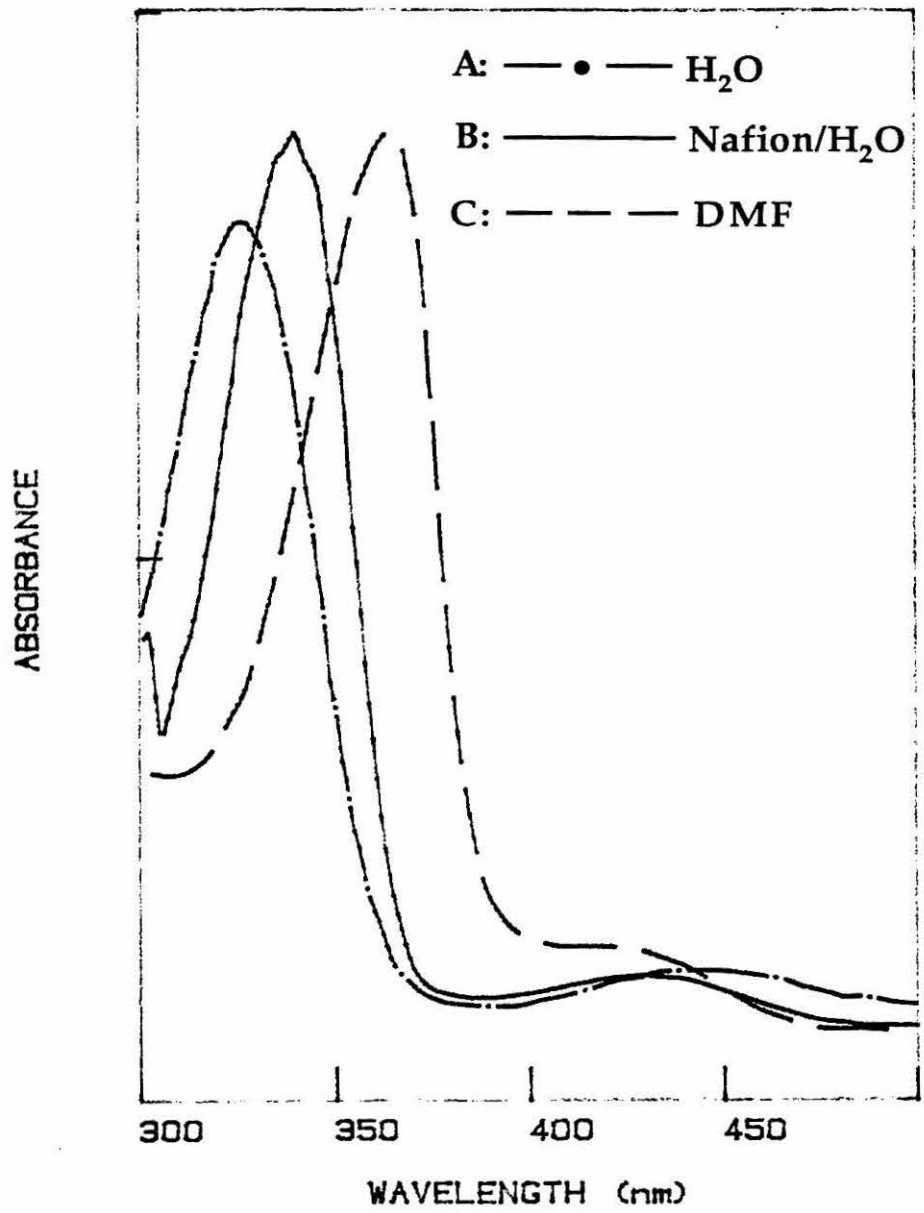
A: — • — H_2O
B: ——— Nafion/H_2O
C: — — — DMF
ABSORBANCE
300
350
400
450
WAVELENGTH (nm)

Figure 4.4. Uncorrected emission spectra of ReO_2^+ in Nafion membranes prepared in (a) H_2O, (b) D_2O.

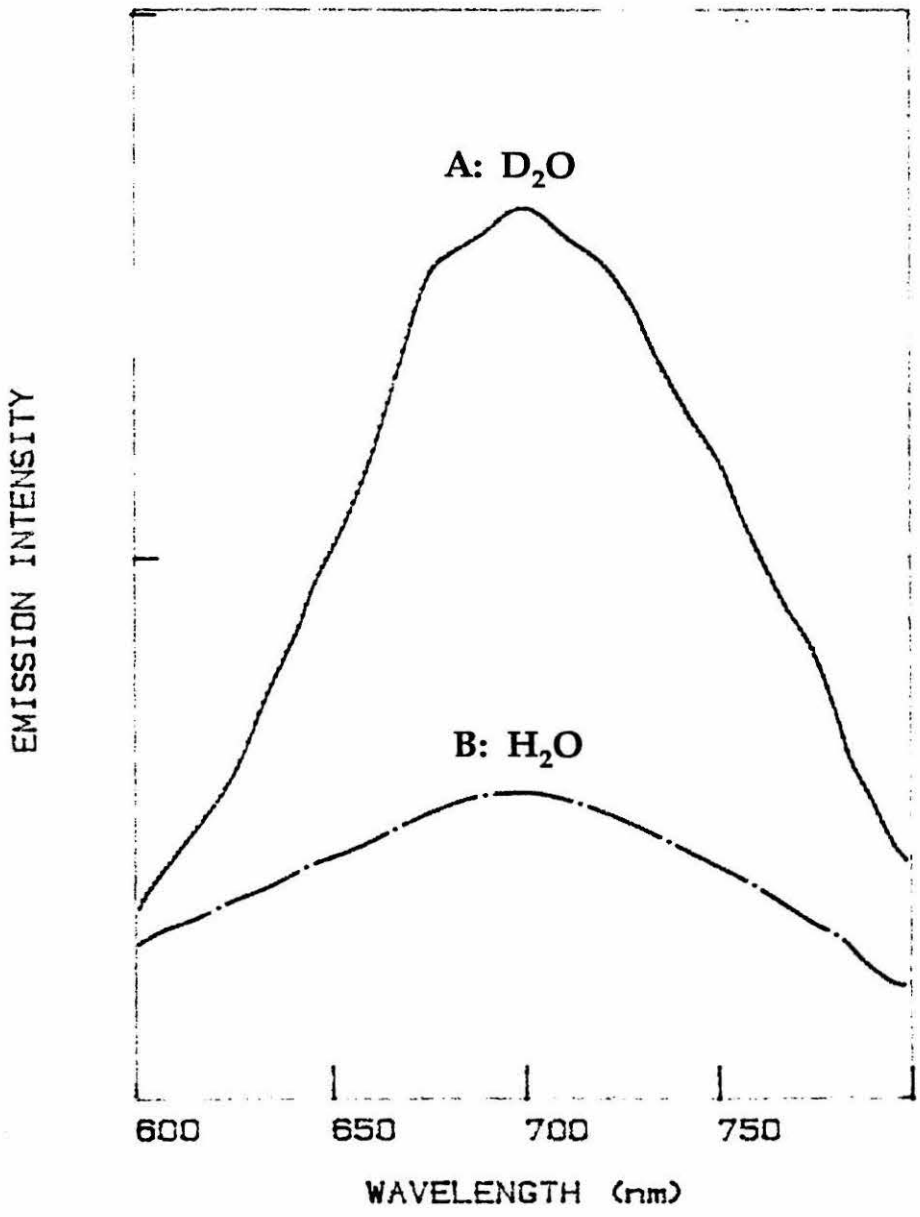
A: D_2O
B: H_2O
EMISSION INTENSITY
600
650
700
750
WAVELENGTH (nm)

Figure 4.5. Emission decay curve of ReO_2^+ in a Nafion membrane prepared in H_2O.

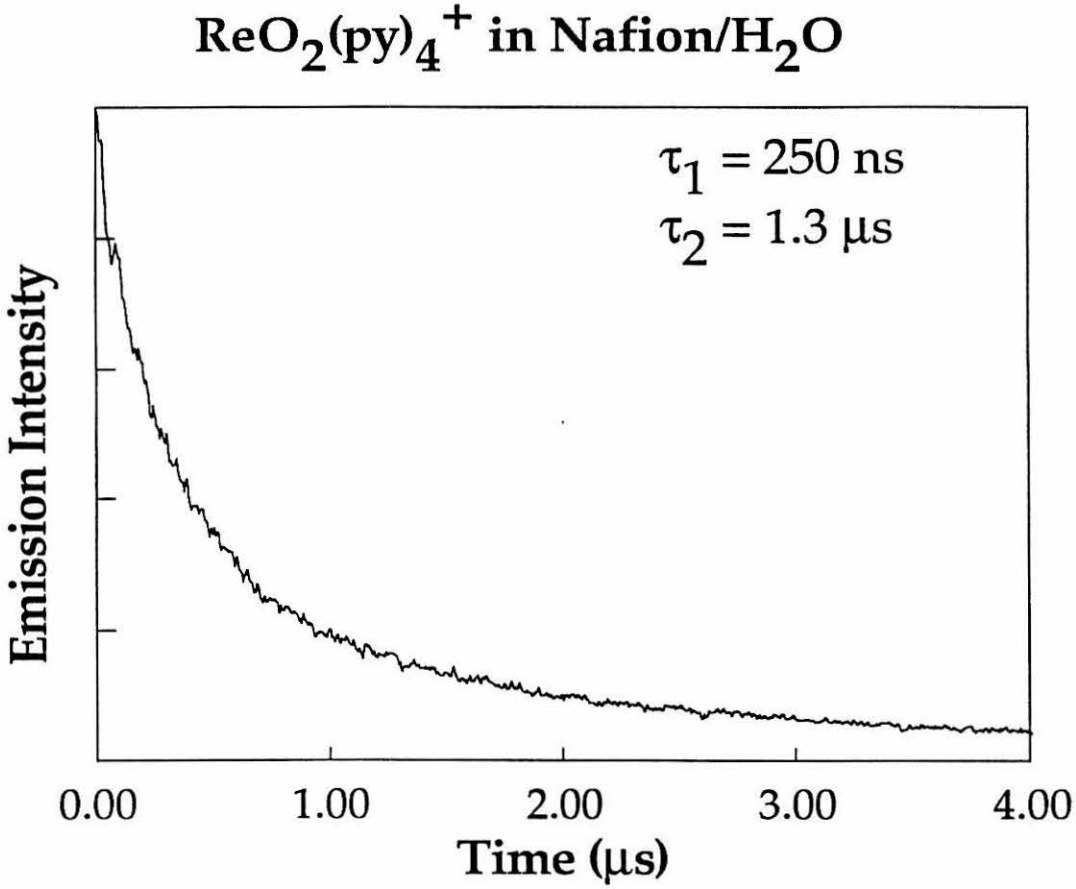
$ReO_2(py)_4^+$ in Nafion/H_2O
τ_1 = 250 ns
τ_2 = 1.3 μs
Emission Intensity
0.00
1.00
2.00
3.00
4.00
Time (μs)

Based on results involving other environments, it is reasonable to assign τ_1 to ReO_2^+ in the ion cluster region and τ_2 to ReO_2^+ in the interfacial region.[5] The hydrophobic region is ruled out because the unsubstituted ReO_2^+ complex does not occupy any hydrophobic region without encouragement from electrostatic interactions. Further, a much larger lifetime (~10 μs) would be expected in a truly hydrophobic region.[11b] The absolute magnitudes for τ_1 and τ_2 in Nafion agree well with decay parameters measured in environments of similar hydrophobic quality. The values of τ_1 are slightly greater than those observed from complexes on the negatively charged surface of aqueous SDS micelles or in the wet region of nonionic micelles.[10] The values of τ_2 are similar to those observed in SDS/ReO_2^+ clusters and $ReO_2(py)_4^+$ electrostatically bound to calf thymus DNA. These comparisons are further supported by the work of Lee and Meisel[9], which shows these regions of Nafion membranes to be quite similar to SDS aggregates. In addition, a larger isotope effect would be expected in the more fluid ion cluster region and this is observed. Thus, the sensitive emission properties of ReO_2^+ can be used to probe two chemically distinct regions in Nafion polymer membranes.

Experimental Section

Materials. Metal complexes were prepared as described in Chapter 2. Nafion and D_2O were purchased from Aldrich and used as received.

Sample Preparation. Nafion membranes were soaked in H_2O or D_2O solutions of $[ReO_2(py)_4]PF_6$ and then placed in between two glass microscope slides. Absorption spectra were measured with a Shimadzu UV260 with a swollen Nafion blank in the reference beam. The membranes were placed at a 45 degree angle to the excitation beam for determination of emission spectra[12] and lifetimes[13] as described previously. Loading levels were

determined from the absorption at 342 nm (ε = 19400 M^{-1} cm^{-1}).[14] Decay curves were deconvoluted as described in Chapter 3.

References

1. Martin, C.R.; Rubinstein, I.; Bard, A.J. *J. Am. Chem. Soc.* **1982**, *104*, 4817.

2. Martin, C.A.; Dollard, K.A. *J. Electroanal. Chem.* **1983**, *159*, 127.

3. McHatton, R.C.; Anson, F.C. *Inorg. Chem.* **1984**, *23*, 3935.

4. Rubinstein, I. *J. Electroanal. Chem.* **1985**, *188*, 227.

5. Yeager, H.L.; Steck, A. *J. Electrochem. Soc.* **1981**, *128*, 1880.

6. Vining, W.J.; Meyer, T.J. *J. Electroanal. Chem.* **1987**, *237*, 191.

7. Buttry, D.A.; Anson, F.C. *J. Am. Chem. Soc.* **1982**, *104*, 4824.

8. Rubinstein, I.; Bard, A.J. *J. Am. Chem. Soc.* **1980**, *102*, 6641.

9. Lee, P.C.; Meisel, D. *J. Am. Chem. Soc.* **1980**, *102*, 5477.

10. Thorp, H.H.; Kumar, C.V.; Turro, N.J.; Gray, H.B. *J. Am. Chem. Soc.* **1989**, In press.

11. a) Thorp, H.H.; Van Houten, J.; Gray, H.B. *Inorg. Chem.* **1989**, *28*, 889. b) Thorp, H.H.; Turro, N.J.; Gray, H.B. Manuscript in preparation.

12. Rice, S.F.; Gray, H.B. *J. Am. Chem. Soc.* **1983**, *105*, 4571.

13. Nocera, D.G.; Winkler, J.R.; Yocum, K.M.; Bordignon, E.; Gray, H.B. *J. Am. Chem. Soc.* **1984**, *106*, 5145.

14. Pipes, D.W.; Meyer, T.J. *Inorg. Chem.* **1986**, *25*, 3256.

Chapter 5.

Photochemistry of Dioxorhenium(V) in DNA: Multiple Binding Regions and Oxidative Cleavage.

Introduction

The interactions of metal complexes with DNA is an area of intense interest.[1-4] The characterization of metal complex binding to DNA has been pursued with the intention of developing sequence-specific DNA cleaving agents based on photo- and redox-active complexes such as $Co(bpy)_3^{3+}$ and $Ru(bpy)_3^{2+}$. Recently, DNA has been reported to be an extremely efficient mediator of long-range electron transfer between complexes of this type.[5-9]

The various modes of metal complex binding to DNA have been assigned from spectroscopic investigations of luminescent ruthenium complexes based on $Ru(bpy)_3^{2+}$ (ligands are shown in Figure 5.1).[10-13] The emission from the MLCT states of $Ru(bpy)_3^{2+}$ is not enhanced substantially by the addition of DNA to a buffer solution.[13] The intensity of $Ru(phen)_3^{2+}$ and $Ru(DIP)_3^{2+}$ emission, however, is enhanced by ~20% in the presence of DNA. Time-resolved measurements show that this enhancement is accompanied by the addition of a long component to the emission decay curve. The short component has been assigned to complexes that are free in solution, electrostatically bound to the phosphate backbone, and surface bound in the DNA minor groove. Thus, changing the ligands from bpy to phen or DIP creates a new binding mode having a lifetime three times greater than the other states present in the solution. This binding mode has been characterized as intercalation of a phen or DIP ligand between the nucleotide polycyclic aromatic rings.

Many bound redox-active metal complexes induce oxidative cleavage of DNA either thermally or photochemically.[4, 14-22] Many of these reactions occur through the sensitization of singlet oxygen; however, the generation of hydroxide radical by strong thermal or photochemical oxidants is the most widely observed mechanism.[4, 19] A hydroxyl radical mechanism has been

Figure 5.1. Pyridyl and polypyridyl ligands used in complexes described in this chapter.

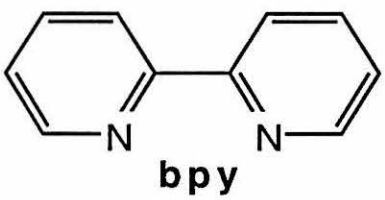

bpy

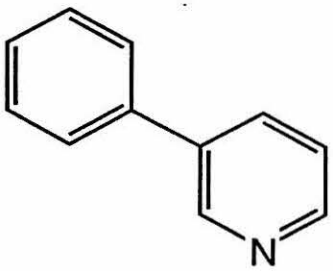

3-Ph-py

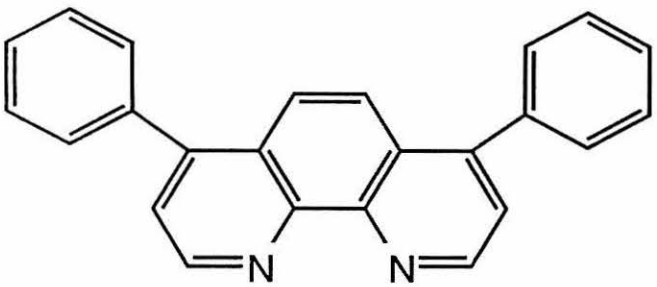

DIP

phen

proposed for the extremely efficient cleavage reactions of $Co(phen)_3^{2+}$ and $Co(DIP)_3^{2+}$.[14]

The photophysics of $ReO_2(py)_4^+$ (ReO_2^+) are altered greatly by binding to DNA. The emissive excited state of ReO_2^+, efficiently quenched in aqueous solution, is long-lived in the presence of sodium dodecyl sulfate at concentrations both above and below the cmc (Chapter 3).[23] Anionic polymers containing potentially hydrophobic regions (i.e., DNA) also induce long-lived emission from aqueous solutions of ReO_2^+. The photophysics of ReO_2^+ in DNA will be interpreted in terms of the general model of Chapter 3 and previous work involving $Ru(bpy)_3^{2+}$. The oxidation of ReO_2^+ bound to DNA by photo-induced electron transfer to methylviologen leads to DNA cleavage. The cyclic voltammetry and optical absorption techniques[24] of Chapter 2 are used to detect this reaction.

Results and Discussion

Photophysics of ReO_2^+ in DNA. Aqueous solutions of ReO_2^+ do not exhibit long-lived emission.[23, 25] Addition of calf thymus DNA to these solutions induces long-lived emission at ~675 nm from ReO_2^+. The decay of this emission is monophasic with a lifetime of 1.7 μs. Since no emission is observed from ReO_2^+ that is free in solution, this emission must arise from an excited complex that is bound to DNA. Solutions of DNA containing $Ru(bpy)_3^{2+}$ show similar behavior except that emission from free metal complexes is observed and cannot be distinguished from emission due to bound excited states.[12, 13] Analogy with these results implies that ReO_2^+ interacts with DNA primarily through electrostatic interactions. It is not surprising that electrostatic association would lead to protection of the complex from the aqueous environment since hydrophilic cations such as Na^+ are known to accumulate in the major and minor grooves of DNA.[26, 27]

Increasing the hydrophobicity of the equatorial ligands leads to a different type of emission profile. The hydrophobic ReO_2^+ derivative, ReO_2(3-Ph-py)$_4^+$,[23] does not dissolve in 2% aqueous ethanol; however, it is soluble in this same medium when 1 mM DNA is present. The absorption spectrum of ReO_2(3-Ph-py)$_4^+$ in calf thymus DNA is shown in Figure 5.2. From the extinction coefficient of this band, it can be determined that the complex is soluble to ~20 μM in the presence of 1 mM DNA-phosphate.

Biphasic emission is observed from ReO_2(3-Ph-py)$_4^+$ bound to DNA (Figure 5.3). The short component, τ_1 = 2.4 μs, is similar to the decay time of the unsubstituted complex in DNA and may arise from the same mode of binding. The long component, τ_2 = 10 μs, is the same as the lifetime in acetonitrile[23, 24] and can thereby be assigned to a very hydrophobic binding mode. Thus, increasing the hydrophobic character (py → 3-Ph-py) of the organic ligands changes the emission decay of ReO_2^+ in the same way as analogous substitution (bpy → phen, DIP) in Ru(bpy)$_3^{2+}$.[13]

Molecular dynamics calculations support the existence of a very hydrophobic ReO_2(3-Ph-py)$_4^+$-DNA adduct. In these calculations, the DNA atoms were fixed and only the metal complex atoms were allowed to move. Docking of the complex in the major groove and minimization of the structure led to a low energy conformation whose solvent-accessible surface did not contain either of the oxo ligands of ReO_2^+. Thus, quenching of the excited state by interaction of water with the oxo ligands can be prevented.

Photochemistry of ReO_2^+ in DNA. The excited state of ReO_2^+ is a mild (-0.7 V vs. SSCE) excited-state reductant in acetonitrile.[24] In this solvent, a reversible electron transfer with methylviologen (MV^{2+}) is observed. The product of this reaction, ReO_2^{2+}, is a strong oxidant and can be scavenged by dichloromethane, leading to net production of MV^+ radical. The oxidized

Figure 5.2. Absorption spectrum of $ReO_2(3\text{-Ph-py})_4^+$ in 1 mM calf thymus DNA.

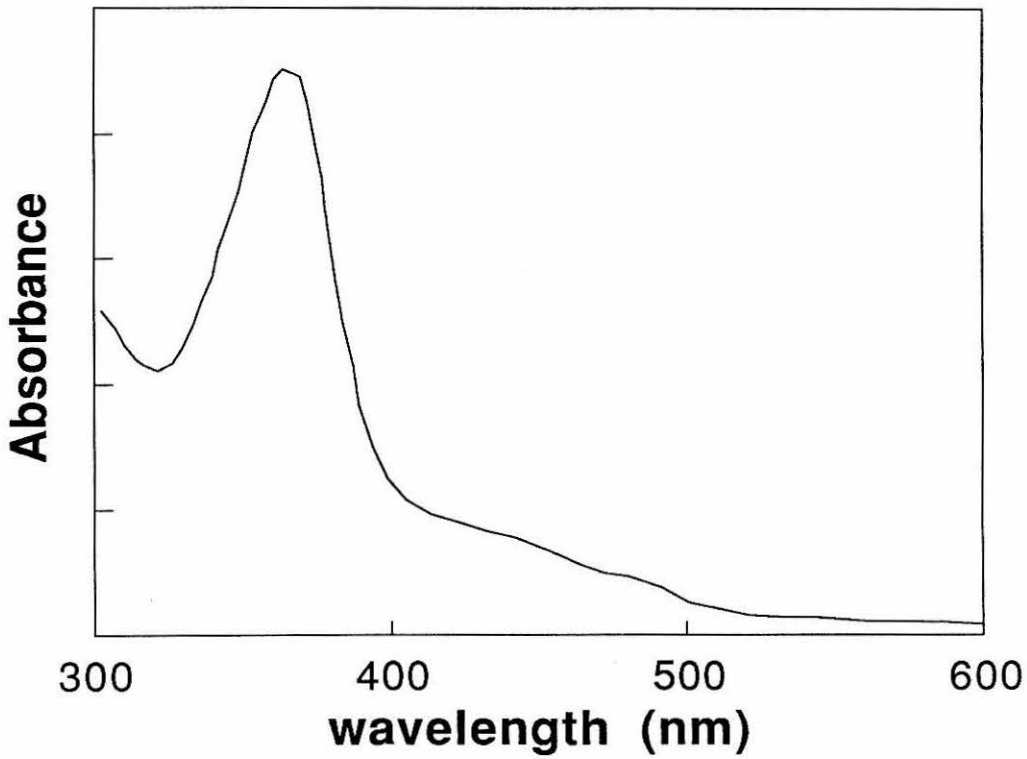
Absorbance
300
400
500
600
wavelength (nm)

Figure 5.3. Emission decay curve of $ReO_2(3\text{-Ph-py})_4^+$ in 1 mM calf thymus DNA.

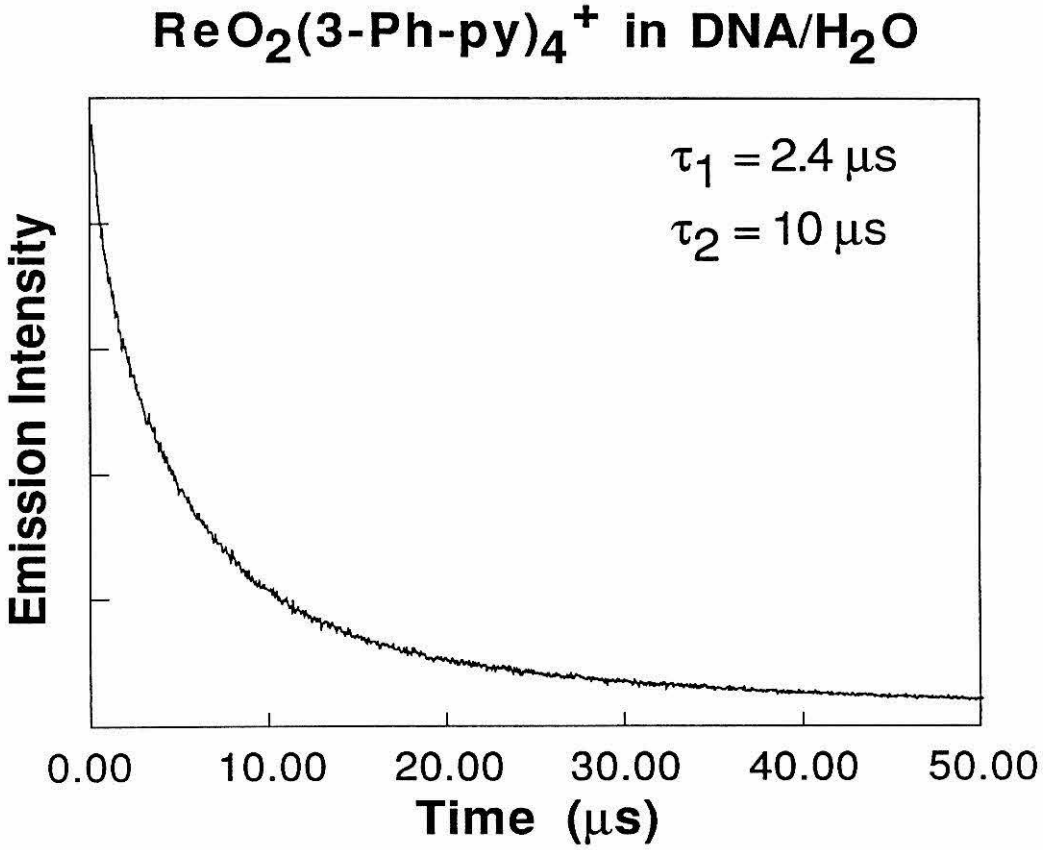
ReO2(3-Ph-py)4+ in DNA/H2O
τ1 = 2.4 μs
τ2 = 10 μs
Emission Intensity
0.00
10.00
20.00
30.00
40.00
50.00
Time (μs)

metal complex shows H-atom abstraction reactivity, catalyzing reactions such as the conversion of secondary alcohols to ketones.

Generation of bound ReO_2^{2+} leads to oxidative cleavage of DNA that can be detected by gel electrophoresis (Figure 5.4). Photolysis ($\lambda > 330$ nm) of phage DNA (ΦX174, rf II) in the presence ReO_2^{+} and MV^{2+} leads to almost total cleavage as seen in lane D. Significant cleavage occurs also, however, in the presence of MV^{2+} alone. This can be explained by excitation of MV^{2+}, which should be a powerful excited state oxidant on its own. In fact, inefficient photocleavage of pBR322 DNA by MV^{2+} has been demonstrated.[28] At this photolysis wavelength, the extinction coefficient for MV^{2+} is very small and the reaction is inefficient.

A product of the oxidative cleavage is MV^{+} radical. This offers a convenient analytical marker for studying the reaction. Photolysis of vacuum-degassed DNA solutions containing ReO_2^{+} and MV^{2+} leads to production of MV^{+} radical (Figure 5.5).[29] Photolysis of DNA control solutions containing only MV^{2+} also generates MV^{+}. Using these absorption spectra, the relative contributions of the two pathways to the overall cleavage can be calculated. This reveals that both pathways produce approximately the same amount of cleavage. This is in qualitative agreement with the electrophoresis data shown in Figure 5.4.

The reaction can also be monitored electrochemically. Cyclic voltammograms of ReO_2^{+} in the presence of silanes and alcohols show loss of return wave current due to chemical reaction of the oxidized metal complex with the added substrate (Chapter 3).[24] With calf thymus DNA as the substrate, the same current loss is observed. Interestingly, this is observed in N_2-degassed solution. Shown in Figure 5.6 is the correlation of current loss with scan rate, which shows that greater current loss is observed at lower scan

Figure 5.4. 1% agarose gel showing ΦX174 (rf II) DNA (12 μM) after 12 h of photolysis at $\lambda > 330$ nm with (left to right): (a) no added compound, (b) 50 μM MV^{2+}, (c) 10 μM ReO_2^+, (d) 50 μM MV^{2+} and 10 μM ReO_2^+.

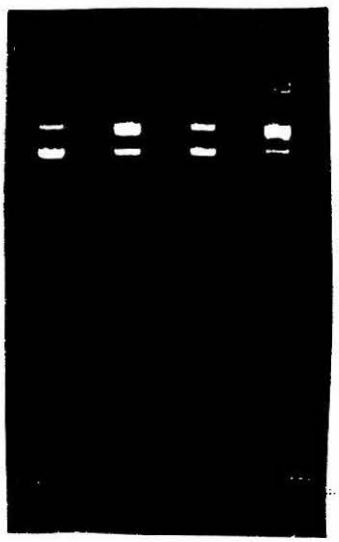

Figure 5.5. Absorption spectrum of a vacuum-degassed solution containing 40 μM ReO_2^+, 1 mM calf thymus DNA, and 50 μM MV^{2+}, after 12 h of photolysis at $\lambda > 330$ nm.

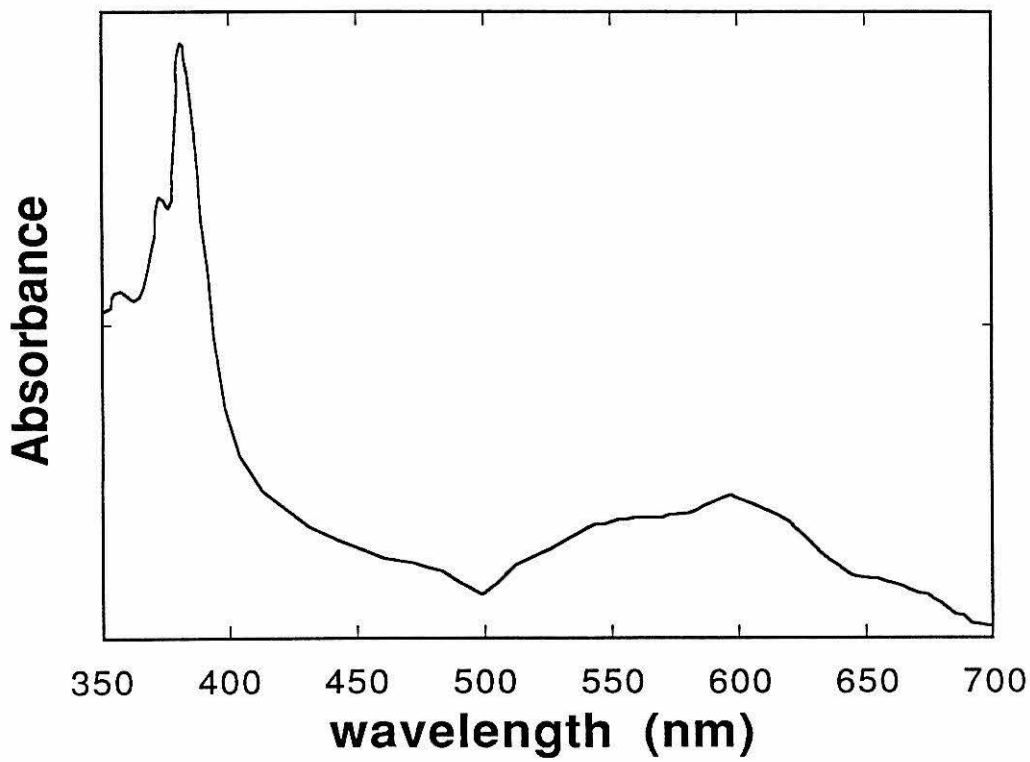
Absorbance
350
400
450
500
550
600
650
700
wavelength (nm)

Figure 5.6. Cathodic current loss of ReO_2^+ rereduction wave (+1.22 V) as a function of scan rate induced by the addition of 2 mM calf thymus DNA to an aqueous solution (Glassy carbon electrode, Ag wire reference, Pt wire auxiliary, 0.05 M KCl, 0.05 M NaOAc, pH 5).

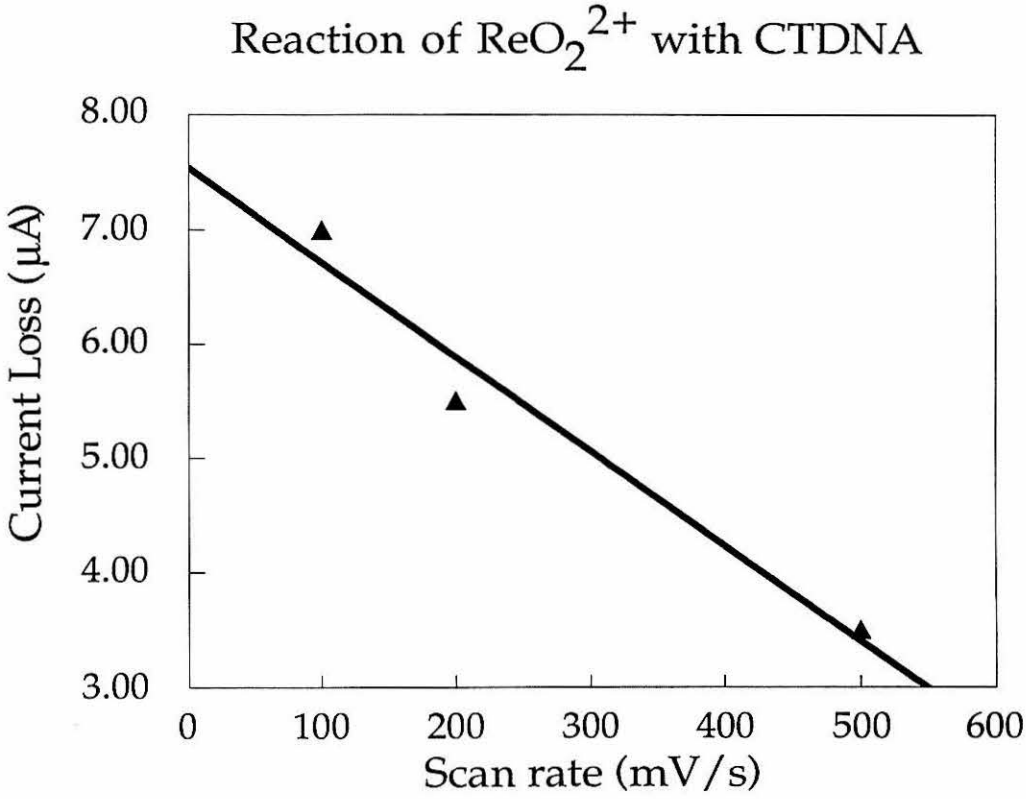
Reaction of ReO_2^{2+} with CTDNA
Current Loss (μA)
8.00
7.00
6.00
5.00
4.00
3.00
0
100
200
300
400
500
600
Scan rate (mV/s)

rates. At lower scan rates, there is more time for the oxidized complex to react with the DNA before rereduction on the return scan. Addition of the DNA causes no loss of oxidation current indicating that the complex is only weakly bound to the DNA.[30] This supports the idea that the interaction of the unsubstituted ReO_2^+ complex is mainly electrostatic. Lack of solubility prevents making this measurement with the 3-Ph-py complex. The electrochemically activated cleavage of DNA by iron bleomycin in aerated solution recently has been reported.[31]

The kinetics of the reduction of MV^{2+} by excited DNA-intercalated ethidium bromide have been measured.[6, 8] It was shown that most of the MV^+ produced is reoxidized rapidly on the DNA strand; however, a small (~2%) fraction escapes from the helix into the aqueous solution.[6] This fraction then is reoxidized via a second-order process ($k = 5.6 \times 10^9\ M^{-1}\ s^{-1}$). Thus, a fraction of the oxidized ethidium bromide has a lifetime on the order of microseconds. The driving forces are similar and it therefore is reasonable to assume that the kinetics of the ReO_2^+ reaction are comparable and that the escape of MV^+ from the helix permits ReO_2^{2+} to react with the DNA. The reaction inefficiency then is consistent with the low yield of MV^+ escape. These findings are summarized by the mechanism shown in Figure 5.7.

The ability of ReO_2^{2+} to oxidatively cleave DNA can be explained by our experiments with organic substrates. Substrate oxidation indicative of H-atom abstraction, such as the conversion of secondary alcohols to ketones, has been observed with ReO_2^{2+}. The oxidative cleavage of DNA by iron bleomycin is believed to occur via abstraction of the ribose 4' hydrogen by an activated "Fe^V=O" intermediate.[32] We have generated a similar intermediate, ReO_2^{2+}, by excited state electron transfer to MV^{2+}. This

Figure 5.7. Proposed mechanism for oxidative cleavage of DNA by ReO_2^+.

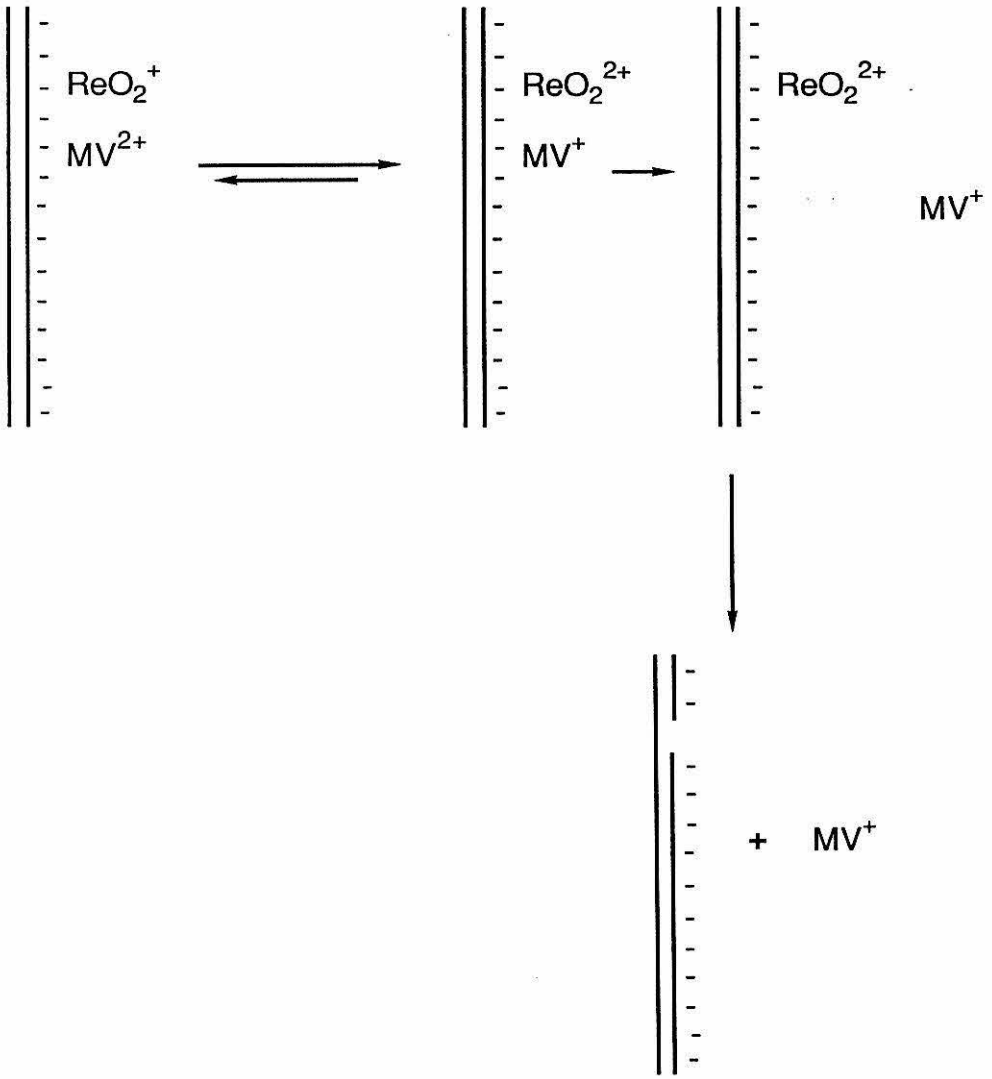
ReO_2^+
MV^{2+}
ReO_2^{2+}
MV^+
ReO_2^{2+}
MV^+
+ MV^+

intermediate should then be capable of abstracting the ribose 4' H-atom, leading to DNA cleavage.

Conclusions

The experiments described in this chapter unify the themes brought forth in Chapters 2 and 3. The environmentally sensitive photophysical properties of ReO_2^+ have been used to probe an environment of intense interest: DNA. The conclusions made from the surfactant experiments have been applied to this medium. Multiple binding regions have been detected and partly characterized.

The photochemical cleavage of DNA by ReO_2^+ utilizes all of the methodology developed in this thesis. Long-lived emission in aqueous solution is brought about by binding of ReO_2^+ to the DNA. An electron transfer reaction is used to generate the strongly oxidizing species, ReO_2^{2+}. This reactive complex then cleaves supercoiled DNA as shown by traditional gel electrophoresis. Techniques of inorganic photo- and redox chemistry can be used to detect this reaction in the same way as with organic substrates. These methods have allowed detection of the reaction in degassed solution, which is difficult using molecular biology techniques.

Experimental Section

Materials. Metal complexes were prepared as described in Chapters 2 and 3. Calf thymus DNA (Sigma) was purified by phenol extraction. Phage DNA ΦX174 (rf II) was purchased from Bethesda Research Laboratories and used as received. Methylviologen dichloride (Aldrich) was used as received.

Solutions of calf thymus DNA containing $[ReO_2(py)_4]PF_6$ and $[ReO_2(3\text{-Ph-py})_4]PF_6$ were vacuum degassed by five freeze-pump-thaw cycles. A liquid nitrogen/*o*-xylene slush bath (-29 °C) was used for slow freezing to insure that the DNA was not nicked. The solutions containing $[ReO_2(3\text{-Ph-py})_4]PF_6$ were prepared by the addition of a saturated ethanol solution of the metal complex to an aqueous solution of DNA. Conditions for the emission experiments were: 1.0 mM DNA-phosphate, 20 mM NaCl and 20 mM Tris, pH 7. Cleavage reactions for analysis by electrophoresis were performed at 12 μM phage DNA-phosphate, 50 μM $MVCl_2$, 10 μM metal complex, 20 mM NaCl and 20 mM Tris, pH 7. Photolysis was performed with a high pressure Hg/Xe arc lamp. Molecular dynamics calculations were performed with BIOGRAF/III version 1.34: BIOGRAF was designed and written by S.L. Mayo, B.D. Olafson and W.A. Goddard III. Electrochemistry was performed at a glassy carbon electrode in 0.05 M KCl, 0.05 M acetate buffer, pH 5. Solutions were degassed with N_2 and kept under an N_2 blanket during the experiment. Voltammograms were corrected for background current due to the addition of DNA. Electrochemical instrumentation was as described previously. Emission spectra[33] and lifetimes[34] were measured as described previously.

Electrophoresis was performed in a homemade apparatus with 1% agarose gels in 40 mM Tris, pH 7.9. Samples were loaded onto the gel using

Ficoll loading buffer. After electrophoresis the gels were stained with ethidium bromide and photographed under UV light.

References

1. Barton, J.K. *Comments Inorg. Chem.* **1985**, *3*, 321.

2. Barton, J.K. *Science* **1986**, *233*, 727.

3. Barton, J.K. *J. Biomol. Struct. Dyn.* **1983**, *1*, 621.

4. Dervan, P.B. *Science* **1986**, *232*, 464.

5. Atherton, S.J.; Beaumont, P.C. *J. Phys. Chem.* **1986**, *90*, 2252.

6. Atherton, S.J.; Beaumont, P.C. *J. Phys. Chem.* **1987**, *91*, 3993.

7. Barton, J.K.; Kumar, C.V.; Turro, N.J. *J. Am. Chem. Soc.* **1986**, *108*, 6391.

8. Fromherz, P.; Rieger, B. *J. Am. Chem. Soc.* **1986**, *108*, 5361.

9. Purugganan, M.D.; Kumar, C.V.; Turro, N.J.; Barton, J.K. *Science* **1988**, *241*, 1645.

10. Barton, J.K.; Dannenberg, J.J.; Raphael, A.L. *J. Am. Chem. Soc.* **1982**, *104*, 4397.

11. Barton, J.K.; Danishefsky, A.T.; Goldberg, J.M. *J. Am. Chem. Soc.* **1984**, *106*, 2172.

12. Barton, J.K.; Goldberg, J.M.; Kumar, C.V.; Turro, N.J. *J. Am. Chem. Soc.* **1986**, *108*, 2081.

13. Kumar, C.V.; Barton, J.B.; Turro, N.J. *J. Am. Chem. Soc.* **1985**, *107*, 5518.

14. Barton, J.K.; Raphael, A.L. *J. Am. Chem. Soc.* **1984**, *106*, 2466.

15. Barton, J.K.; Raphael, A.L. *Proc. Natl. Acad. Sci. USA* **1985**, *82*, 6460.

16. Basile, L.A.; Raphael, A.L.; Barton, J.K. *J. Am. Chem. Soc.* **1987**, *109*, 7550.

17. Basile, L.A.; Barton, J.K. *J. Am. Chem. Soc.* **1987**, *109*, 7548.

18. Chapnick, L.B.; Chasin, L.A.; Raphael, A.L.; Barton, J.K. *Mutat. Res.* **1988**, *201*, 17.

19. Fleisher, M.B.; Waterman, K.C.; Turro, N.J.; Barton, J.K. *Inorg. Chem.* **1986**, *25*, 3549.

20. Graham, D.R.; Marshall, L.E.; Reich, K.A.; Sigman, D.S. *J. Am. Chem. Soc.* **1980**, *102*, 5419.

21. Griffin, J.H.; Dervan, P.B. *J. Am. Chem. Soc.* **1987**, *109*, 6840.

22. Muller, B.C.; Raphael, A.L.; Barton, J.K. *Proc. Natl. Acad. Sci., USA* **1987**, *84*, 1764.

23. Thorp, H.H.; Kumar, C.V.; Turro, N.J.; Gray, H.B. *J. Am. Chem. Soc.* **1989**, in press.

24. Thorp, H.H.; Van Houten, J.; Gray, H.B. *Inorg. Chem.* **1989**, *28*, 889.

25. Winkler, J.R.; Gray, H.B. *Inorg. Chem.* **1985**, *24*, 346.

26. Gueron, M.; Weinbuch, G. *Biopolymers* **1980**, *19*, 353.

27. Manning, G.S. *Q. Rev. Biophys.* **1978**, *11*, 179.

28. Blacker, A.J.; Jazwinski, J.; Lehn, J.-M.; Wilhelm, F.X. *J. Chem. Soc., Chem. Commun.* **1986**, 1035.

29. Kosower, E.M.; Cotter, J.L. *J. Am. Chem. Soc.* **1964**, *86*, 5524.

30. Carter, M.J.; Bard, A.J. *J. Am. Chem. Soc.* **1987**, *109*, 7528.

31. Van Atta, R.B.; Long, E.C.; Hecht, S.M.; van der Marel, G.A.; van Boom, J.H. *J. Am. Chem. Soc.* **1989**, *111*, 2722.

32. Stubbe, J.; Kozarich, J.W. *Chem. Rev.* **1987**, *87*, 1107.

33. Rice, S.F.; Gray, H.B. *J. Am. Chem. Soc.* **1983**, *105*, 4571.

34. Nocera, D.G.; Winkler, J.R.; Yocum, K.M.; Bordignon, E.; Gray, H.B. *J. Am. Chem. Soc.* **1984**, *106*, 5145.

Chapter 6.

Conclusions

An intensely pursued objective has been the development of redox catalysts for the oxidation and reduction of small molecules.[1, 2] Electrochemists have investigated numerous complexes that mediate these conversions upon electrolysis;[3-5] however, realization of these reactions under photochemical conditions often is elusive.[6] The difficulty of initiating electrocatalytic reactions by photoinduced electron transfer arises from the competition of efficient electron recombination with the desired chemical process.[1] Further, multi-electron reactions, readily mediated by a constant-potential electrode, offer puzzling difficulties to photochemists struggling with one-electron sacrificial donors and acceptors. Microheterogeneous environments are a frequent solution to these problems, allowing the organization of reactants in a manner conducive to efficient photocatalysis.[7,8] The experiments described in this thesis show that the dioxorhenium complex, $ReO_2(py)_4^+$, promises to be quite useful in this line of research.

Redox Chemistry

The coupling of photoinduced electron transfer reactions to small molecule activation has been realized in a number of systems.[1, 7-10] With $Ru(bpy)_3^{2+}$, for example, it is possible to effect such conversions as the reduction of water to hydrogen, the oxidation of water to oxygen, and the reduction of CO_2 to CO.[9, 11, 12] Unfortunately, in each of these systems, additional catalysts are required to bring about the reactions (Figure 6.1). Reduced methylviologen, formed by $Ru(bpy)_3^{2+}$-sensitized photoreduction, will reduce water to hydrogen only in the presence of a catalyst such as colloidal Pt;[11] the resulting oxidized sensitizer, $Ru(bpy)_3^{3+}$, will oxidize water to oxygen only in the presence of ruthenium dioxide.[12] The reduction of CO_2

Figure 6.1. Small molecule activations initiated by photoinduced electron transfer.

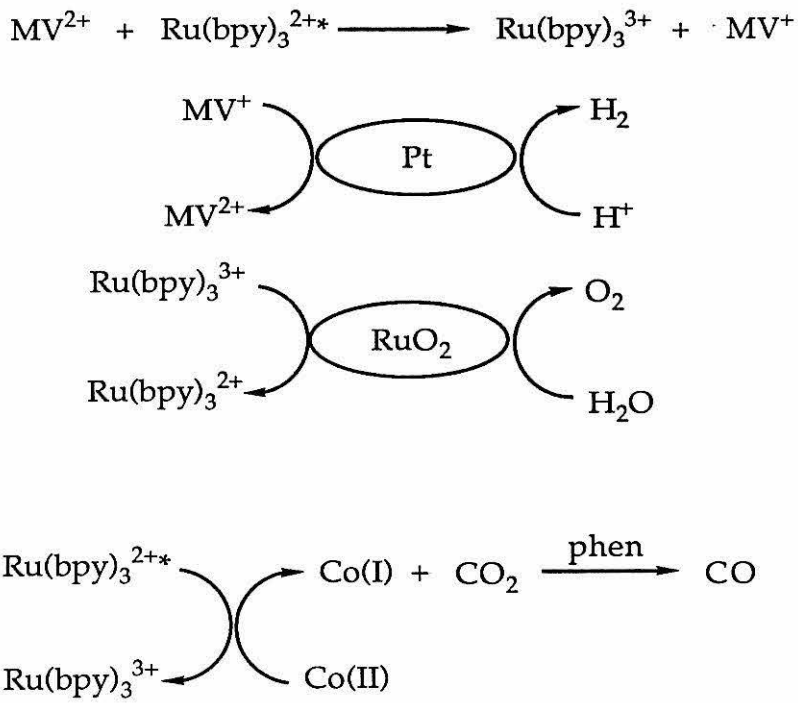
MV2+ + Ru(bpy)3 2+* → Ru(bpy)3 3+ + MV+
MV+
MV2+
Pt
H2
H+
Ru(bpy)3 3+
Ru(bpy)3 2+
RuO2
O2
H2O
Ru(bpy)3 2+*
Ru(bpy)3 3+
Co(I) + CO2
phen
CO
Co(II)

requires a Co(II) complex that can be reduced by $Ru(bpy)_3^{2+*}$ to Co(I), which is known to convert CO_2 to CO.[9]

The reduction of CO_2 to CO by a complex that can act as both sensitizer and catalyst, has been performed (Figure 6.2).[9] Photolysis of $Re(bpy)(CO)_3X$ (X = Cl^- or Br^-) in the presence of a sacrificial donor such as triethanolamine (TEOA) leads to photocatalytic reduction of CO_2 to CO. In this system, photoinduced electron-transfer leads to a reduced metal complex, $Re(bpy)(CO)_3X^-$,[10] which is substitutionally labile. Loss of X^- creates an open metal coordination site that can activate CO_2.[4, 5]

The excited-state redox chemistry of ReO_2^+ signals a similar advance for photocatalytic oxidations. The ^3E_g excited state of ReO_2^+ can reduce sacrificial acceptors such as MV^{2+}.[13] The product of this reaction, ReO_2^{2+}, is a potent oxidant (Figure 6.3). Catalytic amounts of acetophenone have been produced by electrolysis of ReO_2^+ in the presence of *sec*-phenethyl alcohol. Further, oxidation of THF and CH_2Cl_2 has been observed under photolysis conditions. Therefore, ReO_2^+, like its reductive counterpart, $Re(bpy)(CO)_3X$, can act as both sensitizer and catalyst for useful reactions initiated by photoinduced electron transfer. Unlike $Re(bpy)(CO)_3X$, however, electron transfer creates a reactive functionality on the oxo ligand rather than at an open coordination site.

A hydrogen atom abstraction mechanism is strongly implicated in these reactions. All of the conversions have been performed in nonaqueous solution under degassed conditions. Oxidation of ReO_2^+ may impart radical character to the oxo ligands (Figure 2.13). Activation of secondary alcohols, tertiary silanes, and THF has been observed with photocatalysts known to perform H-atom abstraction such as $Pt_2(pop)_4^{4-}$,[14, 15] ketones,[16] and other metal-oxo complexes.[3, 17-19] The oxidative cleavage of DNA is believed to

Figure 6.2. Proposed mechanism for the reduction of CO_2 by $Re(bpy)(CO)_3X$.

$$Re(bpy)(CO)_3X \xrightarrow{h\nu} Re(bpy)(CO)_3X^*$$

$$Re(bpy)(CO)_3X^* + TEOA \longrightarrow Re(bpy)(CO)_3X^- + TEOA^+$$

$$Re(bpy)(CO)_3X^- \longrightarrow Re(bpy)(CO)_3 + X^-$$

$$Re(bpy)(CO)_3 + CO_2 \longrightarrow CO \qquad (< 50 \text{ turnovers})$$

Figure 6.3. Proposed mechanism for the photoactivation of organic substrates by ReO_2^+.

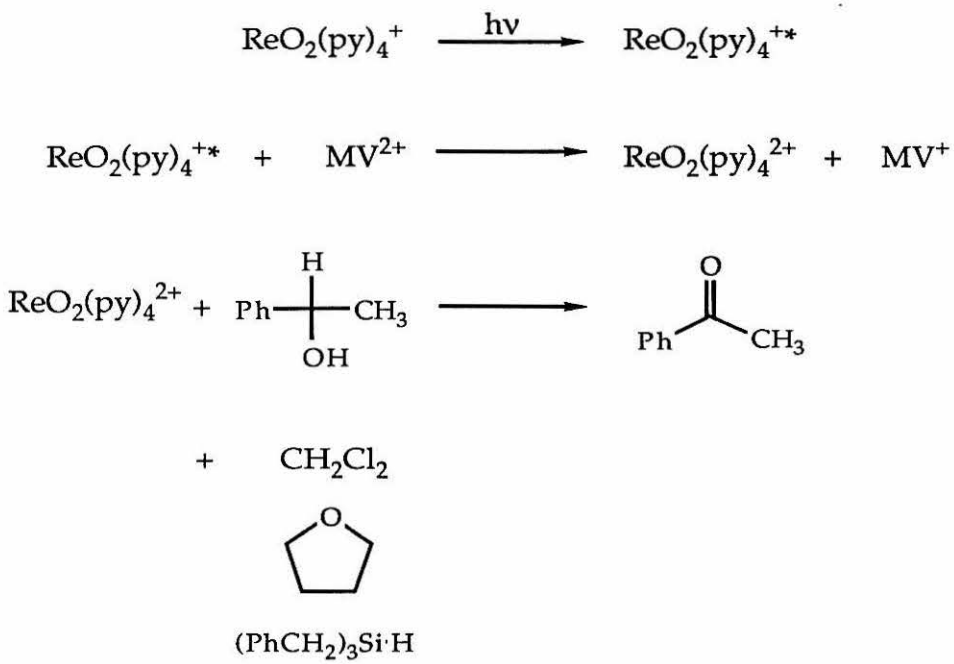
ReO2(py)4+
hν
ReO2(py)4+*
ReO2(py)4+* + MV2+
ReO2(py)42+ + MV+
ReO2(py)42+ +
H
Ph
CH3
OH
O
Ph
CH3
+ CH2Cl2
O
(PhCH2)3Si·H

occur by H-atom abstraction;[20] ReO_2^{2+} also can mediate this reaction in degassed solution.

Photochemistry of Microheterogeneous Environments

The elucidation of micellar structure using emissive metal complexes has been pursued widely.[7, 8, 21] Experiments with $Ru(bpy)_3^{2+}$ and its derivatives are difficult because the lifetime of $Ru(bpy)_3^{2+*}$ is not altered significantly upon binding to aqueous micelles. In fact, the initial observation of premicellar clusters in SDS solutions required hydrophobic quenchers such as 9-methylanthracene.[22] Existence of premicellar clusters was substantiated by the fact that the hydrophobic quenchers were solubilized at surfactant concentrations below the cmc only in the presence of the metal cation. Further, the quencher did affect the lifetime of the clustered $Ru(bpy)_3^{2+}$. With ReO_2^+,[23] the observation of long-lived emission at surfactant concentrations below the cmc is evidence of association. By varying the ionic strength, surfactant concentration, laser power and H_2O/D_2O ratio, it was shown that these clusters can coexist with normal micelles at surfactant concentrations above the cmc. Addition of invasive quenchers was not required because of the extreme sensitivity of the ReO_2^+ lifetime to its environment.

Lifetime data for some metal complexes used as environmental probes are shown in Table 6.1. Hydrophobic $Ru(bpy)_3^{2+}$ derivatives show larger enhancements when bound to SDS micelles, probably because the hydrophobic ligands encourage tighter binding, creating a more rigid environment.[24] The neutral complex, $Ru(bpy)_2(CN)_2$, has a large isotope effect but does not show appreciable change in lifetime upon binding. The lanthanide ions are different in that a change in the number of coordinated

Table 6.1.

Emission Lifetime Data for Metal Complexes in SDS Micelles.

complex	$\tau(H_2O)$, μs	k_H/k_D	τ(SDS), μs	k_H/k_D
Eu^{3+}	103[a]	25.4	100[b]	---
Tb^{3+}	408[a]	8.75	400[b]	---
$Ru(bpy)_3^{2+}$[c]	0.576	1.63	0.80	1.19
$Ru(phen)_2(DIP)^{2+}$[c]	3.07	1.37	6.11	1.07
$Ru(bpy)_2(CN)_2$[c]	0.254	1.80	0.391	1.47
$ReO_2(py)_4^+$	<0.01	(8.6)[d]	0.07	8.6
			0.90	1.0

[a]Reference 25. [b]Reference 26. [c]Reference 24. [d]Measured in homogeneous pyridine solution, reference 55.

H_2O ligands is required to bring about changes in the emission properties.[25] Therefore, for noncoordinating environments such as SDS, lanthanide ion emission is not illustrative.[26] Clearly, examination of the data in Table 6.1 shows the utility of ReO_2^+ as an environmental probe.

The structure of ReO_2^+ contains an interesting combination of hydrophilic and potentially hydrophobic functionality. Synthesis of new complexes shows that four extremely hydrophobic 3-Ph-py ligands can replace the four pyridine ligands of ReO_2^+.[23] This substitution increases greatly the hydrophobic quality of the complex without changing the exquisitely sensitive photophysical properties. Experiments with this molecule also show that a readily observable vibrational progression, arising from an MO_2 stretching mode, can be observed in emission spectra taken in potentially rigid environments. In addition, the absorption and emission maxima for ReO_2^+ complexes reflect the overall polarity of the environment; these data correlate with the other electronic properties.

Experiments on Nafion membranes also are more facile with ReO_2^+. Again, $Ru(bpy)_3^{2+}$ has nearly the same lifetime in water and in the membrane (Table 6.2).[27] Complicated electrochemical experiments involving ferrocene as a neutral, hydrophobic probe[28] have shown that $Ru(bpy)_3^{2+}$ occupies both the ion cluster and interfacial regions of the membrane but, again, emission experiments can not corroborate this interpretation. With ReO_2^+, observation of two-component emission is, in itself, evidence for occupation of distinct regions by the chromophore. The observation of different isotope effects for each component supports the assignment. Finally, emission and absorption measurements show that the overall polarity of the membrane is quite high, similar to ethylene glycol.

Table 6.2.

Emission Properties of Metal Complexes in Anionic Polymer Environments.

complex	$\tau(H_2O)$, μs	environment	τ(μs)
$Ru(bpy)_3^{2+}$	0.576[a]	Nafion/H_2O	0.68[b]
		DNA/H_2O	0.42[c]
$Ru(phen)_3^{2+}$	1.19[d]	DNA/H_2O	0.73[c]
			2.65
ReO_2^+	<0.01	Nafion/H_2O	0.25
			1.3
		Nafion/D_2O	0.75
			2.9
		DNA/H_2O	1.7
$ReO_2(3\text{-Ph-py})_4^+$	<0.01	DNA/H_2O	2.4
			10.

[a]Reference 24. [b]Reference 27. [c]Reference 29. [d]Reference 56.

The characterization of metal complex-DNA interactions by emission lifetime measurements also has been investigated widely.[29-34] Electrostatic association of $Ru(bpy)_3^{2+}$ with the DNA helix induces little change in the emission lifetime (Table 6.2).[29] In contrast, electrostatic binding of ReO_2^+ changes its lifetime by at least three orders of magnitude. Addition of hydrophobic ligands to $Ru(bpy)_3^{2+}$ leads to a longer component; the same effect is observed with ReO_2^+. Again, the changes in lifetime are substantially larger for ReO_2^+.

Oxidative Cleavage of DNA

The oxidative cleavage of DNA by metal complexes is under intense study.[20, 30, 35-43] The reaction of iron bleomycin (Fe-BLM) with DNA leads to oxidative cleavage by a number of well-studied mechanisms.[20] Other metal complexes such as $Cu(phen)_2^+$[39, 40] and methidium-propyl-EDTA-Fe(II)[41] cleave DNA by similar mechanisms. These thermal agents all require oxygen or hydrogen peroxide. The photoactivated cleavage of $Ru(bpy)_3^{2+}$ and $Ru(phen)_3^{2+}$ occurs through sensitization of singlet oxygen.[38, 44] (The singlet oxygen reaction is unique in that it oxidizes the bases, not the sugars). The mechanism for photolytic cleavage of DNA by cobalt bleomycins, $Co(DIP)_3^{3+}$, and $Rh(DIP)_3^{3+}$ is very poorly understood, although it is known that cleavage is mediated by Co-BLM in the absence of oxygen.[20]

The reaction of Fe-BLM is believed to occur through the generation of metal-bound hydroxyl radical, which abstracts the 4' ribose hydrogen from DNA.[20] The resulting ribose radical can degrade via a number of pathways. The cleavage of DNA by ReO_2^{2+} therefore may be explained by an H-atom abstraction mechanism. Photolysis of ReO_2^+ induces electron transfer to methylviologen producing MV^+, which usually recombines rapidly with

ReO_2^{2+} on the helix. After ~2% of the redox events,[45] MV^+ escapes into the bulk solution, allowing ReO_2^{2+} to react with the DNA (Figure 5.7). The efficiency of the process is two orders of magnitude lower than for $Co(phen)_3^{3+}$,[38] consistent with the 2% yield of MV^+ escape.

Novel analytical techniques are possible with this cleavage scheme. The production of MV^+ allows detection of the reaction by absorption spectroscopy, owing to the distinctive spectrum of the radical. The addition of calf thymus DNA to aqueous solutions of ReO_2^+ leads to a decrease in cathodic current for the rereduction wave in cyclic voltammograms of ReO_2^+. This is because on the forward sweep, the oxidizing species, ReO_2^{2+}, is generated and reacts with the DNA. On the reverse sweep, the back wave is smaller because of the chemical reaction of the oxidized complex. The scan-rate dependence of this phenomenon supports this interpretation. Further, this experiment shows that MV^{2+} is not required for reaction of ReO_2^{2+} with the DNA.

It is tempting to consider the mechanism of photocleavage by Co-BLM, $Co(phen)_3^{3+}$, $Co(DIP)_3^{3+}$, and $Rh(DIP)_3^{3+}$. For the polypyridyl complexes, "tight" cleavage patterns have been observed, indicating that no diffusable species is involved.[30, 46-48] As stated, oxygen is not required for activity of Co-BLM.[20] The polypyridyl complexes are strong (~2 V) photooxidants.[47, 49] Cyclic voltammetry of $Rh(bpy)_3^{3+}$ shows irreversible, two-electron reduction, even at sweep rates as high as 100 V s^{-1}.[50] These data are consistent with the mechanism shown in (1) - (3), where reduction of $Rh(bpy)_3^{3+}$ occurs first at the bpy ligand to produce a species that is reduced again at the electrode and goes on to lose a bpy ligand and form a stable, square-planar d^8 complex.

$$Rh(bpy)_3^{3+} + e^- \rightarrow Rh(bpy)_2(bpy^-)^{2+} \qquad (1)$$

$$Rh(bpy)_2(bpy^-)^{2+} + e^- \rightarrow Rh(bpy)_3^+ \quad (2)$$

$$Rh(bpy)_3^+ \rightarrow Rh(bpy)_2^+ + bpy \quad (3)$$

The excited-state properties of these rhodium complexes also are known; $Rh(phen)_3^{3+}$ has a long-lived intraligand (π,π^*) excited state[51] that is a very strong (2.25 V vs. NHE) oxidant.[49]

From the detailed electronic information available for rhodium polypyridyl complexes, the mechanism shown in Figure 6.4 can be proposed. The potential for the one-electron oxidation of water to hydroxyl radical and a proton is +2.33 V (vs. NHE) at pH 7,[52] very close to the potential of $Rh(phen)_3^{3+*/2+}$ (it is being assumed that phen and DIP have similar redox properties).[49] The oxidation of water to hydroxyl radical by $Rh(DIP)_3^{3+}$ produces the two species needed to complete the reaction: a potent H-atom abstractor (OH•), and a good electron acceptor ($Rh(DIP)_2(DIP^-)^{2+}$). Now the reaction can proceed via established mechanisms for bleomycins.[20]

This mechanism has a number of distinct advantages. Direct, one-electron oxidation of the sugar by $Rh(DIP)_3^{3+*}$ might be possible; however, the ribose unit does not possess a readily oxidized functionality. Further, electron recombination between $Rh(DIP)_3^{2+}$ and the "oxidized" sugar probably will be more efficient than the bond cleavage processes necessary for backbone degradation.[16, 53] The reduced rhodium complex is a convenient electron acceptor for conversion of the sugar radical to the 4'-carbocation, a species known to add water and produce cleavage. The one-base cleavage patterns[47] observed for $Rh(DIP)_3^{3+}$ can be accounted for by the need for this proximal electron acceptor. Analogous mechanisms can be proposed for the cobalt complexes and for oxidizing dyes such as 2,7-diazapyrenium cations, which also cleave DNA in the absence of oxygen.[54] Thus, it is possible that

Figure 6.4. New proposed mechanism for the oxidative cleavage of DNA by photoexcited $Rh(DIP)_3^{3+}$.

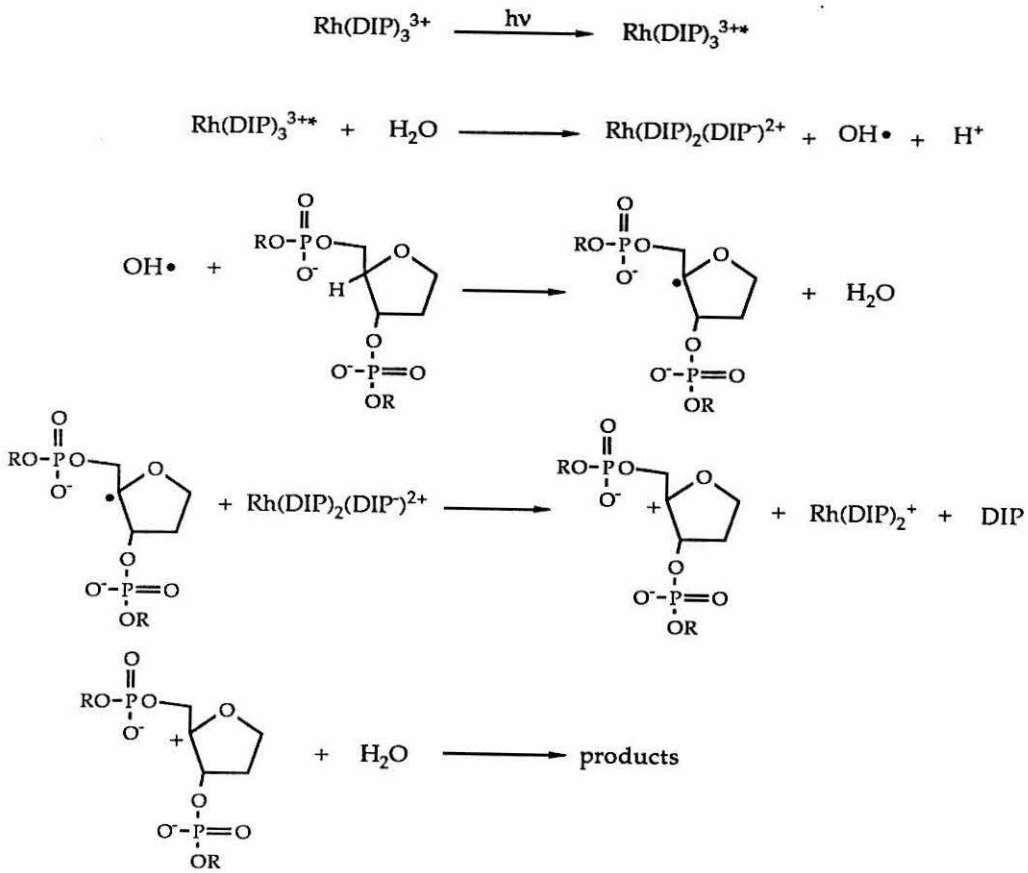
Rh(DIP)3 3+
hν
Rh(DIP)3 3+*
Rh(DIP)3 3+* + H2O
Rh(DIP)2(DIP-)2+ + OH• + H+
OH• +
+ H2O
+ Rh(DIP)2(DIP-)2+
+ Rh(DIP)2+ + DIP
+ H2O
products

these complexes do not oxidize the sugars directly but instead operate by generating a hydroxyl radical.

A mechanism involving water-bound species cannot operate for ReO_2^+. Observation of the reaction under rigorously degassed conditions rules out the involvement of molecular oxygen. Further, the potential for water oxidation is too large for the $ReO_2^{2+/+}$ couple (+1.56 V vs. NHE), ruling out mediation by hydroxyl radical. Experiments involving organic substrates point to an H-atom abstraction mechanism. Reaction with THF has been observed; the chemical resemblance of THF and the DNA ribose is clear. Other dioxo complexes activate THF by abstraction of an H-atom from the α-carbon,[19] a reaction similar to the one proposed here. Thus, direct oxidation of the sugar by ReO_2^{2+} is a probable mechanism.

In conclusion, ReO_2^+ is an attractive photocatalyst because it can undergo photoinduced electron transfer to produce a potent H-atom abstractor capable of oxidizing silanes, alcohols, halocarbons and THF.[13] Using this chemistry, it is possible to perform photoreactions where ReO_2^+ acts as both the sensitizer and catalyst, a previously unrealized goal for the oxidation of organic substrates initiated by photoinduced electron transfer.

The emission properties of ReO_2^+ are ideal for studying microheterogeneous environments because the emission lifetime is strongly dependent on the aqueous character of the medium.[23] Lifetimes spanning five orders of magnitude have been measured in environments of varying solvent accessibility. The remarkably large isotope effect on this emission lifetime also is sensitive to the properties of the environment. The emission and absorption maxima indicate the overall polarity of the environment and give values that are consistent with other techniques.

Experiments in DNA are noteworthy for two reasons. First, the ReO_2^+ chromophore is an excellent probe of binding, and two binding modes readily can be determined. Second, the bound complex can reduce MV^{2+} upon photoexcitation to produce the potent H-atom abstractor ReO_2^{2+}, which can cleave the DNA in a manner possibly analogous to Fe-BLM[20] but without a necessary diffusable intermediate like O_2 or OH•. The spectroscopic and electrochemical properties of the reacting species allow detection of the cleavage reaction by novel techniques. The efficiency of this reaction is low, owing to rapid electron recombination on the helix. Nevertheless, the results indicate that metal-oxo and other complexes known to abstract H-atoms from organic substrates might provide an efficient method for the direct oxidative cleavage of DNA in the absence of any diffusable species.

References

1. Maverick, A.M.; Gray, H.B. *Pure and Appl. Chem.* **1980**, *52*, 2339.

2. Krause, R.A. *Struct. and Bonding* **1987**, *67*, 1.

3. Meyer, T.J. *J. Electrochem. Soc.* **1984**, *131*, 221C.

4. Sullivan, B.P.; Bruce, M.R.M.; O'Toole, T.R.; Bolinger, C.M.; Megehee, E.; Thorp, H.; Meyer, T.J. *ACS Symp. Ser.* **1988**, *363*, 52.

5. Sullivan, B.P.; Siliman, S.; Thorp, H.; Meyer, T.J. *Inorg. Chem.* **1989**, In press.

6. Lees, A.J. *Chem. Rev.* **1987**, *87*, 711.

7. Kalyanasundaram, K., "Photochemistry in Microheterogeneous Systems," Academic Press, London, **1987**.

8. Fendler, J.H., "Membrane Mimetic Chemistry," Wiley-Interscience, New York, **1982**.

9. Hawecker, J.; Lehn, J.-M.; Ziessel, R. *J. Chem. Soc., Chem. Commun.* **1983**, 536.

10. Kutal, C.; Weber, M.A.; Ferraudi, G.; Geiger, D. *Organometallics* **1985**, *4*, 2161.

11. Moroi, Y.; Braun, A.M.; Graetzel, M. *J. Am. Chem. Soc.* **1979**, *101*, 567.

12. Nijs, H.; Fripiat, J.J.; Van Damme, V. *J. Phys. Chem.* **1983**, *87*, 1279.

13. Thorp, H.H.; Van Houten, J.; Gray, H.B. *Inorg. Chem.* **1989**, *28*, 889.

14. Harvey, E.L.; Stiegman, A.E.; Vlcek, A.A.; Gray, H.B. *J. Am. Chem. Soc.* **1987**, *109*, 5233.

15. Vlcek, A.A.; Gray, H.B. *J. Am. Chem. Soc.* **1987**, *109*, 286.

16. Turro, N.J., "Modern Molecular Photochemistry," Benjamin-Cummings, Menlo Park, CA, **1978**.

17. Holm, R.H. *Chem. Rev.* **1987**, *87*, 1401.

18. Che, C.-M.; Yam, V.W.-W.; Cho, K.C.; Gray, H.B. *J. Chem. Soc., Chem. Commun.* **1987**, 948.

19. Yam, V.W.-W.; Che, C.-M.; Tang, W.-T. *J. Chem. Soc., Chem. Commun.* **1988**, 100.

20. Stubbe, J.; Kozarich, J.W. *Chem. Rev.* **1987**, *87*, 1107.

21. Turro, N.J.; Graetzel, M.; Braun, A.M. *Angew. Chem. Int. Ed. Engl.* **1980**, *19*, 675.

22. Baxendale, J.H.; Rodgers, M.A.J. *J. Phys. Chem.* **1982**, *86*, 4906.

23. Thorp, H.H.; Kumar, C.V.; Turro, N.J.; Gray, H.B. *J. Am. Chem. Soc.* **1989**, in press.

24. Hauenstein, B.L.; Dressick, W.J.; Buell, S.L.; Demas, J.N.; DeGraff, B.A. *J. Am. Chem. Soc.* **1983**, *105*, 4251.

25. Horrocks, W.DeW.; Albin, M. *Prog. Inorg. Chem.* **1984**, *31*, 1.

26. Almgren, M.; Greiser, F.; Thomas, J.K. *J. Am. Chem. Soc.* **1979**, *101*, 2021.

27. Buttry, D.A.; Anson, F.C. *J. Am. Chem. Soc.* **1982**, *104*, 4824.

28. Rubinstein, I. *J. Electroanal. Chem.* **1985**, *188*, 227.

29. Kumar, C.V.; Barton, J.K.; Turro, N.J. *J. Am. Chem. Soc.* **1985**, *107*, 5518.

30. Barton, J.K. *Science* **1986**, *233*, 727.

31. Barton, J.K.; Goldberg, J.M.; Kumar, C.V.; Turro, N.J. *J. Am. Chem. Soc.* **1986**, *108*, 2081.

32. Barton, J.K.; Danishefsky, A.T.; Goldberg, J.M. *J. Am. Chem. Soc.* **1984**, *106*, 2172.

33. Barton, J.K. *J. Biomol. Struct. Dyn.* **1983**, *1*, 621.

34. Kelly, J.M.; Tossi, A.M.; McConnell, D.J.; OhUigin, C. *Nucleic Acids Res.* **1985**, *13*, 6017.

35. Barton, J.K.; Raphael, A.L. *J. Am. Chem. Soc.* **1984**, *106*, 2466.

36. Carter, M.J.; Bard, A.J. *J. Am. Chem. Soc.* **1987**, *109*, 7528.

37. Chang, C.H.; Meares, C.F. *Biochemistry* **1982**, *21*, 6332.

38. Fleisher, M.B.; Waterman, K.C.; Turro, N.J.; Barton, J.K. *Inorg. Chem.* **1986**, *25*, 3549.

39. Basile, L.A.; Raphael, A.L.; Barton, J.K. *J. Am. Chem. Soc.* **1987**, *109*, 7550.

40. Graham, D.R.; Marshall, L.E.; Reich, K.A.; Sigman, D.S. *J. Am. Chem. Soc.* **1980**, *102*, 5419.

41. Dervan, P.B. *Science* **1986**, *232*, 464.

42. "Bleomycin: Chemical, Biochemical and Biological Aspects," Hecht, S.M., Ed., Springer-Verlag, New York, **1979.**

43. Van Atta, R.B.; Long, E.C.; Hecht, S.M.; van der Marel, G.A.; van Boom, J.H. *J. Am. Chem. Soc.* **1989**, *111*, 2722.

44. Mei, H.-Y.; Barton, J.K. *Proc. Natl. Acad. Sci., USA* **1988**, *85*, 1339.

45. Atherton, S.J.; Beaumont, P.C. *J. Phys. Chem.* **1987**, *91*, 3993.

46. Barton, J.K.; Raphael, A.L. *Proc. Natl. Acad. Sci. USA* **1985**, *82*, 6460.

47. Kirshenbaum, M.R.; Tribolet, R.; Barton, J.K. *Nucleic Acids Res.* **1988**, *16*, 7943.

48. Muller, B.C.; Raphael, A.L.; Barton, J.K. *Proc. Natl. Acad. Sci., USA* **1987**, *84*, 1764.

49. Ballardini, R.; Varani, G.; Balzani, V. *J. Am. Chem. Soc.* **1980**, *102*, 1719.

50. Creutz, C.; Keller, A.D.; Sutin, N.; Zipp, A.P. *J. Am. Chem. Soc.* **1982**, *104*, 3618.

51. Watts, R.J.; Van Houten, J. *J. Am. Chem. Soc.* **1978**, *100*, 1718.

52. George, P., in "Oxidases and Related Redox Systems," T. E. King, H. S. Mason, M. Morrison, Eds. (John Wiley and Sons, New York, 1964), p. 3.

53. Marcus, R.A.; Sutin, N. *Biochim. Biophys. Acta* **1985**, *811*, 265.

54. Blacker, A.J.; Jazwinski, J.; Lehn, J.-M.; Wilhelm, F.X. *J. Chem. Soc., Chem. Commun.* **1986**, 1035.

55. Winkler, J.R.; Gray, H.B. *Inorg. Chem.* **1985**, *24*, 346.

56. Duveneck, G.L.; Kumar, C.V.; Turro, N.J.; Barton, J.K. *J. Phys. Chem.* **1988**, *92*, 2028.